



UNIVERSITAT DE  
BARCELONA

## Towards Novel Therapeutical Strategies for NUT Carcinoma

Carmen Escudero Iriarte

**ADVERTIMENT.** La consulta d'aquesta tesi queda condicionada a l'acceptació de les següents condicions d'ús: La difusió d'aquesta tesi per mitjà del servei TDX ([www.tdx.cat](http://www.tdx.cat)) i a través del Dipòsit Digital de la UB ([diposit.ub.edu](http://diposit.ub.edu)) ha estat autoritzada pels titulars dels drets de propietat intel·lectual únicament per a usos privats emmarcats en activitats d'investigació i docència. No s'autoritza la seva reproducció amb finalitats de lucre ni la seva difusió i posada a disposició des d'un lloc aliè al servei TDX ni al Dipòsit Digital de la UB. No s'autoritza la presentació del seu contingut en una finestra o marc aliè a TDX o al Dipòsit Digital de la UB (framing). Aquesta reserva de drets afecta tant al resum de presentació de la tesi com als seus continguts. En la utilització o cita de parts de la tesi és obligat indicar el nom de la persona autora.

**ADVERTENCIA.** La consulta de esta tesis queda condicionada a la aceptación de las siguientes condiciones de uso: La difusión de esta tesis por medio del servicio TDR ([www.tdx.cat](http://www.tdx.cat)) y a través del Repositorio Digital de la UB ([diposit.ub.edu](http://diposit.ub.edu)) ha sido autorizada por los titulares de los derechos de propiedad intelectual únicamente para usos privados enmarcados en actividades de investigación y docencia. No se autoriza su reproducción con finalidades de lucro ni su difusión y puesta a disposición desde un sitio ajeno al servicio TDR o al Repositorio Digital de la UB. No se autoriza la presentación de su contenido en una ventana o marco ajeno a TDR o al Repositorio Digital de la UB (framing). Esta reserva de derechos afecta tanto al resumen de presentación de la tesis como a sus contenidos. En la utilización o cita de partes de la tesis es obligado indicar el nombre de la persona autora.

**WARNING.** On having consulted this thesis you're accepting the following use conditions: Spreading this thesis by the TDX ([www.tdx.cat](http://www.tdx.cat)) service and by the UB Digital Repository ([diposit.ub.edu](http://diposit.ub.edu)) has been authorized by the titular of the intellectual property rights only for private uses placed in investigation and teaching activities. Reproduction with lucrative aims is not authorized nor its spreading and availability from a site foreign to the TDX service or to the UB Digital Repository. Introducing its content in a window or frame foreign to the TDX service or to the UB Digital Repository is not authorized (framing). Those rights affect to the presentation summary of the thesis as well as to its contents. In the using or citation of parts of the thesis it's obliged to indicate the name of the author.



UNIVERSITAT DE  
BARCELONA



VALL D'HEBRON  
Institute  
of Oncology

Biomedicine Doctoral Program  
Faculty of Medicine-Campus Clinic  
of Universitat de Barcelona

# Towards Novel Therapeutical Strategies for NUT Carcinoma

**Carmen Escudero Iriarte**

This work was developed under the supervision of  
**Dr. Tian Tian** and **Dr. Teresa Macarulla**  
at the Vall d'Hebron Institute of Oncology (VHIO)

Tutor: **Neus Agell Jané**



# INDEX



# INDEX

ACKNOWLEDGEMENTS .....	16
ABBREVIATIONS.....	23
SUMMARY .....	30
RESUMEN .....	33
INTRODUCTION.....	36
<b>1. NUT CARCINOMA.....</b>	<b>38</b>
<b>1.1 Definition and epidemiology.....</b>	<b>38</b>
1.1.1 Epidemiology of NC.....	38
1.1.2 Prevalence and prognosis of NC .....	40
<b>1.2 Molecular basis of NUT Carcinoma oncogenesis.....</b>	<b>42</b>
1.2.1 NUT fusion partners in NC.....	42
1.2.2 Molecular mechanism behind NUT-fusion in NC. ....	43
1.2.3 Megadomains of histone acetylation in NC .....	45
1.2.4 Cells of origin of NC .....	46
1.2.5 Fusion protein as a driver factor in NC disease. ....	46
<b>1.3 Diagnosis .....</b>	<b>47</b>
1.3.1 Clinical symptoms and histopathologic features .....	47
1.3.2 NUT detection to diagnose NC .....	47
1.3.3 NC as an aggressive subtype of NUT-rearranged neoplasms (NRNs) .....	48
<b>1.4 Clinical management.....</b>	<b>51</b>

1.4.1 Surgical resection as the best but uncommon option for NC patients.....	51
1.4.2 Chemo and radiotherapy regimens for NC patients .....	52
1.4.3 Targeted therapies for NC.....	52
1.4.4 Immunotherapy as an emerging option for NC .....	54
<b>2. EPIGENETICS .....</b>	<b>55</b>
<b>2.1 Chromatin structure and organization.....</b>	<b>55</b>
2.1.1 The different levels of chromatin compaction.....	55
2.1.2 The interplay between chromatin architecture and transcription .....	57
<b>2.2 Histone post-translational modifications with a particular focus on acetylation.....</b>	<b>58</b>
2.2.1 A brief overview of chromatin chemical modifications, highlighting histone PTMs. ....	58
2.2.2 Histone acetylation. ....	60
<b>2.3 Epigenetics and NUT Carcinoma .....</b>	<b>65</b>
2.3.1 NC is an epigenetic-driven cancer.....	65
2.3.2 The model of megadomain formation extends to other NUT fusion partners beyond BRD4. ....	66
2.3.3 Megadomains of acetylation: origin, organization, and impact on NC cells. ....	67
2.3.4 The connection between megadomains and condensate formation .....	70
2.3.5 Epigenetic alterations of NC beyond BRD4-NUT and p300-dependent megadomains.....	71
<b>3. SOURCES AND PATHWAYS INVOLVED IN DNA DAMAGE RESPONSE.....</b>	<b>73</b>
<b>3.1 Sources of DNA damage response .....</b>	<b>73</b>

<b>3.2 DNA repair mechanisms.</b>	<b>75</b>
3.2.1 Single-strand DNA repair	75
3.2.2 Double-strand DNA repair	76
3.2.3. DNA damage sensors	76
3.2.4 Chromatin and DNA damage response	79
3.2.5 DDR and NC	80
<b>3.3 Replication stress as a source of DNA damage</b>	<b>81</b>
3.3.1 Mechanisms of replication fork rescue	81
3.3.2 Sources of RS	83
3.3.3 R-loops as a critical player in the RS	85
3.3.4 The bidirectional regulation between RS and chromatin structure.	86
<b>3.4 The implication of RS in cancer</b>	<b>87</b>
<b>3.5 Targeting DDR as a therapeutical strategy in cancer</b>	<b>88</b>
<b>HYPOTHESIS AND OBJECTIVES</b>	<b>90</b>
<b>MATERIALS AND METHODS</b>	<b>94</b>
<b>Cell lines and culture conditions</b>	<b>96</b>
<b>Drug treatments</b>	<b>97</b>
<b>Patient samples information</b>	<b>100</b>
<b>Immunofluorescence</b>	<b>102</b>
<b>Image analysis</b>	<b>104</b>
<b>Western blot</b>	<b>105</b>
<b>DNA fiber assay</b>	<b>106</b>
<b>Global transcription detection. EU assay</b>	<b>107</b>
<b>Cell viability assay. MTT</b>	<b>107</b>
<b>Apoptosis assay</b>	<b>108</b>
<b>HR reporter assay</b>	<b>108</b>

Knockout cell generation.....	109
RAD51 assay.....	110
Drug efficacy studies <i>in vivo</i> .....	110
BrdU assay.....	111
RNA sequencing.....	112
<b>RESULTS</b> .....	<b>113</b>

**PART 1. The impact of BRD4-NUT fusion on RS in NC cells as a novel targetable vulnerability ..... 115**

<b>1. BRD4-NUT fusion is involved in an increased RS in NC ....</b>	<b>115</b>
1.1. Modulation of the expression of BRD4-NUT fusion using degrader MZ1.....	115
1.2 MZ1 treatment resulted in decreased expression of RS markers, and their recovery occurred upon MZ1 removal.....	117
1.3 BRD4-NUT impacts on replication fork speed.....	118
<b>2. The NUT moiety of the BRD4-NUT fusion affects the RS status in NC cells.....</b>	<b>119</b>
2.1. Generation and validation of ectopic expression models to study the involvement of BRD4-NUT fusion in RS.....	119
2.2. BRD4-NUT increases RS markers through the NUT moiety of the fusion.....	121
<b>3. p300 acetyltransferase and hyperacetylated chromatin megadomain formation are involved in BRD4-NUT fusion-induced RS in NC cells. ....</b>	<b>123</b>
3.1. BRD4-NUT degradation decreases the formation of megadomains in NC cell lines. ....	123
3.2. p300 degradation with dCBP1 PROTAC degrader can lead to decreased hyperacetylated megadomain in NC cells. ....	124
3.3. p300 and associated megadomains are required for BRD4-NUT-induced RS in NC cells. ....	125

<b>4.</b>	<b>Transcription is required for BRD4-NUT-induced RS in NC cells.</b>	<b>128</b>
4.1.	MZ1 treatment affects transcription levels, and this is recovered upon its removal. ....	128
4.2.	p300 is required for the recovery in overall transcription observed upon BRD4-NUT restoration. ....	130
4.3.	Transcription is required for the BRD4-NUT-induced RS in NC cells.	131
<b>5.</b>	<b>R-loops are also involved in BRD4-NUT-induced RS in NC cells.</b>	<b>134</b>
5.1.	p300 and transcription are required for the BRD4-NUT-induced accumulation of R-loops in NC cells. ....	135
5.2.	R-loop elimination by RNH1 abrogates BRD4-NUT-induced RS in NC cells. ....	137
<b>6.</b>	<b>Proposed model for the involvement of BRD4-NUT fusion in RS of NC cells.</b>	<b>139</b>
<b>7.</b>	<b>NC cells exhibit sensitivity to a range of inhibitors that target factors implicated in the RS response pathways.</b>	<b>141</b>
7.1.	A drug screening focused on DDRi revealed that NC cells are sensitive to inhibitors targeting factors involved in RS response pathways. ....	141
7.2.	The sensitivity of the selected drug candidates was confirmed through further validation. ....	142
7.3.	Candidate drugs can induce apoptotic effects in NC cell lines.	143
<b>8.</b>	<b>NC cell lines are not Homologous Recombination Deficient.</b>	<b>145</b>
8.1.	HR reporter assay shows HR proficiency in NC cells. ....	145
8.2.	NC cell lines and patient samples showed HR proficiency using RAD51-related functional assays. ....	147

9.	The combined treatment of PARPi and ATRi significantly inhibits the growth of NC cells <i>in vivo</i> .....	149
<b>PART 2. Targeting MYC as a novel therapeutic strategy for patients with NUT Carcinoma.....</b>		<b>152</b>
10.	Novel MYC inhibitor OMO-103 showed remarkable sensitivity in NC cell lines.....	152
10.1.	NC cells are sensitive to OMO-103 in vitro.....	152
10.2.	OMO-103 treatment in vitro enhances differentiation and induced apoptosis while halting the cell cycle progression in NC cell lines.	153
11.	Transcriptional analysis showed that OMO-103 treatment led to downregulating proliferation and cell cycle-related pathways.	156
12.	OMO-103 can inhibit NC xenograft growth <i>in vivo</i> , particularly when combined with chemotherapy.....	158
<b>PART 3. Efficacy study of novel chemotherapy regimen for NC treatment.....</b>		<b>160</b>
13.	Lurbinectedin, an approved treatment for SCLC, demonstrated significant sensitivity in NC cells. ....	160
14.	Irinotecan, an approved treatment for solid tumors, showed significant efficacy in NC cells.....	161
<b>DISCUSSION .....</b>		<b>163</b>
1.	Addressing the complexities of research and advancement in treating rare cancers .....	165
2.	Limitations of experimental models in NUT Carcinoma research .....	166
3.	Strategies for modulating BRD4-NUT expression in NC cells.....	167

4. Epigenetic-driven cancers: understanding the impact of BRD4 in cancer development and progression. ....	168
5. Targeting replication stress in NUT Carcinoma. ....	170
6. The effect of PARP inhibitors beyond Homologous Recombination deficiency. ....	173
7. The emerging role of <i>MYC</i> oncogene in NUT Carcinoma.....	174
8. A possible connection between RS and <i>MYC</i> in NC oncogenesis. ....	175
CONCLUSIONS .....	179
REFERENCES.....	183
APPENDIX .....	203

# FIGURE INDEX

Figure 1. Overall survival of three subgroups of NC patients.....	41
Figure 2. Schematic representation of NUT fusion proteins and WT counterparts.....	43
Figure 3. Scheme of BRD4-NUT-dependent megadomains of acetylation. .	44
Figure 4. Schematic representation of NUT fusion interaction complex. ....	45
Figure 5. Diagnosis of NC by NUT immunohistochemistry. ....	48
Figure 6. NUT fusion partners in NRNs. ....	49
Figure 7. First NC treatment guideline proposed at the First International Symposium of NUT Carcinoma. ....	51
Figure 8. Schematic representation of the organization of the eukaryotic genome.....	55
Figure 9. Scheme of the interplay between writers, erasers, and readers across chromatin. ....	60
Figure 10. Scheme of histone acetylation.....	61
Figure 11. Schematic representation of p300's involvement in transcription. ....	62
Figure 12. Scheme of BRD4 isoforms. ....	64
Figure 13. Schematic representation of key domains in BRD4-NUT and p300.....	66
Figure 14. Schematic representation of the different proposed models of megadomain formation.....	68
Figure 15. Scheme of chromatin organization of megadomains.....	69
Figure 16. Schematic representation of the model of condensate formation. ....	71
Figure 17. DNA damage sources.....	74

Figure 18. Scheme of recruitment, activation, and consequences of DNA-PK, ATM, and ATR kinase pathways.....	77
Figure 19. Scheme of fork rescue mechanisms.....	82
Figure 20. Scheme of the different directionalities of TRCs.....	85
Figure 21. Scheme of R-loop structure.....	85
Figure 22. Schematic representation of RS-focused hypothesis.....	92
Figure 23. Schematic representation of MYC-driven hypothesis.....	93
Figure 24. Scheme of the OE constructs.....	97
Figure 25. Mechanism of action of MZ1.....	98
Figure 26. Mechanism of action of dCBP-1.....	98
Figure 27. Mechanism of action of OMO-103.....	100
Figure 28. MZ1 treatment led to the elimination of BRD4-NUT fusion, and the removal of MZ1 (WO) could restore its expression in NC cells.....	116
Figure 29. MZ1 treatment decreased the presence of the RS marker pRPA S33, but its expression can be restored in WO conditions.....	117
Figure 30. MZ1 treatment can decrease the fork velocity, and it can be restored in WO conditions.....	118
Figure 31. Validation of cell lines expressing inducible forms of GFP, BRD4s, NUT, and BRD4-NUT.....	120
Figure 32. Ectopic expression of BRD4-NUT and NUT moiety of the fusion can increase the expression of RS markers.....	121
Figure 33. Schematic representation of the model (1).....	122
Figure 34. Effects of BRD4-NUT degradation by MZ1 treatment on megadomain formation, reversed upon MZ1 removal.....	123
Figure 35. dCBP-1 degrades p300 and decreases megadomains in NC cells.....	125
Figure 36. dCBP-1 treatment led to the impairment of BRD4-NUT-induced RS in NC cells.....	126

Figure 37. Schematic representation of the model (2).....	127
Figure 38. Transcription is affected by MZ1 treatment and partially restored upon its removal. ....	129
Figure 39. Transcription recovery after the removal of MZ1 was abrogated upon dCBP-1 treatment. ....	130
Figure 40. Transcription modulation alters the BRD4-NUT-induced RS in NC cells. ....	132
Figure 41. Schematic representation of the model (3).....	133
Figure 42. S9.6 staining in NC cells.....	135
Figure 43. p300 and transcription are required for NRD4-NUT-induced R-loops accumulation. ....	136
Figure 44. R-loops are required for BRD4-NUT-induced RS in NC cells. ...	138
Figure 45. Scheme of the proposed model for the molecular mechanism. ....	140
Figure 46. A DDRi-focused drug screening evidenced several sensitive candidates in NC cells. ....	142
Figure 47. IC <sub>50</sub> values of the selected candidate DDRi in NC cells.....	143
Figure 48. Drug candidates induced apoptosis in NC cells. FACS analysis of apoptosis marker. ....	144
Figure 49. NC cells PER624 is HR proficient.....	147
Figure 50. NC cell lines and patient samples demonstrated HR proficiency using RAD51-related assays. ....	148
Figure 51. PER624 xenografts show sensitivity to ATRi and PARPi combinatorial treatment. ....	150
Figure 52. PER403 xenografts show sensitivity to ATRi and PARPi combinatorial treatment. ....	151
Figure 53. NC cells are sensitive to OMO-103 in vitro.....	153
Figure 54. OMO-103 induces differentiation, apoptosis, and cell cycle arrest in NC cells in vitro.....	155

Figure 55. OMO-103 treatment resulted in a downregulation of MYC signatures. ....	157
Figure 56. The combination of OMO-103 and chemotherapy inhibited PER624 xenografts in vivo. ....	159
Figure 57. NC cells are sensitive to lurbinectedin in vitro. ....	161
Figure 58. NC cells are sensitive to irinotecan in vitro. ....	162
Figure 59. BRD4 and MYC roles in nuclear processes. ....	176
Figure 60. Scheme of the potential connection between RS and MYC in NC. ....	178

# TABLE INDEX

Table 1. Comparison of clinical characteristics of two comprehensive studies of NC. ....	39
Table 2. List of acetyl-lysine modifications of histones with roles in DSB signaling and repair. ....	79
Table 3. Information about patient-derived samples.....	96
Table 4. Table of DDRi for the focused screening. ....	99
Table 5. Patient information of paraffin samples. ....	100
Table 6. List of the antibodies used. ....	103
Table 7. List of drugs used in vivo. ....	111

# ACKNOWLEDGEMENTS



Llegando al final de este proceso tan largo solo puedo terminar de confirmar una idea que siempre he tenido bastante clara: la tesis no la hace una sola. Esta tesis está firmada por mí, pero hecha gracias a muchas más personas que han contribuido, de manera más o menos académica, a que haya podido existir.

Antes de nada, quiero dar las gracias a **Sandra Peiró**, que me aceptó en su laboratorio y me dio la oportunidad de embarcarme en el doctorado. Durante su época como capitana del barco aprendí muchísimo. Y hablando de esa época inicial no puedo dejar de mencionar a dos personas que me recibieron con los brazos abiertos desde el primer día. **Gemma**, gracias por tener un ojo siempre en mí sin que nadie te lo hubiera pedido, fuiste el referente que en muchas ocasiones necesité y la persona que me metió en el mundo de la divulgación, y, significando lo que significa eso para a día de hoy, te voy a estar siempre agradecida, amiga. **Marc**, qué te digo, has sido casa y espacio seguro en el laboratorio y en Barcelona en momentos en los que me hacía falta de verdad, me entiendes mucho diciéndote lo justo. Sé que te voy a tener siempre, y tú a mí también.

Después, a media tesis, el grupo dio un giro de 180° y Tian tomó el rumbo. **Tian**, muchas gracias por haber tomado aquella responsabilidad cuando no tenías ninguna intención de ser jefe. Nunca me olvidaré de que, en esos días de mucha incertidumbre, me dijiste que pasase lo que pasase con el grupo, tú te quedarías hasta que yo terminase mi doctorado. Gracias a ti estoy hoy aquí terminando esto, y eso lo recordaré siempre. Y por supuesto, quiero dar las gracias también a **Teresa Macarulla** por habernos permitido hacer todo esto bajo su paraguas, habéis creado entre los dos un equipo increíble, ha sido muy bonito verlo surgir desde cero hasta llegar a lo que se ha convertido.

Y hablando de lo que se ha generado, vaya grupo... Vaya grupo bonito unido, que se cuida y que se quiere. **Mariana**, eres un sol, cuando llegaste con **Nuria** no os disteis cuenta, pero lo llenasteis todo de luz, qué suerte fue. Cuidas en silencio, desde la distancia, sin molestar, pero cuidas mucho y bien y se agradece muchísimo, hermani. **Cheska**, how fortunate that our paths have crossed, I can't help but see a little of myself in you and your intense way of living and feeling. It's not a bad thing. Not at all. Don't ever forget it. **Natalia**, me quedé impresionada desde que te conocí, siempre dispuesta a aprender y a conocer todo lo nuevo que la vida te quiera dar, sin juicio y con muchas ganas. Gracias por recordarme muchas veces, sin darte cuenta, el motivo por el que me metí en esto hace mucho. **Sofía**, qué maravilla la energía que traes cada día, mantén esa fuerza, que es muy buena para ti y muy inspiradora para las demás. **Jess**, qué habría hecho yo sin ti a mi lado todos estos años...

probablemente nada porque no habría encontrado ninguna cosa, no habría sabido solucionar ningún problema y no me habría reído ni la mitad. No te creas que esto se ha acabado, te voy a seguir llamando para preguntarte cosas desde allá donde esté, y para comer croquetas veganas.

Me dejo para el final a mis hijos favoritos, mis alumnos predilectos, dos de las personas más importantes para que esta tesis materialmente salga adelante y dos de las personas que más me han aguantado y acompañado durante esos años. **Iker**, había tenido más estudiantes pero tus ganas de aprender de verdad y tu manera de verme como un referente me despertaron las ganas de serlo. Aprendimos juntos, porque mientras tu aprendías a hacer inmunos yo aprendía a transmitir ciencia y a decidir qué valores quiero inculcar y aportar a las siguientes generaciones. **Joel**, parecía que llegar a la altura de mi relación con Iker no era posible y llegaste tú. Te has comido conmigo la parte más difícil de mi tesis y has trabajado como nadie, sin una queja, sin un paso en falso, y has estado sosteniéndome dentro y fuera del laboratorio como hace un amigo, no un estudiante. Gran parte de esta tesis es gracias a ti, te lo voy a agradecer siempre. Por último, a los que habéis pasado en algún momento por el laboratorio y no os he mencionado específicamente, gracias por todos los ratitos buenos que hayamos podido tener y espero que hayáis tenido una experiencia bonita y os hayáis sentido a gusto. A los que habéis llegado más tarde y no hemos podido coincidir tanto, solo os pido una cosa: cuidad esto que se ha formado, cuidaros mucho, esto no se tiene siempre y vale su peso en oro.

Por supuesto, esta tesis tampoco se habría podido hacer sin la ayuda de personas clave de VHIO. Gracias al laboratorio de **Laura Soucek**, especialmente a ella y a **Jony**, por la confianza en el proyecto, la ayuda y los buenos consejos, y a **Hugo** por ser mi drug dealer de confianza darme todo el omomyc que necesitaba en todo momento. Gracias al Laboratorio de **Lara Nonell**, especialmente a ella y a **Irene Agustí**, por todo el análisis bioinformático y por estar disponibles siempre que las he necesitado. Gracias al laboratorio de **Violeta Serra**, en especial a **Cristina Molina** y **Alba Llop** por los análisis de RAD51 en pacientes, a **Heura** por los experimentos de DNA fibers, y a **Olga** y a **Marta** por acogerme en el animalario, guiarme y ser un referente de conocimiento cuando me hacía falta uno. También quiero dar las gracias a **Irene Braña** por ser un enlace fundamental con la clínica y con los pacientes y sus muestras, así como darles las gracias a los **pacientes** que han cedido sus muestras para que podamos intentar avanzar en el conocimiento de esta enfermedad tan horrible hoy en día. Por último, como seres importantísimos en el desarrollo de esta tesis, quiero dar las gracias a los **ratones** involucrados en los experimentos. No tengo claro con qué

derecho he hecho esto, creo que me supondrá muchos más años de reflexión todavía, pero lo que deseo de todo corazón es que, sea o no justificable, todos los experimentos con esos ratones sirvan para algo bueno.

También quiero mirar un segundo atrás y dar las gracias al laboratorio que me terminó de despertar el gusanillo científico, gracias **SNAILS** por acogerme tan bien, enseñarme tanto y hacerme tan agradable el aterrizaje en Barcelona. Sobre todo, gracias a **Héctor** por ser una suerte de mentor y ahora un buen amigo más allá de la ciencia, y gracias a **Jordi, Marina, Rubén, Aida, Guillem, Bea, Raúl** y todos los que estuvisteis ahí en esa época tan bonita.

Como la tesis y la ciencia van más allá de los apoyos estrictamente científicos, no quiero dejar de lado a todas las personas de VHIO que han sido un apoyo para mí. **Cate, Paula**, me siento muy afortunada de haber compartido forzosamente el laboratorio con vosotras en diferentes momentos y que el resultado sea haber acabado teniéndooos tan cerquita. **Marta, Alex, Paula Carrillo, Berta** y toda la gente de **GreenVHIO**, me hace muy feliz encontrarme a gente con ganas de mejorar un poquito el mundo en el que vive y hacerlo a vuestro lado, sacando tiempo que no tenemos de nuestros días a días porque consideramos que hay cosas que son más importantes, ha sido muy bonito. **Bianca y todo el equipo de comunicación**, gracias por acogerme como a una más desde el primer día y por permitirme compaginar mi actividad investigadora con la comunicadora, que cada vez estoy disfrutando más. Me muero de ganas de ver hasta donde llegamos con este nuevo proyecto. **Andrea, Íñigo, Iris, Almudena, Pablo, Andreu, María, Caye, Laura, Ari, Fabio, Agus, Enrique, Olivia** y los que me esté dejando (no me lo tengáis en cuenta, sabéis como soy...), gracias por haber llenado el hueco que supone mudarse a 600km de tu familia y tus amigos de siempre. Gracias por estar siempre dispuesto/as a hacer planes divertidos, diferentes, llenando los sábados de amigos y los domingos de familia. Gracias también por acudir a un Julito's cuando hace falta desahogar, porque entendéis lo que es trabajar en esto y no hace falta explicar demasiado.

Y por supuesto, mención especial para **Ester, Joanna y mis Saras**, agradeceros a vosotras lo que habéis hecho para que termine esta tesis ocuparía otra tesis, así que os lo digo en otro momento con una cervecita en la mano. **Ester**, qué feliz me hace dar con gente tan genuinamente buena. Tener una amiga que cuida tanto y tan bien, y a la vez es tan divertida no es una cosa que pase todos los días, te quiero siempre en mi equipo hermani. **Joanna**, igual el mundo ha tenido que ponerte delante de mi tres veces, pero ya no te voy a soltar nunca, te lo prometo, eres una suerte, y tú y **Óscar** sois

familia para mí. **Sara Arce**, ojalá todo el mundo pudiera tener una Sara Arce a la que llamar a cualquier hora por cualquier motivo con la certeza de que, si está en su mano, va a estar ahí para ti sea lo que sea. **Sara Belón**, qué bonito espacio seguro hemos generado para ser, equivocarnos, cambiar, volver a ser, volver a cambiar, y sobre todo cuidarnos. Chicas, de corazón, mil gracias, os quiero muchísimo.

También, quiero dar las gracias a mis amigos de fuera del trabajo, por haber entendido, o por lo menos respetado y aceptado, que ya es mucho, mis idas y venidas, mis épocas de desaparición durante este proceso, y haberme acogido con los brazos abiertos cuando sí estaba en Madrid, cuando sí tenía tiempo, cuando sí estaba disponible.

A **Los de atrás**, ese grupo idílico de amigos muy diferentes que se conocen en primero de carrera y se quieren, respetan, divierten y cuidan y siguen siendo un grupo increíble de amigos 10 años después, con el que todo el mundo sueña y pocos tienen. No estoy exagerando si os digo que sois lo que hace que valga la pena haber pasado por esa carrera. Hemos creado una red fuerte de apoyo y sois grandes referentes para mí, todos. De cada uno saco algo que me ha ayudado a llegar a ser la científica que soy hoy, aunque no lo creáis. **Laurita y Manu**, siempre seréis casa, siempre. **Guerre**, si tu respuesta es igual que la mía a mí me vale como buena, para todo en la vida y para siempre. **Santi**, qué bonito que hayamos caído en el mismo sitio y tenerte tan cerquita, siento que nos hemos redescubierto y me hace muy feliz. Os quiero mucho a todos, de verdad.

A mis amigos *de toda la vida*, los de Valdemorillo, con los que he crecido y los que han aparecido por el camino. **Cris, Carol, Alba, Jose, Alfredo, Diana**, gracias por seguir ahí muchos años y muchos kilómetros después, dispuestos a ponernos al día cada vez que vuelvo al pueblo. La sensación de volver a casa no la pierdo por muchos años que pase fuera. Necesito mencionar especialmente a **Cris y Carol**, por ser la amistad más sólida e inquebrantable que se puede tener, toda una vida, hermanis, y lo que nos queda. Qué ganas de celebrar este éxito con vosotras.

Para terminar, quiero darle las gracias a mi familia, por haberme ayudado a convertirme en la persona que soy, capaz de haber llegado hasta aquí. **Abuela**, gracias por ver sólo cosas buenas en mí y recordarme siempre que lo necesito que, a través de tus ojos, soy la persona más capaz del mundo y te voy a tener a mi lado siempre. También hago esto, en parte, por ti y por todas las mujeres con un increíble potencial a las que les habría encantado poder conquistar el mundo laboral como yo lo estoy haciendo. **María**, la prima

menos prima y más hermana que se puede tener. Has sido un espejo en el que mirarme desde que tengo uso de razón, un referente de persona empoderada, inteligente, divertida y cuidadora en el que me he mirado muchos años y con el que ahora disfruto de celebrar cada éxito de una o de otra. **Lucía**, toda una vida juntas, mano a mano creciendo física y emocionalmente. Gracias por hacer mi vida más divertida y por hacerme fácil estar lejos estos años, porque sé que por allí está todo bajo control. Gracias por estar siempre en mi equipo y por encargarte de pensar tú uno de cada dos días si hace falta. **Mamá**, el mejor ejemplo lo he tenido siempre en casa, una mujer comprometida, trabajadora y con un corazón enorme que se desvive por los demás. **Papá**, otro gran ejemplo de que se puede compaginar la excelencia científica con invertir toda tu energía en dejar una pequeña huella en el mundo que lo haga un poquito mejor. Entre los dos me habéis hecho fuerte, sensible y segura y habéis eliminado por completo de mi cabeza la idea de que no tengo la capacidad de volar alto. Os quiero mucho.

Y finalmente, **Javi**, no sé por dónde empezar. Has llegado en un momento complicado y no es que hayas estado a la altura, es que has roto toda expectativa. Gracias por estar incondicionalmente, por escuchar, por no juzgar, por acompañar y por ayudarme a llegar hasta aquí. Sola habría podido, pero contigo ha sido mucho más fácil, divertido y feliz. Eres una suerte titi. A partir de ahora viene lo mejor. Te quiero muchísimo.

# ABBREVIATIONS



---

**A**

ACIN1 · *Apoptotic chromatin condensation inducer 1*  
ActD · *Actinomycin D*  
AD1 · *Acidic transcriptional activation domain 1*  
AD2 · *Acidic transcriptional activation domain 2*  
AML · *Acute Myeloid Leukemia*  
ANOVA · *Analysis of variance*  
ATAT1 ·  *$\alpha$ -tubulin N-acetyltransferase 1*  
ATM · *Ataxia telangiectasia mutated*  
ATR · *Ataxia telangiectasia and Rad3-related*  
ATRi · *ATR inhibitor*  
ATRIP · *ATR-interacting protein*

---

**B**

B-AALs · *B-cell acute lymphoblastic leukemias*  
BD · *Bromodomain*  
BER · *Base excision repair*  
BET · *Bromodomain and extra-terminal domain*  
BETi · *BET inhibitors*  
BFP · *Blue fluorescent protein*  
BRD2 · *Bromodomain containing protein 2*  
BRD3 · *Bromodomain containing protein 3*  
BRD4 · *Bromodomain containing protein 4*  
BRD4l · *BRD4 long*  
BRD4s · *BRD4 short*  
BRD9 · *Bromodomain containing protein 9*  
BRDt · *Bromodomain testis-associated protein*  
BSA · *Bovine serum albumin*

---

**C**

CEEA · *Ethical committee for the use of experimental animals*  
CIC · *Capicua transcriptional repressor*  
CTD · *Carboxi-terminal domain*

---

**Ch**

ChIP · *Chromatin immunoprecipitation*  
CHK1 · *Checkpoint kinase 1*

---

**D**

DAPI · *4',6-Diamidino-2-phenylindole*  
DDR · *DNA damage response*  
DDRi · *DDR inhibitors*  
DDT · *DNA damage tolerance*  
DEGs · *Differentially expressed genes*  
DMEM · *Dulbecco's modified Eagle's medium*  
DNA-PK · *DNA-Dependent Protein Kinase*  
DNMTs · *DNA methyltransferases*  
DRIP · *DNA-RNA immunoprecipitation*  
DSB · *double-strand break*  
dsDNA · *double-strand DNA*

---

**E**

ecDNA · *Extrachromosomal DNA*  
ECL · *Enhanced chemiluminescence*  
ET · *extra-terminal domain*  
EU · *5-Ethynyl uridine*

---

**F**

FBS · *Fetal bovine serum*  
FDR · *False discovery rate*  
FISH · *Fluorescence in situ Hybridization*

---

**G**

GEMM · *Genetically engineered mouse model*  
GFP · *Green fluorescent protein*  
GSEA · *Gene set enrichment analysis*

---

## **H**

HATs · *Histone acetyltransferases*  
HDAC · *Histone deacetylase*  
HR · *Homologous recombination*  
HRD · *HR deficient*  
HRP · *Horseradish peroxidase, HR proficient*

---

## **I**

IC<sub>50</sub> · *Half-maximal inhibitory concentration*  
IF · *Immunofluorescence*  
IHC · *Immunohistochemistry*  
IRBs · *Institutional review boards*

---

## **K**

KO · *Knock out*

---

## **L**

LLPS · *liquid-liquid phase separation*

---

## **M**

MAD · *MAX dimerization gene family*  
MCM · *Minichromosome maintenance helicase complex*  
MMR · *Mismatch repair*  
MSigDB · *Molecular signature database*  
MTT · *3-(4,5-dimethylthiazol-2-yl)-2,5-diphenyltetrazolium bromide*

---

## **N**

NAD · *Nicotinamide adenine dinucleotide*  
NC · *NUT Carcinoma*  
NER · *Nucleotide excision repair*  
NES · *Nuclear export signal*  
NGS · *Next-generation sequencing*  
NHEJ · *Non-Homologous end joining*  
NLS · *Nuclear localization sequence*

NMC · *NUT midline Carcinoma*  
NRNs · *NUT-rearranged neoplasms*  
NSCLC · *Non-small cell lung cancer*  
NSD3 · *Nuclear receptor binding SET domain protein 3*  
NUT · *NUT Midline Carcinoma Family Member 1 protein*

---

## **O**

OE · *Overexpression*  
ORR · *Objective response rate*  
OS · *Overall survival*

---

## **P**

p300 · *E1A binding protein 300kDa*  
PAR · *poly(ADP-ribose)*  
PARP · *poly(ADP-ribose) protein*  
PARPis · *PARP inhibitors*  
PBS · *Phosphate-buffered saline*  
pCHK1 · *phosphorylated CHK1*  
PDX · *Patient-derived xenograft*  
PFA · *Paraformaldehyde*  
PFS · *Progression-free survival*  
PRC2 · *Polycomb repressive complex 2*  
PROTAC · *Proteolysis Targeted Chimeras*  
pRPA S33 · *phosphorylated RPA at serine 33*  
P-TEFb · *Positive transcription elongation factor B*  
PTMs · *Post-translational modifications*

---

## **Q**

qPCR · *quantitative Polymerase chain reaction*

---

## **R**

replication protein A · *Replication protein A*  
RNH1 · *RNase H1*  
ROS · *Reactive oxygen species*  
RPMI · *Roswell Park Memorial Institute*  
RS · *Replication stress*

RT · *Room temperature*

---

## **S**

SCLC · *Small cell lung cancer*  
SE · *Super-enhancer*  
SNF · *SWItch/Sucrose Non-Fermentable*  
SSBs · *Single-strand breaks*  
ssDNA · *Single-strand DNA*

---

## **T**

TADs · *Topologically associated domains, Transactivation domains*  
TEAD · *Transcriptional enhancer domain*  
TGS · *Tris-glycine-SDS buffer*  
TLS · *Translesion synthesis*  
TMB · *Tumor mutational burden*  
TMM · *Trimmed mean method*  
TNBC · *Triple-negative breast cancer*  
TRCs · *Transcription-replication conflicts*  
TRE · *Tet response element*  
TS · *Template switching*

---

## **V**

VHIO · *Vall d'Hebron Institute of oncology*  
VHIR · *Vall d'Hebron Institute of research*

---

## **W**

WB · *Western blot*  
WO · *Washout*  
WT · *Wildtype*

# SUMMARY



NUT Carcinoma (NC) is a rare and aggressive cancer lacking effective treatment, with a dismal prognosis of less than seven months after diagnosis. It is characterized by chromosomal rearrangements that involve the testis-specific *NUT* gene and genes encoding for epigenetic regulators or transcription factors, mainly BRD4. Of note, it has been shown that NUT fusion proteins are associated with epigenetic and transcriptional changes that promote cell proliferation while impeding cell differentiation. Several genes, including *P63*, *SOX2*, and *MYC*, have been identified as being modulated by NUT fusion proteins. This study aims to investigate the molecular mechanism underlying NC oncogenesis and identify targetable vulnerabilities that could be transferred to the clinical setting. We found that BRD4-NUT is associated with increased replication stress (RS) in NC cells. This leads to an addiction of NC cells to RS response pathways, such as ATR and PARP pathways. Targeting these pathways using specific inhibitors yields promising outcomes *in vitro* and *in vivo*, both as monotherapy and in combination setting. Furthermore, we also found that NC cells are sensitive to the MYC inhibitor OMO-103, and this inhibitor could induce apoptosis, cell cycle arrest, and differentiation in NC cells. Of note, treatment with OMO-103 *in vivo*, particularly in combination with chemotherapy, significantly reduced tumor growth. Finally, the preclinical exploration unveiled notable sensitivity of lurbinectedin and irinotecan in NC cell lines. Taken together, this study advances our understanding of the molecular mechanisms underlying NC and presents promising therapeutic avenues for this challenging and aggressive cancer type.

# RESUMEN



NUT Carcinoma (NC) es un cáncer muy infrecuente y agresivo que carece de tratamiento eficaz, con un pronóstico desalentador de menos de siete meses tras el diagnóstico. Se caracteriza por reordenamientos cromosómicos que implican al gen *NUT*, específicamente expresado en testículos en condiciones normales, y a genes que codifican para reguladores epigenéticos o factores de transcripción, principalmente BRD4. Se ha demostrado que las proteínas de fusión NUT están asociadas a cambios epigenéticos y transcripcionales que promueven la proliferación celular al tiempo que impiden la diferenciación celular en NC. Algunos genes como *P63*, *SOX2* y *MYC*, se han identificado como modulados por estas proteínas de fusión. El objetivo de este estudio es investigar el mecanismo molecular que subyace a la oncogénesis de NC e identificar vulnerabilidades abordables terapéuticamente que puedan trasladarse al ámbito clínico. Durante este estudio, hemos descubierto que BRD4-NUT se asocia con un aumento de estrés replicativo (RS) en las células de NC. Esto confiere una adicción de estas células a las vías de respuesta de RS, como las vías de ATR y PARP. El ataque a estas vías utilizando inhibidores específicos ha demostrado resultados prometedores *in vitro* e *in vivo*, tanto en monoterapia como en combinación. Además, también hemos descubierto que las células de NC son sensibles al inhibidor de MYC OMO-103, y que este inhibidor podría inducir apoptosis, arresto del ciclo celular y diferenciación en las células de NC. Cabe destacar que el tratamiento con OMO-103 *in vivo*, especialmente en combinación con quimioterapia, ha demostrado reducir significativamente el crecimiento tumoral. Por último, una exploración preclínica ha revelado una notable sensibilidad de lurbinectedina e irinotecán en líneas celulares de NC. En conjunto, este estudio permite avanzar en el conocimiento de los mecanismos moleculares subyacentes al NC y presenta prometedoras vías terapéuticas para este tipo de cáncer tan difícil y agresivo.

# INTRODUCTION



# 1. NUT CARCINOMA

## 1.1 Definition and epidemiology

NUT Carcinoma (NC) is a rare, aggressive, and recently described cancer type. The first cases were reported in 1991 in two young patients with poorly differentiated carcinomas with a thymic origin that were refractory to chemotherapy<sup>1,2</sup>. Both patients had a chromosomal rearrangement resulting in the translocation t(15;19)(q13, p13.1). This caused the formation of a fusion between the gene that encodes the NUT Midline Carcinoma Family Member 1 protein (NUTM1 or NUT), which is specifically expressed in the testis, and the gene that encodes the Bromodomain-containing protein 4 (BRD4), a ubiquitously expressed epigenetic factor. However, it was only in 2003, after identifying accumulative cases of aggressive and poorly differentiated carcinomas with NUT-involved fusions, that French *et al.* defined and described this new cancer type, namely NUT Carcinoma<sup>3</sup>. To date, NC is one of the first and most aggressive cancer types defined by a gene fusion<sup>4</sup>.

### 1.1.1 Epidemiology of NC

Although the number of reported patients with NC is scarce due to its rarity and the need for more awareness about this disease among clinicians, a few comprehensive studies have been conducted to obtain clinical characteristics of this fatal disease. Notably, the studies by Chau *et al.*<sup>5</sup> and Girighad *et al.*<sup>6</sup> included 141 and 119 patients with NC respectively, being the two most significant cohorts published to date. Specifically, Chau *et al.* performed a retrospective study using the cohort from the International NUT Carcinoma Registry ([www.NMCRRegistry.org](http://www.NMCRRegistry.org)), an international registry enabling the collection of NC clinical data and tissue to facilitate translational research. In parallel, Girighad *et al.* conducted a systematic review and gathered the published data until 2018. A comparison of the clinical characteristics between the two studies is presented in **Table 1**.

**Table 1. Comparison of clinical characteristics of two comprehensive studies of NC.**

		<b>Chau <i>et al.</i></b>	<b>Giridhar <i>et al.</i></b>
<b>Sample size</b>		141	119
<b>Source</b>		NMC registry	Systematic bibliographic review
<b>Age</b>	<b>Range</b>	0-80 <18 years 47/124 (38%) >18 years 77/124 (62%) Unknown 17	0-68 <13 years 19 (15.9%) 13-20 years 27 (22.8%) 21-30 years 33 (27.7%) 31-40 years 21 (17.6%) 41-50 years 7 (5.9%) 51-60 years 5 (4.2%) 61-70 years 7 (5.9%)
	<b>Mean</b>	23.6	23
<b>Sex</b>	<b>Women</b>	74/141 (52%)	58/118 (49%)
	<b>Men</b>	67/141 (48%)	60/118 (51%)
<b>Location</b>	<b>Thoracic</b>	71/140 (51%)	73/119 (61%)
	<b>Head and neck</b>	58/140 (41%)	40/119 (34%)
	<b>Other</b>	11/140 (8%)	6/119 (5%)
<b>Overall survival</b>		6.5 months	5 months
<b>NUT fusion partner</b>	<b>BRD4</b>	99/127 (78%)	84/102 (82%)
	<b>BRD3</b>	19/127 (15%)	5/102 (5%)
	<b>other</b>	9/127 (7%)	13/103 (13%)
<b>Metastatic disease</b>	<b>Yes</b>	71/113 (63%)	37/93 (40%)
	<b>No</b>	42/113 (37)	56/93 (60%)
<b>Year of publication</b>		2019	2018

Interestingly, both studies derived similar findings. First, NC can occur at any age, ranging from 0 to 80 years, and in the last years, new reports have been published describing patients up to 84 years old<sup>7</sup>. It preferentially affects adolescents and young adults. The mean age of diagnosis in both studies is approximately 23 years, and most patients were diagnosed between the second and the third decade of life. Secondly, the disease can affect men and women without significant enrichment in any gender. Third, both studies suggested that the preferred anatomical location of NC is the thorax, mainly lung and mediastinum, followed by the head and neck regions. This agrees with previous reports with smaller cohorts<sup>8</sup>. Interestingly, as NC was initially found only in “midline organs,” it was originally named “NUT Midline Carcinoma” (NMC)<sup>3</sup>. However, recent evidence has shown that NC can arise

in various locations. There are cases reported in the thymus, bladder<sup>9,10</sup>, thyroid<sup>1,2</sup>, liver/pancreas<sup>11</sup>, adrenal gland<sup>8,12</sup>, kidney, soft tissue, stomach, brain<sup>13</sup> or bone<sup>9,14</sup> among others. Thus, there is a consensus on naming it NUT Carcinoma.

### 1.1.2 Prevalence and prognosis of NC

Unfortunately, the accurate prevalence of NC is unknown, and no significant risk factor has been associated with it so far. Using next-generation sequencing (NGS) screenings in solid tumors, researchers could estimate an annual incidence of approximately 1080-3600 NC cases in the United States<sup>15</sup>. However, another study presented at the ASCO 2023 annual meeting claimed only 40-50 yearly diagnoses of NC in the same country<sup>16</sup>. Several reasons could explain this discrepancy.

It is believed that the lack of awareness of NC among clinicians is a significant reason for late or misdiagnosis of the disease<sup>4</sup>. Indeed, several retrospective studies reported that 1% (4/362) of poorly differentiated or undifferentiated head and neck carcinomas<sup>17</sup>, 3.5% (4/114) of poorly differentiated carcinomas or unclassified mediastinal<sup>18</sup>, 2% (3/151) of primary sinonasal carcinomas, especially 15% of the undifferentiated subtype (2/13)<sup>19</sup>, and 7% of poorly/undifferentiated carcinomas in children and young adults<sup>10</sup> were NUT-positive. None of them were diagnosed as NC. Thus, a standardized NC screening protocol must be implemented in clinical practice.

It is worth noting that raising awareness of this disease has contributed to more NC case identification. For example, a study demonstrated that although only 17 NC patients were diagnosed in the head and neck region from 1993 to 2011, twenty-two cases (130% increase) were diagnosed from 2012 to 2014<sup>5</sup>. These data suggested that due to the deepened understanding and heightened awareness of the disease, there has been a significant rise in the number of NC diagnoses in the last two years compared to the past 20 years. In line with this, although 63 NC patients were registered in the NMC registry in 2012<sup>8</sup>, the number has increased to 141 patients in 2017, indicating a growth of 124% in the last 5 years compared to the previous 20 years<sup>5</sup>.

Patients diagnosed with NC have a poor prognosis, with a median overall survival of 5-6.5 months (**Table 1**). The 1-year and 5-year survival rates are 24.99% and 7.09%, respectively<sup>6</sup>. The poor prognosis of NC patients is due to aggressive tumors, late diagnosis, misdiagnosis, and lack of effective treatments<sup>4</sup>. Interestingly, Chau *et al.* proposed a risk classification system in which thoracic primary NC tumors are associated with the worst prognosis, followed by non-thoracic tumors harboring BRD4-NUT fusion and, finally, non-thoracic tumors harboring a non-BRD4 fusion partner with a relatively higher overall survival (OS)<sup>5</sup> (**Figure 1**).

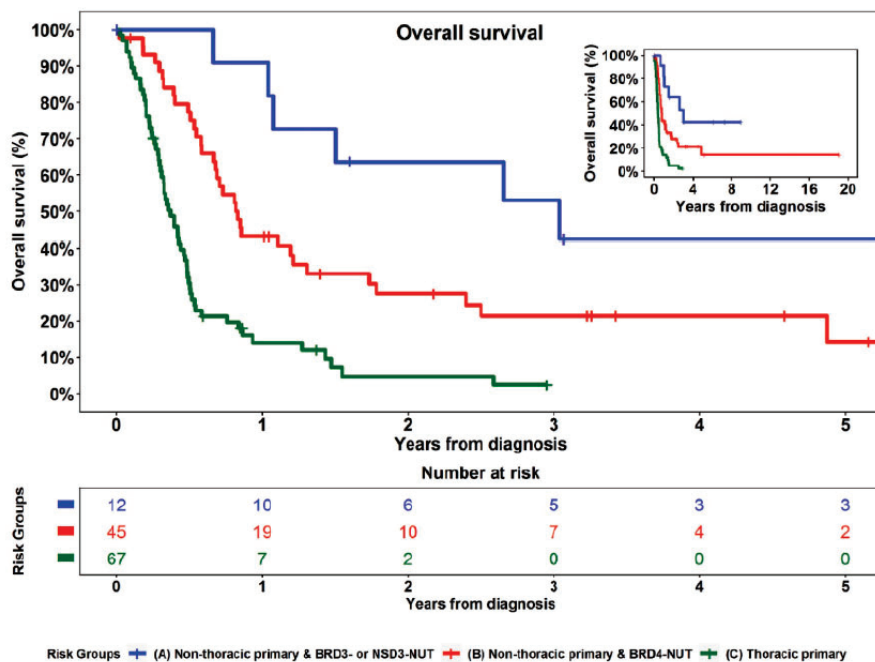


**Figure 1. Overall survival of three subgroups of NC patients.**

The figure shows the overall survival (above) and number of patients at risk (below) of three subgroups of NC patients. Image from Chau *et al.*<sup>5</sup>

Taken together, NC is a rare disease with a poor prognosis. We must increase awareness of this disease and implement NC screening as a routine part of clinical practice. In the following section, we will delve into the molecular basis of NC.

## 1.2 Molecular basis of NUT Carcinoma oncogenesis

NC is defined by a chromosomal rearrangement involving the *NUT* gene<sup>3</sup>. The physiological function of the *NUT* gene and the corresponding NUT protein still need further investigation. Nevertheless, Shiota *et al.* recently discovered that NUT is an unstructured protein specifically expressed in the testis with a unique role in post-meiotic spermatogenic cells<sup>20</sup>. Under normal conditions, it promotes histone H4 hyperacetylation through the interaction with the acetyltransferase E1A binding protein 300kDa (p300). Subsequently, the acetylated chromatin could be recognized and bound by Bromodomain Testis-Associated protein (BRDt), a testis-specific member of the Bromodomain and extra-terminal domain (BET) family. This process is responsible for histone-to-protamine removal and is indispensable for the completion of spermatogenesis<sup>20</sup>.

### 1.2.1 NUT fusion partners in NC

In NC, the *NUT* gene is fused to genes that encode for epigenetic regulators or transcription factors due to chromosomal translocations. As shown in **Table 1**, in 80% of the described cases, NUT is fused to BRD4. However, in 5-15% of cases, the fusion partner is bromodomain-containing protein 3 (BRD3). Other fusion partners, such as nuclear receptor binding SET domain protein 3 (NSD3) and zinc finger-containing proteins like ZNF532 and ZNF592, have also been reported to a lesser extent<sup>5,21,22</sup>. A recent case has been described where bromodomain-containing protein 2 (BRD2) can also act as a fusion partner of NUT in NC<sup>23</sup>.

The fusion genes found in NC involved almost the entire coding region of *NUT*, including its two acidic transcriptional activation domains (AD1 and AD2), a nuclear localization sequence (NLS), and a nuclear export signal (NES). Regarding the NUT fusion partner, in the case of the BRD4-NUT fusion, the BRD4 part of the fusion corresponds to the short isoform of BRD4, including two bromodomains (BD 1 and 2), the extra-terminal (ET) domain, and a bipartite NLS. Notably, the BRD4 moiety included in the fusion lacks the carboxy-terminal domain (CTD), a region restricted to the BRD4 long isoform that can interact with the positive transcription elongation factor B (P-TEFb). In the case of BRD3 as a fusion partner (BRD3-NUT), the fusion protein

includes BRD3's BD1, BD2, ET, and NLS domains, similar to BRD4-NUT fusion. In the case of NSD3, the fusion protein contains only one of the two Proline-Tryptophan-Tryptophan-Proline motif (PWWP) domains (protein interaction domains). Moreover, when it comes to the zinc finger-containing proteins as fusion partners, the length and the number of zinc finger domains included in the fusion proteins differ<sup>24</sup> (**Figure 2**).

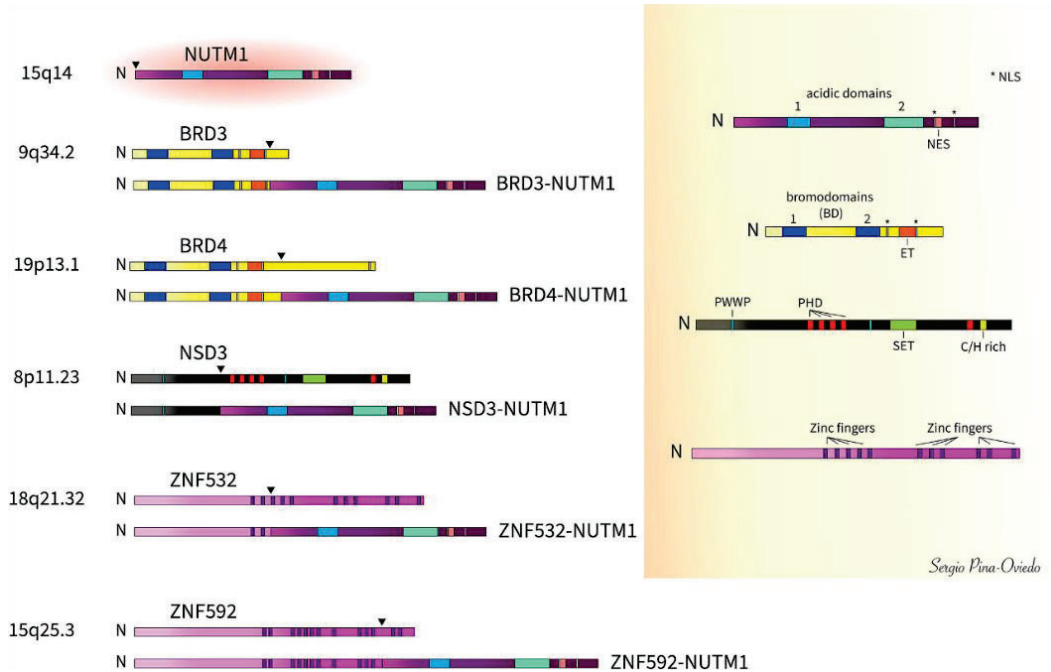


**Figure 2. Schematic representation of NUT fusion proteins and WT counterparts.**

N: amino- or N-terminal; NLS: nuclear localization signal; NES: nuclear export signal; BD: bromodomains (BD1 and BD2); ET: extra-terminal domain; PWWP: Proline-Tryptophan-Tryptophan-Proline domain; PHD: plant homeo-domain-type zinc-finger motifs; SET: Su(var)3-9, Enhancer-of-zeste and Trithorax (SET) domain; C/H rich: SET-associated Cys-His-rich (SAC) domain. Image from Moreno *et al.*<sup>24</sup>

### 1.2.2 Molecular mechanism behind NUT-fusion in NC.

Our understanding of the molecular mechanism behind the oncogenesis of NC and fusion protein is currently limited. However, several research groups have explored the effects of the fusion protein in cell models, with a particular focus on BRD4-NUT fusion as it is the most common fusion found in patients. As we will discuss later, the fusion protein binds to existing acetylated regions in the chromatin through the bromodomains of the BRD4 portion.

Subsequently, the NUT moiety can recruit acetyltransferase enzyme p300, which then acetylates the surrounding chromatin. Notably, the newly acetylated residues can be recognized by the BRD4 component of the BRD4-NUT protein, which in turn recruits more p300, leading to more acetylation and generating a positive feedback loop of chromatin acetylation, resulting in the formation of large hyperacetylated chromatin regions known as 'megadomains'<sup>25,26</sup> (**Figure 3**). This event promotes a redistribution of acetylation on the chromatin and ultimately leads to a significant modification of the transcriptional landscape in NC cells, increasing the expression of pro-proliferative genes and decreasing the expression of pro-differentiation genes.

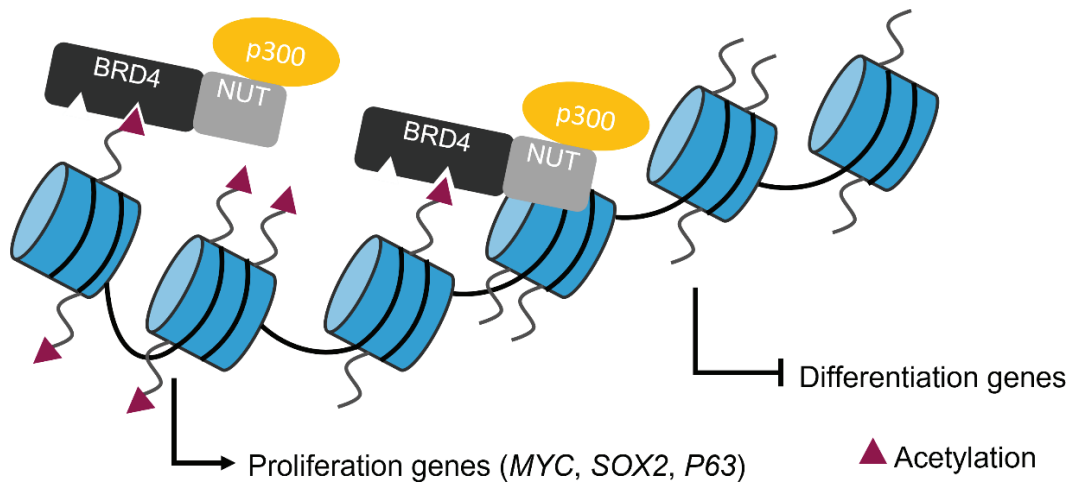


**Figure 3. Scheme of BRD4-NUT-dependent megadomains of acetylation.**

Of note, although the aforementioned mechanism of action described the oncogenic role of BRD4-NUT fusion protein through megadomain formation, this can be potentially extrapolated to the rest of NUT fusion partners. The interaction of NUT with BRD4 is necessary to bring p300 to the chromatin and generate megadomains of acetylated chromatin. This event can occur either directly (BRD4-NUT fusion) or indirectly, as the rest of the described fusion partners (ZNF532, NSD3, or BRD3) have been demonstrated to be interactors of BRD4 and thus the BRD4-NUT complex<sup>26</sup> (**Figure 4**). This will be explained in detail in the following sections.

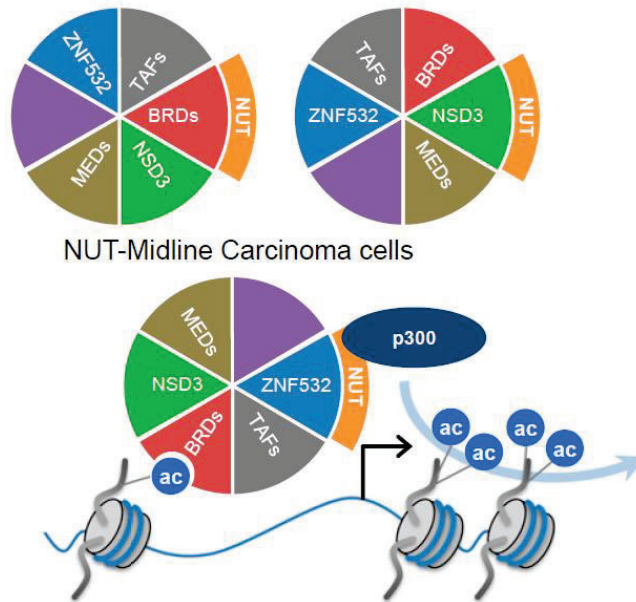


**Figure 4. Schematic representation of NUT fusion interaction complex.**

MEDs: mediator complex subunits; TAFs: TATA box-binding protein-associated factors. Image from Alekseyenko *et al.*<sup>26</sup>

### 1.2.3 Megadomains of histone acetylation in NC

Megadomains are regions of the chromatin that can extend up to 2Mb. Although the size and composition are consistent among cell lines, the location of these acetylated regions is highly variable<sup>27</sup>. However, the fusion consistently inhibits cell differentiation and stimulates cell growth across NC models<sup>28,29</sup>. Interestingly, while only a few genes are consistently found within the megadomains, there are still a small number of cancer-related genes that have been identified to be consistently encompassed within the megadomains, including *MYC*<sup>29,30</sup>, *SOX2*<sup>31</sup>, and *P63*<sup>27</sup>.

Taken together, the NUT fusion protein promotes oncogenesis through the remodeling of the epigenetic landscape of NC cells. The fusion, together with p300, generates megadomains of acetylation in the chromatin that promote the expression of pro-proliferative genes (included inside the megadomains) and the silencing of differentiation genes (excluded from the megadomains).

#### 1.2.4 Cells of origin of NC

NC cell origin is unknown, although its epithelial origin is suspected. There is a consensus that the preexisting epigenetic state of original cells is highly determinant in the construction of megadomains and their location. Megadomain's location in the chromatin is, at least in part, determined by several initial seed sites of acetylation along the chromatin<sup>30</sup>. As the epigenetic landscape of a cell is highly lineage-specific, the original cell state and identity shape the formation, location, and pattern of megadomains of acetylation<sup>32</sup>. Thus, the inconsistency among megadomain location patterns across patients may be determined by specific cell contexts.

#### 1.2.5 Fusion protein as a driver factor in NC disease.

For many years, the study of NC's cell of origin and the transformation capacity of BRD4-NUT fusion has been limited by the highly toxic effect of the BRD4-NUT overexpression in most non-NC cell lines. Probably, at least in part, because of the identity of the used cell lines (and thus their epigenetic landscape), and the level of ectopic expression of BRD4-NUT fusion protein<sup>15,33</sup>.

However, in 2023, two studies successfully generated genetically engineered mouse models for NUT Carcinoma. One of them overexpressed Brd4-Nut fusion protein under the regulation of the endogenous Brd4 promoter upon tamoxifen induction of Sox2-driven Cre<sup>15</sup>. In the other case, they genetically modified the appropriate introns of Brd4 and Nut in mice to allow the stochastic induction of the translocation<sup>34</sup>. Both models proved the BRD4-NUT driver capacity in NC oncogenesis, as the ectopic expression of the fusion protein could induce aggressive NC-like tumors that phenocopied NC patient sample characteristics. Indeed, these murine tumors were poorly differentiated squamous carcinomas, and the presence of megadomains and high expression of Myc and P63 could be observed. In these mouse models, tumors arise from the epithelial progenitor cells<sup>34</sup> or squamous epithelium<sup>15</sup>.

Furthermore, the existence of these mouse models will enable the study of cell-extrinsic mechanisms of NC generation, progression, and metastasis, such as the immune system.

## 1.3 Diagnosis

### 1.3.1 Clinical symptoms and histopathologic features

Clinical symptoms are frequently absent in early stages, and the variability of location intrinsically implies a high variability and a lack of consistency that makes its diagnosis difficult. Clinical symptoms, when developed, often include fatigue and weight loss. Despite the high variability in location, the most common symptoms include painless lumps, pain, persistent cough, shortness of breath, and nasal congestion or obstruction<sup>4</sup>.

Although no morphological features are unique to NC, several histological characteristics are associated with the disease and can be used as a clinical criterion. NCs are poorly differentiated squamous carcinomas that, in approximately one-third of cases, show focal squamous differentiation. In addition, NC samples display monomorphic round-oval cells with scant-to-moderate amounts of pink-to-clear cytoplasm, demonstrate frequent mitoses, and show single-cell or regional necrosis. They also present a nuclear diffuse staining and speckled appearance. Furthermore, although there is an occasional lymphocyte infiltration, the presence of neutrophils infiltrated in tumor samples is commonly observed<sup>35,36</sup>.

### 1.3.2 NUT detection to diagnose NC

NC is a type of tumor that relies on the identification of the fusion for its diagnosis. As a result, various techniques have been developed for NC diagnosis involving the detection of NUT, due to its testis-restricted expression under normal conditions. These diagnostic techniques include the detection of NUT through immunohistochemistry (IHC), or the use of Fluorescence in situ Hybridization (FISH), quantitative Polymerase Chain Reaction (qPCR), and NGS to identify the presence of NUT fusion and its partner. Currently, in cases of poorly differentiated non-cutaneous carcinomas that exhibit a monomorphic appearance, with or without local squamous differentiation, it is recommended to consider performing a NUT staining test by IHC for differential diagnosis of NC<sup>35,36</sup>.

In 2009, Haack *et al.* reported the NUT IHC protocol using a NUT-specific antibody, which was found to have 87% sensitivity and 100% specificity for

NC diagnosis. Interestingly, although germ cells express NUT, they were proven to do it to a lesser extent<sup>9</sup>. It is worth noting that this NUT IHC protocol has been validated retrospectively by other researchers, becoming a valuable tool for clinicians in the early and accurate diagnosis of the disease<sup>37</sup> (**Figure 5**).

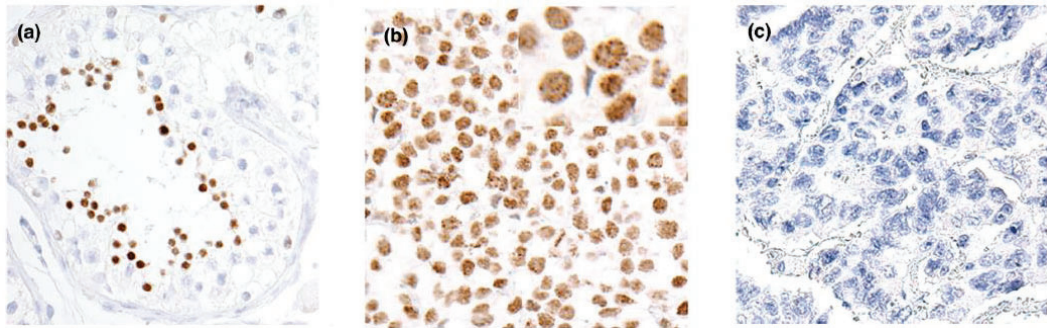


**Figure 5. Diagnosis of NC by NUT immunohistochemistry.**

**A** NUT IHC in seminiferous tubules of adult testes staining post-meiotic spermatids. **B** NUT IHC in the NC sample shows diffuse nuclear staining, often with a speckled pattern. **C** NUT IHC in the non-NC sample reveals no staining. Image adapted from French *et al.*<sup>35</sup>

It is important to note that, while IHC is currently considered the gold standard for NC diagnosis, this technique cannot discriminate the partner of the NUT fusion. Identification of the fusion partner is relevant, as it has been shown that "non-BRD4" NCs have a better prognosis, as reported by Chau *et al.*<sup>5</sup> As a result, DNA and RNA-based next-generation sequencing techniques are also implemented in NC studies to identify the fusion partner and provide further insight into the disease.

### 1.3.3 NC as an aggressive subtype of NUT-rearranged neoplasms (NRNs)

Unexpectedly, recent studies have revealed a wide variety of NUT fusion partners in diverse neoplasms<sup>38,39</sup>. For instance, different sarcoma-like tumors have been reported to harbor fusion rearrangements involving NUT protein fused to members of the MAX dimerization (MAD) gene family<sup>40</sup> or fused to the capicua transcriptional repressor (CIC)<sup>41</sup>. This last example is specifically interesting because it contains two fusion partners that independently define a tumor category, creating a newly discovered sarcoma subtype that has been investigated in recent years<sup>42</sup>. Furthermore, different NUT-rearranged cases have been reported in hematologic malignancies such as B-cell acute

lymphoblastic leukemias (B-AALs). NUT B-AALs are primarily found in pediatric cases and, again, the fusion partners diverge from NUT Carcinoma ones, even though there is an interesting representation of epigenetic-related partners such as apoptotic chromatin condensation inducer 1 (ACIN1) or bromodomain containing 9 (BRD9)<sup>39,43</sup>. Additionally, NUT rearrangements have been found in other cases, depicted in **Figure 6**, including poromas/cutaneous adnexal tumors in which NUT mainly fuses to transcription factors such as YAP1, WWTR1, or transcriptional enhancer domain (TEAD) activators<sup>38,39</sup>.

Differences in the nosology and clinical outcomes and the biology of NUT partners suggest differences in the oncogenic mechanism among these tumor entities that are dependent on the fusion partner rather than the location or the histological features. Thus, in recent years, it has been proposed to group all these malignancies as NUT-rearranged neoplasms (NRNs). NC is the most aggressive and resistant to standard therapies subtype, as significantly better clinical outcomes have been observed in the newly described NRN with non-BRD-related fusion partners<sup>38,39,43</sup>.

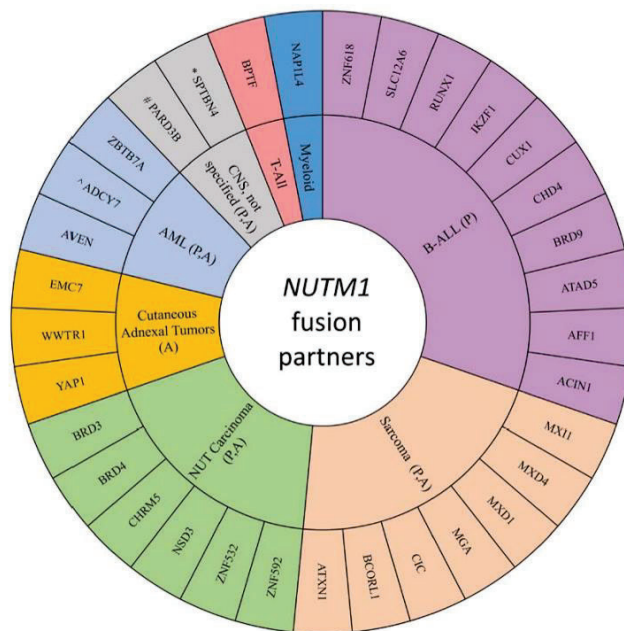


**Figure 6. NUT fusion partners in NRNs.**

Associations between NUT fusion partners (outer circle) and neoplasm types (inner circle). P: pediatric; A: Adult. Image from Charlab *et al.*<sup>39</sup>

## 1.4 Clinical management

Due to their rarity and the difficulty of conducting clinical trials for NC patients, there has been no consensus or guideline for their standard of care for a long time. However, an expert guideline was recently proposed at the first international symposium of NUT Carcinoma<sup>4</sup> (**Figure 7**).

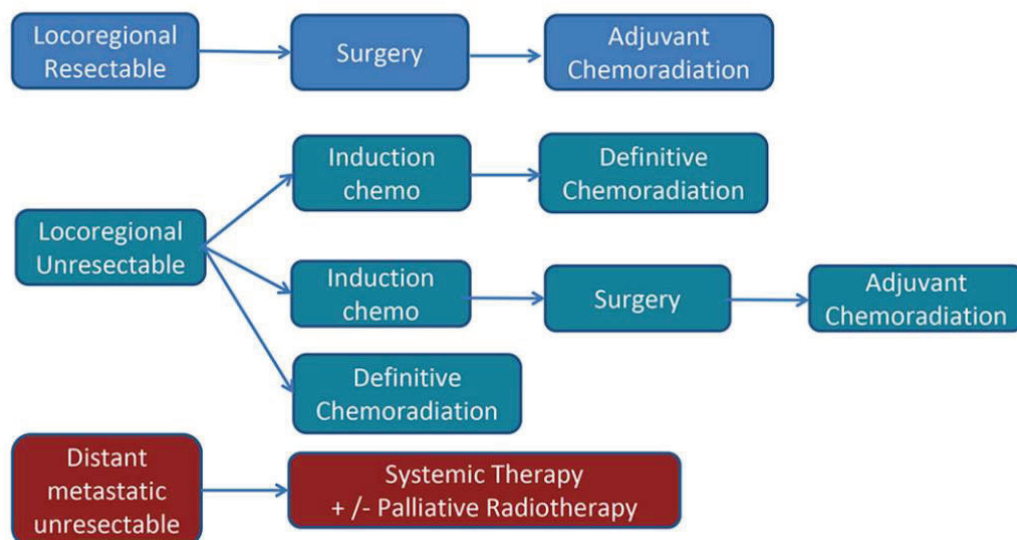


**Figure 7. First NC treatment guideline proposed at the First International Symposium of NUT Carcinoma<sup>4</sup>.**

### 1.4.1 Surgical resection as the best but uncommon option for NC patients

Surgical resection and adjuvant chemoradiation are the most effective treatment for NC. A retrospective study with a cohort of 63 NC patients showed a significantly improved progression-free survival (PFS) and overall survival (OS) with complete resection compared to incomplete or absent surgical resection (from less than 20% 2-year OS to 80%)<sup>8</sup>. Furthermore, an additional retrospective study of a cohort of 48 head and neck NC patients corroborated that an aggressive initial surgical resection with or without postoperative chemoradiation or radiation is associated with significantly enhanced survival, improving the 2-year OS of 7% in patients with no surgical resection up to 50% for patients undergoing surgical resection<sup>44</sup>. However, an important amount of NC cases are found in the advanced stage at diagnosis, where

surgical resections are no longer an option<sup>5,44</sup>. Thus, systemic therapy is nearly always required.

#### 1.4.2 Chemo and radiotherapy regimens for NC patients

Several cytotoxic chemotherapy regimens can be used for advanced NC, including ifosfamide-based regimens such as ifosfamide combined with etoposide, and ifosfamide combined with etoposide and vorinostat. In addition, platinum-based chemotherapies, such as etoposide combined with platinum, or platinum combined with paclitaxel have also been used as a frontline treatment in NC<sup>4,45</sup>. However, systemic chemotherapy is generally not effective for NC treatment due to low response rates and acquired resistance during the therapy<sup>4,24,46</sup>. Interestingly, Luo *et al.* have recently suggested that ifosfamide-based therapy may have a higher objective response rate (ORR) compared to platinum-based therapy but with limited durability. The study also highlights the need to develop effective combination targeted therapies<sup>45</sup>.

Radiotherapy has also demonstrated clinical benefit as part of the initial treatment strategy, positively impacting the OS rate. Patients receiving radiotherapy as initial treatment showed a 2.8 times lower risk of progression and 2.2 lower risk of death than patients who did not receive it<sup>44</sup>.

#### 1.4.3 Targeted therapies for NC

Targeted therapy has been explored in recent years as a potential option for treating patients with rare tumors in addition to radio- or chemotherapy. Particularly, epigenetic modifiers have been the focus of research<sup>4,24,47</sup>. The importance of BRD-related proteins in the oncogenesis of NC tumors has led to the development of small molecules that target the BET family of proteins. These molecules, known as BET inhibitors (BETi), were first described in 2010<sup>48</sup>. They competitively inhibit the interaction of bromodomains of BET proteins with their target acetylated lysine residues. As a result, BETis have shown promising results by displacing BRD4-NUT from the chromatin and disrupting megadomains<sup>48</sup>. Moreover, they have been demonstrated to promote cell growth arrest and differentiation in NC cell lines *in vitro* and *in vivo*. These findings provided a strong rationale for performing clinical trials.

Several phase I/II clinical trials have been conducted to test BETi in NC. These include trials investigating birabresib, molibresib<sup>49</sup>, RO6870810<sup>50</sup>, ODM-207<sup>51</sup> and BMS-986158<sup>52</sup>. Unfortunately, the development of resistances and observed toxicity effects such as thrombocytopenia, gastrointestinal symptoms, anemia, or fatigue, limited the clinical benefits of NC patients<sup>4,24</sup>.

To decrease the toxicity and increase the therapeutic window, next-generation BETi that selectively inhibit either BD1 or BD2 bromodomains, such as BI-894999, are being developed<sup>4,53</sup>. Furthermore, researchers are exploring various approaches to use BET inhibition in combination with other reagents. One such strategy involves combining BETis with p300 inhibitors using two different drugs or a dual inhibitor. This combination has been found to synergistically inhibit cell growth and promote cell differentiation in NC preclinical models<sup>54,55</sup>.

Alternative strategies that do not involve BET inhibition are also being developed. The BRD4-NUT-dependent rearrangement of acetylation in NC cells, which results in the silencing of differentiation genes and the promotion of proliferation (see section **1.2 Molecular basis of NUT Carcinoma oncogenesis** of Introduction), has led to the exploration of therapeutic strategies that disrupt the acetylation process. In support of this idea, a high-throughput chemical screen using a dCAS9-based GFP-reporter was conducted to identify small molecules that inhibit NUT-dependent gene activation and histone deacetylase (HDAC) inhibitors were identified as the top hits<sup>56</sup>. Some studies have demonstrated that HDAC inhibitors such as vorinostat can disrupt the already described megadomain formation, thus enabling the transcription of previously silenced regions responsible for the promotion of squamous differentiation and growth arrest<sup>47,57</sup>. However, the high toxicity observed upon HDAC inhibition in the clinical setting has limited the feasibility of this therapeutic approach<sup>57</sup>.

#### 1.4.4 Immunotherapy as an emerging option for NC

Immunotherapy has emerged as an effective treatment option for various cancer types, such as melanoma<sup>58</sup>. Thus, an immune-oncologic approach is also being explored for NC patients. Although immunotherapy response is frequently associated with a high tumor mutational burden (TMB)<sup>5,17</sup>, and NC samples have been demonstrated to be genetically stable<sup>5,17</sup>, there is a possibility that NC harbor antigenic tumor-specific neoantigens caused by NC fusion proteins. Interestingly, it has been shown that a subset of NC tumors expresses PD-L1, and several studies have been published reporting durable disease stability in PD-L1-high NCs treated with nivolumab or pembrolizumab<sup>59,60</sup>. However, to date, the reported responses to immunotherapy are variable<sup>16,61</sup>, and further study is needed.

In summary, NC is a highly aggressive tumor type with scarce therapeutic options that commonly presents an advanced stage at diagnosis, limiting the surgical resection, which is the most effective strategy. Although its response to different systemic radio- and chemotherapy regimens is very limited, other targeted therapies are currently being developed, with focusing on epigenetic-targeting small molecules inhibiting BET proteins or HDACs.

## 2. EPIGENETICS

### 2.1 Chromatin structure and organization

#### 2.1.1 The different levels of chromatin compaction

The information that human cells contain in their nuclei, encompassing around two meters of DNA, must be confined within the nucleus. This involves a complex and tightly regulated multilayered process of chromatin compaction. Importantly, this compaction must be coordinated to enable essential cell processes such as transcription, DNA replication, or repair. To achieve this, DNA is packaged in a dynamic nucleoprotein complex, namely nucleosomes<sup>62</sup>. Nucleosomes are the basic unit of chromatin, consisting of 147 base pairs of DNA wrapped around an octamer of histone proteins (H2A, H2B, H3, and H4) and a linker histone H1, which is located outside the octamer to stabilize DNA wrapping around the nucleosomes<sup>63</sup>. Chromatin can be compacted to varying degrees to form a high-order chromatin structure, as shown in **Figure 8**.

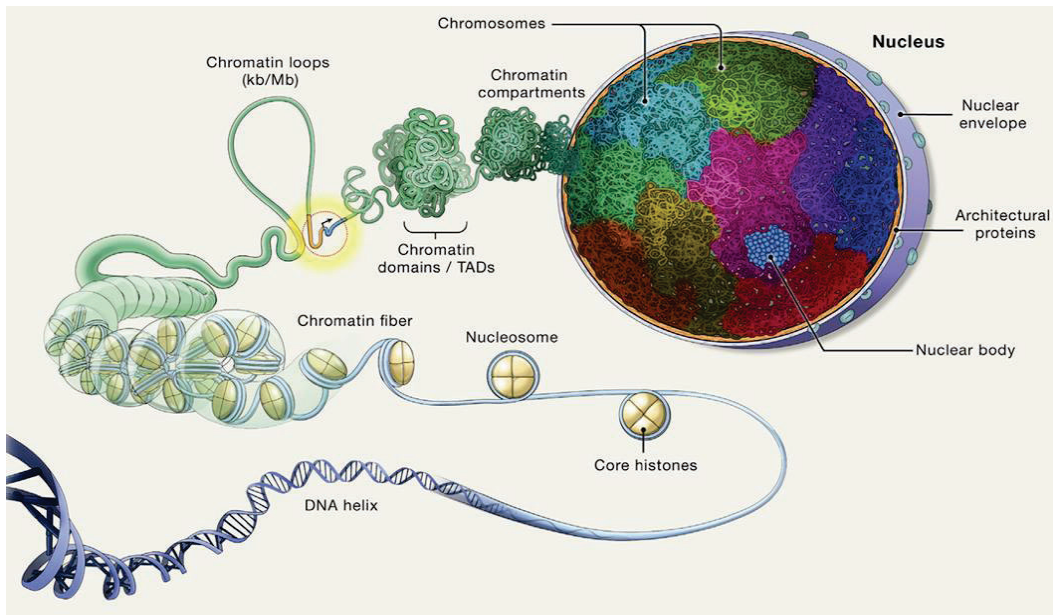


**Figure 8. Schematic representation of the organization of the eukaryotic genome.** Image from Misteli *et al.*<sup>64</sup>

Nucleosomes are folded to create the chromatin fibers. These fibers, in turn, get irregularly folded into high-ordered features named loops via intra-polymer self-associations<sup>64</sup>. Loops mediate the interaction of spaced regulatory elements, often enhancers and promoters<sup>64</sup>.

The next level of compaction is the creation of chromosomal domains. These domains are genome regions that preferentially interact with each other rather than with their surroundings and, because of that, are called topologically associated domains (TADs)<sup>64</sup>. They are structural and functional units exhibiting correlations with synchronized gene expression, histone modification patterns, and DNA replication timing. Moreover, their boundaries are notably enriched with insulator proteins such as CTCF, markers of active transcription, and repetitive elements<sup>65</sup>.

Subsequently, chromatin domains assemble into higher-order chromatin compartments, thus promoting spatial segregation of different chromatin regions. Two major compartments have been described, termed A and B. While compartment A typically harbors a plethora of genes, exhibiting elevated transcriptional activity and accessibility, fewer genes and a repressed state mark compartment B, indicative of a more constrained regulatory landscape<sup>66</sup>.

Finally, chromosomes have the highest levels of genome compaction. Chromosome formation only occurs during cell division. Thus, during interphase, they usually exist in the nucleus as chromosome territories<sup>67,68</sup>.

### 2.1.2 The interplay between chromatin architecture and transcription

All these chromatin organization and compaction levels are essential in regulating gene expression. The spatial organization of the genome is intricately connected to its biological functionality, as it governs the accessibility of chromatin to different protein factors, bringing regulatory elements and genes into close spatial proximity to ensure proper gene expression for each cell context and identity<sup>64</sup>. Furthermore, the organization of the genome across different scales has been proposed to entail the creation of biomolecular condensates through liquid-liquid phase separation (LLPS). This process consists of the formation of membrane-less organelles and condensates caused by weak multivalent interactions between macromolecules, in this case, DNA molecules and different proteins that promote the action of different transcription-modulating proteins due to their proximity<sup>69</sup>.

In parallel, recent studies depicted a requirement for the transcription process and machinery to originate and maintain chromatin structure and genome topology. Although it does not seem to affect the higher-level genome organization significantly, it influences the formation of subcompartments and subdomains and stabilizes enhancer-promoter interactions<sup>70</sup>.

Thus, the morphological representation of the genome of a cell is ultimately shaped by the bidirectional and dynamic interaction between the architectural characteristics and the functional transcriptional status. Alterations in these folding units at any level are associated with multiple diseases and cancer<sup>71</sup>, as discussed in the following sections.

Of note, NUT Carcinoma is a comprehensive example of the importance of chromatin-associated proteins as drivers of genome architecture remodeling events that, ultimately, lead to an important transcriptional switch that directly affects cell behavior.

## 2.2 Histone post-translational modifications with a particular focus on acetylation

### 2.2.1 A brief overview of chromatin chemical modifications, highlighting histone PTMs.

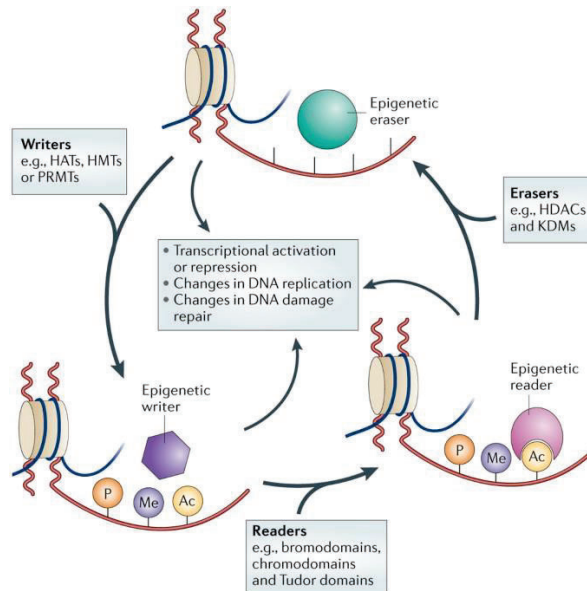
Chromatin undergoes various chemical modifications to achieve the mentioned dynamic properties. In some cases, these modifications can directly affect the DNA molecule, as exemplified by DNA methylation. This epigenetic process involves enzymes called DNA methyltransferases (DNMTs) that transfer a methyl group covalently to the cytosine residue, thereby silencing gene expression<sup>72</sup>. Additionally, ATP-dependent chromatin remodeling complexes (CRCs), such as the SWItch/Sucrose Non-Fermentable (SWI/SNF) family, utilize ATP hydrolysis to mobilize, destabilize, eject, or restructure nucleosomes, impacting chromatin organization<sup>73</sup>.

Another mechanism that modulates chromatin configuration is the post-translational modifications (PTMs) of histone proteins within nucleosomes. Remarkably, the histone tails, which extend from the nucleosome core, are rich in lysine and arginine residues, making them susceptible to these PTMs, including acetylation, methylation, phosphorylation, ubiquitination, SUMOylation, and others<sup>63,69,74</sup>.

Importantly, these diverse PTMs of histone proteins collectively contribute to the dynamic regulation of chromatin structure and gene expression in response to various cellular signals and environmental cues. They exert their effects either directly, altering the chromatin structure, or indirectly, modulating the availability of binding of proteins that promote or repress DNA transcription<sup>69,75</sup>. For instance, acetylation of histone lysine residues generally correlates with transcriptional activation<sup>76</sup>. It alters histone charge by reducing the positivity of histone residues and, thus, disrupting the stabilizing influence of electrostatic interaction between DNA (negatively charged) and histones (positively charged), leading to a more open chromatin structure that allows for increased accessibility of transcriptional machinery to the DNA<sup>75</sup>. Additionally, methylation of histones affects lysine and arginine residues and can either activate or repress gene expression, depending on the specific residue that is methylated and the number of methyl groups added<sup>77</sup>. For

example, trimethylation of lysine 4 on histone H3 (H3K4me3) is associated with active transcription, while trimethylation of lysine 9 on histone H3 (H3K9me3) is typically linked to gene repression<sup>78</sup>. Complementary, phosphorylation of histone serine or threonine residues can also regulate gene expression by influencing chromatin compaction or recruiting specific proteins involved in transcriptional regulation<sup>79</sup>. Lastly, ubiquitination and SUMOylation, as well as other described histone PTMs, can regulate various chromatin processes, including transcriptional activation, repression, and DNA repair<sup>69</sup>.

A multitude of interconnected enzymes and pathways orchestrates the intricate tapestry of histone PTMs within chromatin. These enzymes, often referred to as "writers," are responsible for catalyzing the addition of PTMs, ensuring their proper formation and distribution across histone proteins. Conversely, "erasers" can remove these modifications, facilitating chromatin remodeling and dynamic regulation of gene expression. Furthermore, specialized proteins known as "readers" recognize and interpret these PTMs, thereby influencing downstream chromatin-associated processes<sup>80</sup>. Together, these interrelated mechanisms sculpt the histone PTM landscape, finely tuning chromatin structure and gene expression in response to cellular signals and environmental cues<sup>69,81,82</sup> (**Figure 9**).



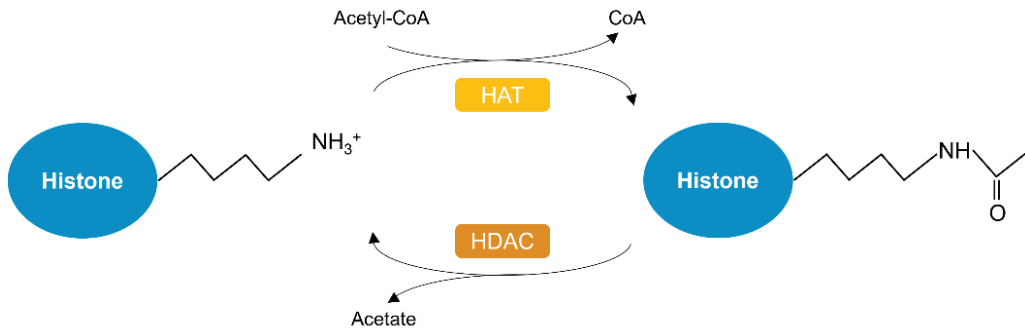
**Figure 9. Scheme of the interplay between writers, erasers, and readers across chromatin.**

Image from Falkenberg *et al.*<sup>82</sup>

### 2.2.2 Histone acetylation.

To understand the role of epigenetic dysregulation in NUT Carcinoma, here we will mainly focus on histone acetylation. This extensively studied histone PTM was first elucidated by Allfrey *et al.* in 1964<sup>83</sup>. Primarily targeting lysine residues within histone tails, histone acetylation plays a pivotal role in chromatin dynamics<sup>84</sup>. The disruption of the electrostatic interaction with negatively charged DNA enhances DNA accessibility, rendering it more susceptible to interactions with proteins, including transcription factors that recruit transcription machinery<sup>75,76</sup>. Consequently, histone acetylation exhibits a strong association with transcriptional activity and is often found in active promoters, enhancers, and other accessible chromatin regions<sup>85</sup>.

Histone acetylation is a dynamic process involving the action of histone acetyltransferases (HATs) for addition and histone deacetylases (HDACs) to remove the acetyl group. HATs utilize acetyl-CoA as a cofactor to facilitate the transfer of an acetyl group onto the  $\epsilon$ -amino group of lysine chains (**Figure 10**).



**Figure 10. Scheme of histone acetylation.**

HAT: histone acetyltransferase; HDAC: histone deacetylase.

To date, two types of HATs have been documented: type A and type B<sup>86</sup>. Type B HATs are predominantly cytoplasmic, exhibiting high conservation, and are responsible for acetylating free histones in the cytosol, an important event in histone deposition. Type A HATs function in the acetylation of histone proteins within the nuclear chromatin and display greater diversity. Typically, these proteins are associated with large multiprotein complexes<sup>87</sup>. Type A HATs can be further categorized into five groups based on their amino-acid sequence homology and structural conformation<sup>75,88</sup>.

- GNAT class, representing the classical HAT family.
- MYST class, characterized by the presence of a highly conserved MYST domain, containing an Acetyl-CoA-binding motif and a zinc finger.
- CBP/p300 class, closely linked to cell differentiation and apoptosis, with multiple non-histone substrates and consistently contains four separate transactivation domains, including cysteine–histidine-rich region 1, kinase-induced domain interacting with CREB, another cysteine–histidine-rich region, and a nuclear receptor coactivator binding domain.
- TAFII230/250 class, integral components of the transcription factor complex TAFIID.
- Lastly, a fifth category includes other unclassified HATs, such as  $\alpha$ -tubulin N-acetyltransferase 1 (ATAT1).

As mentioned earlier (see **1.2 Molecular basis of NUT Carcinoma oncogenesis** of Introduction), p300 emerges as a pivotal acetyltransferase within the molecular framework of NC. It is a histone acetyltransferase first reported by Lundblad *et al.* in 1995<sup>89</sup> that has a multifaceted role in physiological contexts, orchestrating fundamental cellular processes such as proliferation and differentiation<sup>90,91</sup>. Beyond its enzymatic capacity as an acetyltransferase, p300 is also a transcriptional co-activator<sup>92</sup>, as it orchestrates the recruitment of transcription factors and the transcription machinery, thereby instigating the activation of gene expression at precise loci<sup>93</sup> (**Figure 11**). This multifunctional process positions p300 as a central orchestrator in the intricate symphony of molecular events underlying cellular regulation and function<sup>92</sup>.

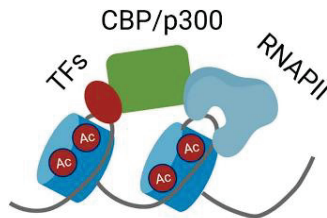


**Figure 11. Schematic representation of p300's involvement in transcription.**

TFs: Transcription factors; Ac: acetylation; CBP is an analog of p300. Image from Gou *et al.*<sup>92</sup>

HDACs, conversely, function as enzymes that can catalyze the removal of acetylation from lysine residues, thereby restoring their positive charge and predominantly acting as transcriptional repressors. According to phylogenetic analyses and sequence homologies, these enzymes can be classified into four classes.

- Class I (HDACs 1, 2, 3, 8) comprises HDAC proteins phylogenetically related to yeast proteins Rpd3, Hos1 and Hos2.
- Class II (HDACs 4, 5, 6, 7, 9, 10) are related to yeast proteins Hda1 and Hos3.
- Class III is constituted by sirtuins, which have a completely different mechanism of action and are phylogenetically more separated from the others.
- Class IV includes an HDAC only expressed in higher eukaryotes named HDAC11.

Classes I, II, and IV proteins are evolutionarily linked and share a common enzymatic mechanism involving Zn-catalyzed hydrolysis of the acetyl-lysine amide bond. However, class III HDACs (sirtuins) function as a family of nicotinamide adenine dinucleotide (NAD<sup>+</sup>)-dependent deacetylases, catalyzing the transfer of the acetyl group onto the sugar moiety of NAD<sup>+</sup> <sup>88,94</sup>. Despite their classification, HDACs individually exhibit relatively low substrate specificity, as a single enzyme can deacetylate multiple sites within histones. Similar to HATs, they are often found in large protein complexes<sup>75</sup>.

Apart from histone PTM writers and erases, epigenetics readers play a crucial role in histone PTMs and are involved in transcription and cell identity. Notably, there are proteins that specialize in recognizing acetylated residues. Among these acetylation readers, the BET family of proteins, particularly BRD4, holds important significance in NC oncogenesis.

The BET family, which comprises BRD2, BRD3, BRD4, and the testis-specific BRDt, is characterized by harboring two tandem bromodomains (BD1 and BD2) that bind to lysine-acetylated histones. Moreover, they possess an extra-terminal (ET) domain facilitating protein-protein interaction, condensate formation, and recruitment of BET proteins to specific genomic loci<sup>95</sup>. They are important transcriptional regulators and key readers of lysine acetylation, orchestrating the assembly of transcriptional regulator complexes and initiating transcriptional programs that can lead to phenotypic changes<sup>96,97</sup>. They can also recruit coactivators to target gene sites and activate RNA polymerase II for transcription elongation<sup>95</sup>.

BRD4, a member of this family, is well known for its implication in epigenetic modulation, cell cycle regulation, and DNA damage response. It is notably involved in organizing super-enhancers (SEs) and regulating the expression of oncogenes such as *MYC* or *NOTCH3*<sup>98,99</sup>. There are two main isoforms of BRD4: BRD4 long (BRD4l) and BRD4 short (BRD4s). Both isoforms contain bromodomains, and BRD4s lacks the C-terminal domain present in BRD4l, as well as the HAT domain, and thus, the histone acetyltransferase catalytic activity<sup>99,100</sup> (**Figure 12**). Both isoforms display diverse characteristics, such as transcriptional activity or interaction patterns, with different effects on gene regulation. Furthermore, BRD4s demonstrates oncogenic properties, whereas BRD4l acts as a tumor suppressor in breast cancer models<sup>99,101</sup>.

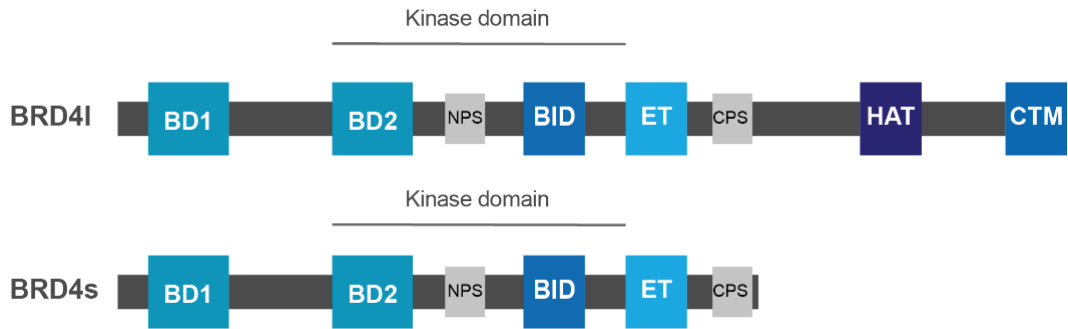


**Figure 12. Scheme of BRD4 isoforms.**

BD1: bromodomain 1; BD2: bromodomain 2; NPS: N-terminal cluster of phosphorylation sites; BID: basis residue enriched interaction domain; ET: extra-terminal domain; CPS: C-terminal cluster of phosphorylation sites; HAT: histone acetyltransferase catalytic domain; CTM: C-terminal motif.

## 2.3 Epigenetics and NUT Carcinoma

Dysfunctions in chromatin regulation can have profoundly detrimental effects, commonly leading to various diseases, including cancer. Research indicates that mutations in genes responsible for chromatin organization and regulation are present in over 50% of cancer cases<sup>102</sup>. Moreover, changes in global patterns of histone modifications are frequently observed in diverse types of cancers<sup>103,104</sup>.

### 2.3.1 NC is an epigenetic-driven cancer.

NUT Carcinoma is a paradigm example of epigenetic-driven cancers, as it is triggered by chromosomal rearrangements leading to the expression of NUT-containing fusion proteins. A single event likely initiates these rearrangements<sup>15,34</sup>. Interestingly, NC cells exhibit genetic stability with minimal additional genetic alterations<sup>5,17</sup>. Furthermore, these additional genetic alterations vary widely and lack a clear pattern among patients<sup>59</sup>. Indeed, the relatively young age of diagnosis and the absence of common mutagenic risk factors, such as tobacco use, further support the lack of common genetic mutations associated with NC<sup>4</sup>.

However, the effect of this NUT-fusion protein, although isolated, seems to be enough to promote oncogenesis<sup>15,34</sup>. This is facilitated by several associated events. Firstly, the fusion of NUT protein with BRD4 (or other molecules) results in its permanent localization within the nucleus and bound to chromatin, losing its inherent ability to migrate between the nucleus and cytoplasm due to its NES/NLS regions<sup>105</sup>. Secondly, the interaction between BRD4-NUT and p300 leads to the activation of p300 and the loss of its autoinhibitory capacity<sup>106</sup>. Of note, it has been shown that BRD4-NUT fusion contains two transactivation domains (TADs) in the NUT moiety that bind to the four-helical bundle TAZ2 domain in p300 protein<sup>25,106</sup> (**Figure 13**). The TAD/TAZ2 bipartite binding in BRD4-NUT/p300 triggers allosteric activation of p300 by promoting a conformational change in p300 protein that relieves TAZ2 autoinhibitory function on the HAT activity<sup>106</sup>.

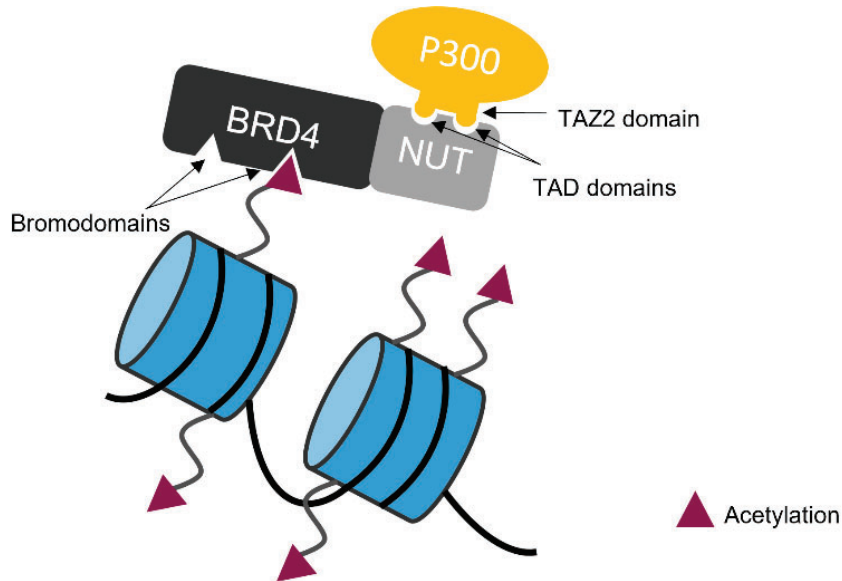


**Figure 13. Schematic representation of key domains in BRD4-NUT and p300.**

These events eventually lead to a distortion of NUT functionality, contributing to the systemic epigenetic remodeling of the NC cell's chromatin that contributes to its oncogenesis.

### 2.3.2 The model of megadomain formation extends to other NUT fusion partners beyond BRD4.

Activation of p300 by BRD4-NUT is pivotal for initiating the positive feedback loop of chromatin hyperacetylation, ultimately leading to the formation of megadomains in NC cells. However, this mechanism that generates hyperacetylated regions along the chromatin of NC cells may also extend to other fusion partners as well. In a study comparing the protein interactome of cells expressing BRD4 and BRD4-NUT, ZNF532 was identified as a BRD4-NUT interacting protein<sup>26</sup>. Furthermore, ZNF532 was found to be a novel NUT fusion partner, and the newly discovered ZNF532-NUT fusion protein was demonstrated to form megadomains of hyperacetylated chromatin, including at the *MYC* locus, which mirrors the mechanism described for BRD4-NUT fusion and responsive to BET inhibitors<sup>26</sup>. Additionally, BRD3 and NSD3, two other common NUT partners in NC cells, were also shown to interact with BRD4<sup>21,28</sup>. Moreover, Shiota *et al.* reported ZNF592, another zinc finger-containing protein, as a NUT fusion partner<sup>22</sup>. Interestingly, ZNF592 was also

identified as a component of the BRD4-NUT complex<sup>26</sup> (see **Figure 4**). Collectively, these findings led to the establishment of a model where all fusion variants interact with BRD4. Interestingly, this discovery opens avenues for exploring BET inhibitors and other potential treatments studied in BRD4-NUT models for all NC cases, regardless of their fusion partners.

Thus, the BRD4-NUT fusion-dependent model of megadomain formation could apply to all NC models regardless of the NUT fusion partner. In all cases, BRD4 binds acetylated histone residues and recruits NUT and p300 to establish positive feedback loops that culminate in the formation of acetylation megadomains.

### 2.3.3 Megadomains of acetylation: origin, organization, and impact on NC cells.

Megadomains of chromatin decorated with histone acetylation were initially identified as H3K27ac nuclear foci in immunofluorescence assays that perfectly colocalize with BRD4-NUT staining in NC cells or non-NC cells with ectopic overexpression of BRD4-NUT<sup>25</sup>. Later, using chromatin immunoprecipitation combined with sequencing (ChIP-seq), it was found that NC cells have about 100-200 large regions of acetylated chromatin marked with H3K27ac. These areas were surprisingly bigger than the usual acetylated regions<sup>30,32</sup>.

Interestingly, upon analyzing different cell lines expressing BRD4-NUT, variations in the distribution of megadomains along the chromatin were observed, while their size and quantity remained consistent. This discrepancy in megadomain location could be explained by their origin and formation process. Megadomains emerge in response to the preexisting transcriptional or epigenetic state of host cells, originating from H3K27ac-enriched seed regions such as enhancers and regulatory regions<sup>30,32</sup>. Three potential processes for megadomain formation have been proposed. Firstly, a megadomain may stem from a single seed enhancer where the BRD4-NUT fusion binds and triggers the positive feedback loop. Secondly, megadomain formation might involve multiple seed enhancers, possibly resulting from the fusion of distinct enhancers due to megadomain expansion. Thirdly, some megadomains may arise without preexisting enhancers<sup>30</sup> (**Figure 14**).

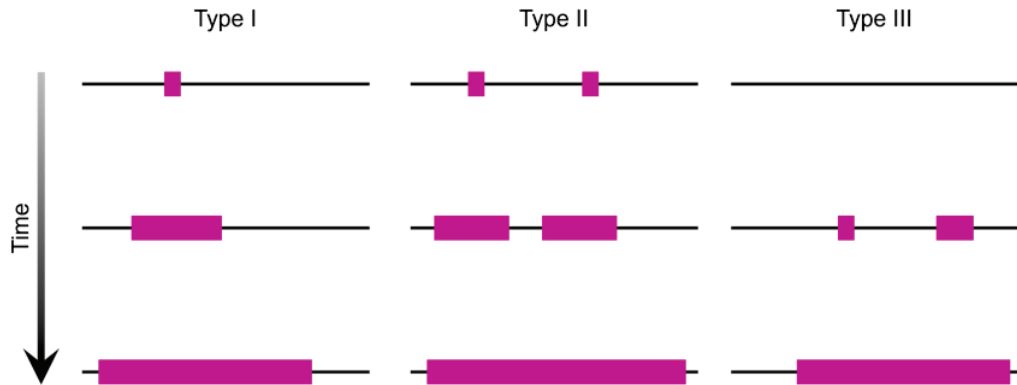


**Figure 14. Schematic representation of the different proposed models of megadomain formation.**

Histone acetylation is represented in purple.

A comparison of the localization of megadomains and previously generated Hi-C data demonstrated that most megadomains are bounded by the extent of a TAD. Similarly to TADs, megadomain boundaries showed significant enrichment in active enhancers, CTCF binding, and transcription start sites<sup>30</sup>. However, in some cases, megadomains do not show well-defined boundaries, possibly reflecting the dynamic balance of acetylation and deacetylation within them<sup>30</sup>. Furthermore, Rosencrance *et al.* described that megadomains spatially clustered in the nucleus. They found elevated megadomain-megadomain interactions, both intra and inter-chromosomal, over hundreds of megabases, resulting in the establishment of a distinct nuclear subcompartment that they named subcompartment M. It entailed elevated transcription activity and was demonstrated to be BRD4-NUT-dependent as it was abrogated upon fusion degradations and restored upon fusion expression restoration<sup>107</sup> (**Figure 15**).

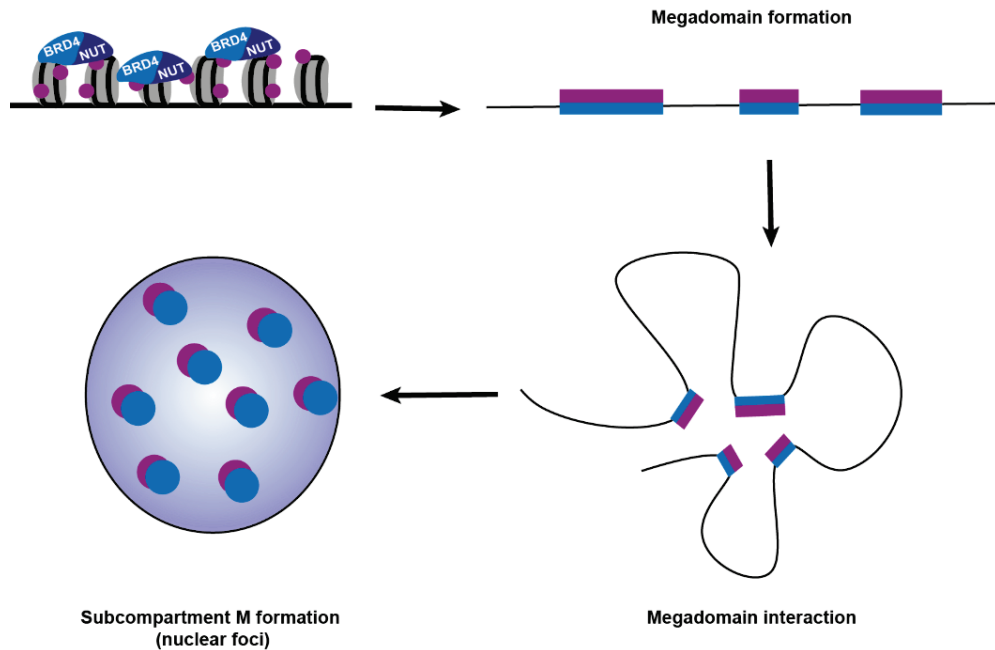


**Figure 15. Scheme of chromatin organization of megadomains.**  
Acetylation is represented in purple.

While megadomain distribution may vary between different cell lines, the behavior of NC remains similar across these lines due to a consistent presence of pro-proliferative genes within megadomains. Additionally, pro-differentiation genes are currently suppressed, as they are excluded from megadomains and consequently under-transcribed<sup>30</sup>. However, a few cancer-related genes, such as *TP63*, *SOX2*, and *MYC*, have been consistently found to be included within megadomains across various cell lines.

*TP63* is an epithelial-specific developmental gene<sup>108</sup> encoding a transcription factor associated with squamous carcinomas<sup>109</sup>. It was found coincidentally inside megadomains in several NC cell lines and its expression is decreased upon JQ1 (BETi) treatment<sup>30</sup>. Furthermore, *TP63* silencing significantly decreased NC cell viability<sup>30</sup>.

*SOX2* is a well-known transcription factor indispensable for embryonic development and is pivotal in preserving the pluripotency of embryonic cells and diverse adult stem cell populations<sup>110</sup>. It has been demonstrated that NC cells express remarkably high levels of *SOX2* and can grow into stem cell-like

spheres in a BRD4-NUT fusion-dependent manner. In addition, SOX2 elimination phenocopies BRD4-NUT silencing as it promotes differentiation, cell growth inhibition, reduced SOX2 expression, and abrogation of sphere formation. However, these features are restored upon SOX2 rescue by overexpression<sup>31</sup>.

Lastly, and with particular importance in this project, the *MYC* gene is one of the few cancer-related genes consistently placed inside megadomains across NC cell lines. It is a master transcription factor that modulates the expression of several genes involved in different processes such as cell proliferation, growth, or metabolism<sup>111</sup>. BRD4-NUT associates with the *MYC* promoter and is required to maintain *MYC* expression in NC cell lines. Its elimination induces NC cell differentiation, and its overexpression can restore it<sup>29</sup>. Moreover, expression profiling studies performed to identify BRD4-NUT-dependent potential transcriptional differences using gene set enrichment analysis (GSEA) showed that the most highly correlated oncogene target signature corresponded to that of *MYC*<sup>29</sup>. Thus, *MYC* is a downstream target of BRD4-NUT required to maintain NC cells in an undifferentiated, proliferative state.

#### 2.3.4 The connection between megadomains and condensate formation

The formation of chromatin condensates plays a crucial role in how epigenetic changes influence transcriptional regulation. Kosno *et al.* proposed a model suggesting that the BRD4-NUT-p300 complex is involved in condensate formation through a combination of positive feedback and phase separation processes<sup>105</sup>. In this study, they demonstrated that BRD4-NUT forms condensate to a greater extent than BRD4 and NUT alone. These condensates recruit p300 and drive changes in gene expression in NC. Moreover, a minimal fragment of the NUT part of the fusion involving the p300 binding region encompassing the 355-505 residues, is necessary and sufficient to bind p300 and form condensates. Regarding the p300 part, its intrinsically disordered regions, transcription factor-binding domains, and HAT activity collectively contribute to condensate formation<sup>105</sup> (**Figure 16**).

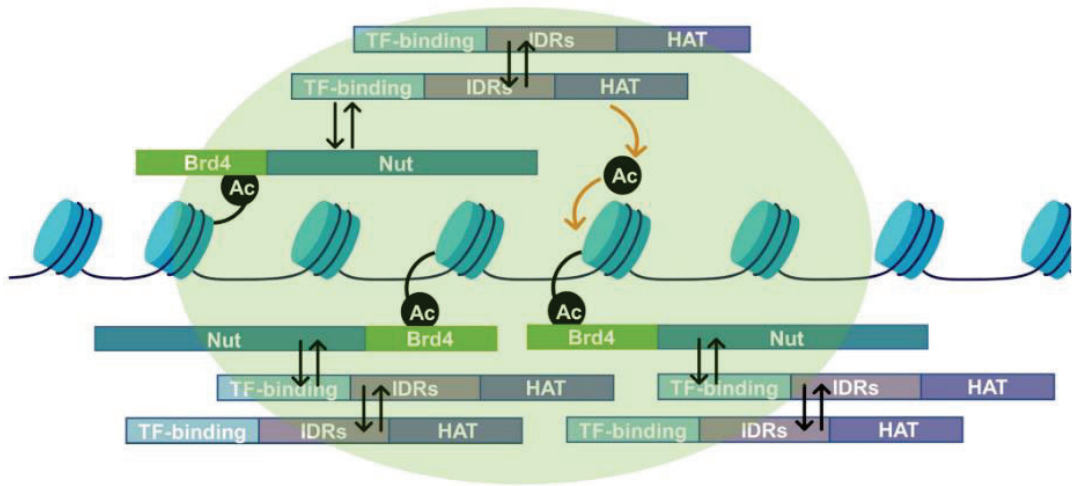


**Figure 16. Schematic representation of the model of condensate formation.**

Image from Kosno *et al.*<sup>105</sup>

### 2.3.5 Epigenetic alterations of NC beyond BRD4-NUT and p300-dependent megadomains

Recently, an intriguing connection has emerged between NC and a well-known epigenetic complex, the Polycomb repressive complex 2 (PRC2)<sup>112</sup>. PRC2 is a protein complex that plays a role in gene signaling initiation by catalyzing the trimethylation of histone H3 at lysine 27 (H3K27me3). Among its components, EZH2 stands out as the catalytic subunit responsible for this methylation reaction<sup>113</sup>. In the study by Huang *et al.*, EZH2 was identified as a critical factor for NC. Inhibition of EZH2 using tazemestostat resulted in the suppression of NC cell growth. Furthermore, EZH2-specific H3K27me3 marks were found to silence the expression of a set of tumor suppressor genes. Interestingly, it was observed that EZH2-dependent H3K27me3 marks and H3K27ac marks of megadomains were mutually exclusive. This finding suggests a complementary molecular mechanism underlying the enhanced proliferation and aggressiveness phenotype of NC cells<sup>112</sup>. However, further investigations are needed to better understand this process and its interconnection with the model of megadomain formation.

In conclusion, NC is a cancer type driven by epigenetic factors. Although there has been increasing knowledge about this disease in recent years, a deeper understanding of its oncogenesis, progression, and clinical characteristics is still urgently needed. Various epigenetic drug trials have assessed therapeutic efficacy but have been unsuccessful. This failure is attributed to the narrow therapeutic windows of these drugs. Hence, further studies are required to explore new therapeutic strategies.

### 3. SOURCES AND PATHWAYS INVOLVED IN DNA DAMAGE RESPONSE.

#### 3. 1 Sources of DNA damage response

Similar to the intricate regulation of gene expression through epigenetic mechanisms, the preservation of genomic integrity via DNA damage response (DDR) mechanisms is crucial for maintaining cell identity and functionality<sup>114,115</sup>.

The DDR comprises a multitude of biochemical pathways that safeguard genomic integrity<sup>116,117</sup>. It coordinates processes such as DNA repair, activation of cell-cycle checkpoints, and regulation of DNA replication or damage tolerance processes<sup>118–120</sup>. These pathways play a vital role in maintaining cellular function and ensuring the faithful transmission of the genome during cell division by orchestrating a complex network of processes to overcome genomic problems and maintain cellular homeostasis<sup>116</sup>. DNA damage that triggers various DDR pathways arises from diverse sources (**Figure 17**).

Firstly, environmental factors can compromise DNA integrity<sup>121</sup>. UV radiation, for instance, can induce the formation of pyrimidine dimers<sup>122</sup>, while ionizing radiation, such as X-rays, can generate free radicals within cells, leading to mutations<sup>123</sup>. In addition, exposure to genotoxic chemicals is also a threat to DNA integrity<sup>124</sup>.

Secondly, several endogenous sources can impact DNA integrity<sup>121</sup>. Errors occurring during DNA replication, such as misincorporation of nucleotides<sup>125</sup> or stalled replication forks<sup>126</sup>, can trigger DDR pathway activation. Cellular metabolism itself can also produce intermediates that harm DNA. For example, oxidative damage generates reactive oxygen species (ROS) capable of oxidizing DNA bases, resulting in alterations and DNA breaks<sup>127</sup>. Finally, spontaneous base modifications, such as hydrolysis of DNA bases leading to deamination, can cause mismatches and mutations<sup>128</sup>.

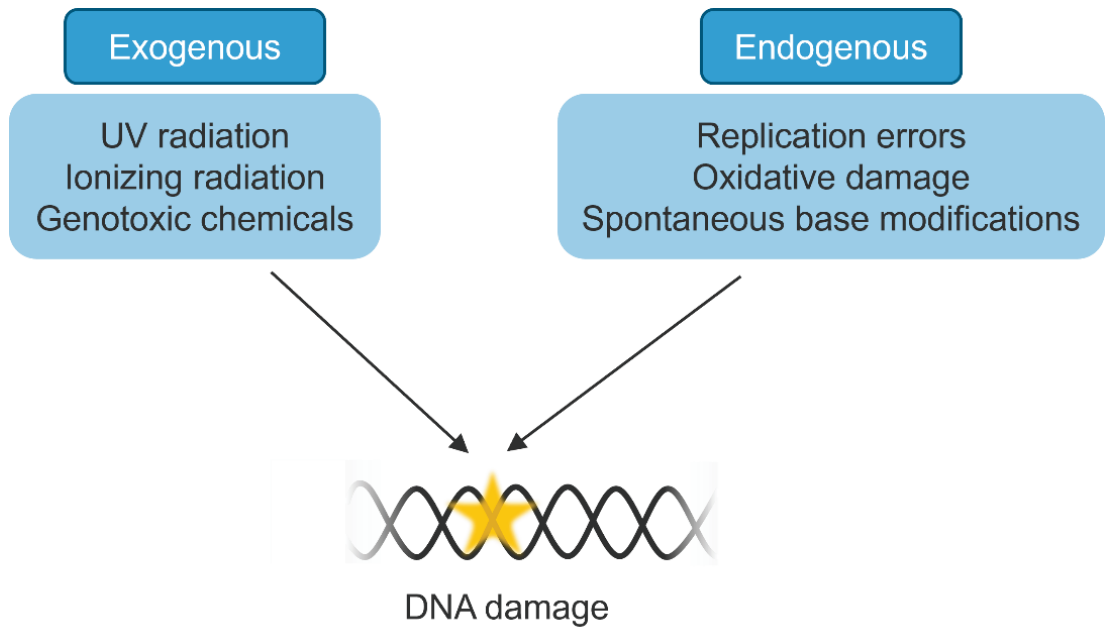


Figure 17. DNA damage sources.

## 3.2 DNA repair mechanisms.

Various types of DNA damage prompt distinct responses by specific repair mechanisms and signaling pathways. Here, we will summarize the main types of DNA damage repair and their principal characteristics<sup>129</sup>.

### 3.2.1 Single-strand DNA repair

Base Excision Repair (BER): This pathway addresses small non-helix-distorting lesions such as base modifications and single-strand (ssDNA) breaks (SSBs), a prevalent form of DNA damage. It involves the sequential removal of the damaged base by DNA glycosylases, cleavage of the DNA backbone at the resulting apurinic site by endonucleases, filling of the gap with the appropriate nucleotide by DNA polymerases, and finally, the ligation of the DNA strand by DNA ligases<sup>130</sup>.

Nucleotide Excision Repair (NER): NER targets bulky DNA lesions that distort the helical structure of DNA, caused by factors like UV radiation or platinum salts, along with transcription-coupled repair. The process entails recognition of the lesion by specific proteins, excision of a small segment of ssDNA containing the lesion, gap filling with the correct nucleotide by DNA polymerases using the intact single strand as a template, and ultimately, ligation of the DNA strand by DNA ligases<sup>131</sup>.

Mismatch Repair (MMR): MMR rectifies base mismatches and small insertion/deletion loops in DNA arising from errors in DNA replication or recombination, ensuring the fidelity of the genetic code. It involves the recognition of the mismatch by MutS, the recruitment of MutL triggering downstream repair steps, the excision of the mismatched segment, the resynthesis by DNA polymerase with the correct nucleotides, and the ultimate ligation by DNA ligases<sup>132</sup>.

### 3.2.2 Double-strand DNA repair

Non-Homologous End Joining (NHEJ): This is a low-fidelity double-strand (dsDNA) break (DSB) repair process capable of fixing DSBs without an intact sister chromatid as a template. It may introduce DNA rearrangements by directly ligating the broken DNA ends<sup>133</sup>.

Homologous Recombination (HR): HR represents a more accurate and efficient repair pathway, dependent on the presence of an intact sister chromatid as a template. HR involves resection of the broken DNA ends, invasion of the intact DNA template by the broken ends, DNA synthesis, and resolution of the recombination intermediate<sup>134</sup>.

### 3.2.3. DNA damage sensors

The most important factors controlling the DNA damage response are ATM, ATR, and DNA-PK<sup>135</sup> (**Figure 18**).

DNA-Dependent Protein Kinase (DNA-PK) Pathway: The DNA-PK pathway is involved in sensing and repairing DSBs, playing a critical role in maintaining genomic stability<sup>136</sup>. Upon detection of DSBs, DNA-PK forms a complex with the Ku70/Ku80 heterodimer, leading to DNA-PK activation. This activated complex then phosphorylates various downstream targets involved in DNA repair processes, mainly NHEJ<sup>137</sup>.

Ataxia Telangiectasia Mutated (ATM) Pathway: This pathway is primarily activated in response to DSBs, often facilitated by the recruitment of the MRE11-RAD50-NBS1 (MRN) complex. Upon recruitment and activation, ATM phosphorylates histone H2AX and MDC1 to activate a phosphorylation-ubiquitylation signaling cascade involving various transducer and effector proteins<sup>138</sup>. This activation leads to profound effects on cellular processes, including modulation of protein activity, stability, translocation, and interaction, as well as regulation of gene expression<sup>139</sup>. Consequently, ATM activation promotes diverse cellular responses such as DNA repair (via NHEJ or HR), cell cycle arrest (at G1/S or G2/M checkpoints), regulation of transcription, modulation of signaling and metabolic pathways, and, in certain instances, induction of senescence or apoptosis<sup>135</sup>.

Ataxia Telangiectasia and Rad3-Related (ATR) Pathway: This pathway responds to various forms of DNA damage and RS, particularly those inducing SSBs. ATR is recruited to regions of ssDNA coated by the replication protein A (RPA). This occurs through the formation of a heterodimer of ATR and ATR-interacting protein (ATRIP)<sup>140</sup>. Together with other activators such as TopBP1 and ETAA1<sup>141,142</sup>, ATR initiates a cascade of downstream kinase activations, beginning with checkpoint kinase 1 (CHK1)<sup>143</sup>. Activated CHK1 coordinates cell cycle progression and DNA repair by phosphorylating and activating numerous target proteins<sup>144</sup>. It induces cell cycle arrest<sup>145</sup> and prevents replication fork collapse by delaying replication origin firing to allow time for handling unrepaired DNA damage, modulating key replication components, or regulating the availability of deoxyribonucleotides<sup>146</sup>. Therefore, it prevents under-replicated DNA regions from progressing beyond the S-phase, and it is also crucial for stabilizing stalled replication forks and promoting fork restart during RS<sup>144</sup>.

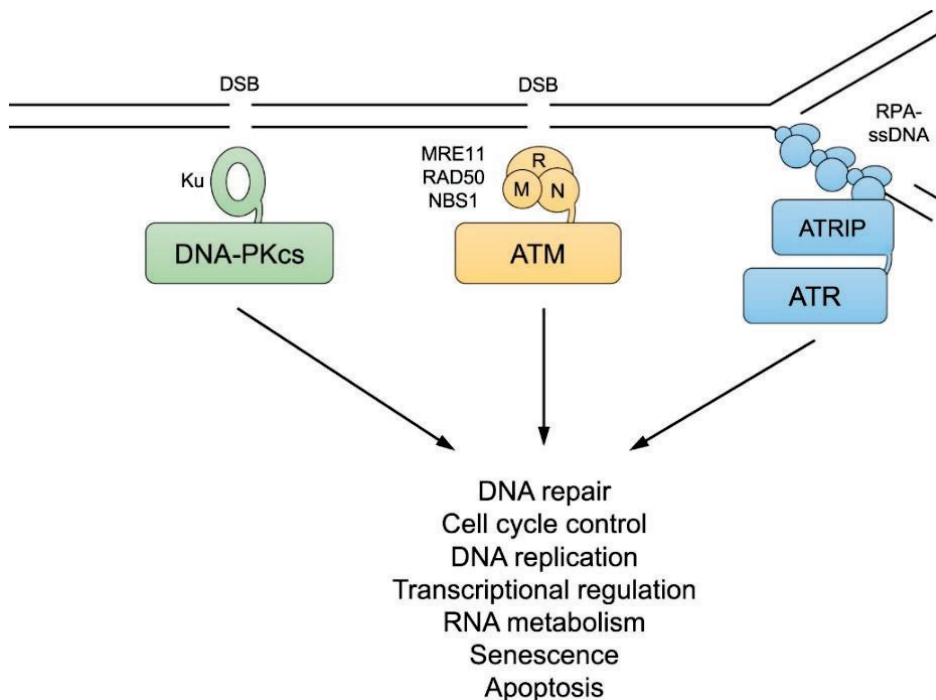


**Figure 18. Scheme of recruitment, activation, and consequences of DNA-PK, ATM, and ATR kinase pathways.**

Image obtained from Blackford *et al.*<sup>135</sup>

Altogether, depending on the lesion's nature and time, a sensing mechanism is activated in a tightly regulated manner. When activated, they create a time window through their involvement in checkpoint signaling and cell cycle progression. Depending on the nature and the time of the lesion, the cell cycle can be arrested at G1/S, intra-S, or G2/M transitions. The G1/S checkpoint is believed to be controlled primarily by ATM rather than ATR. By contrast, both ATM and ATR contribute to the establishment and maintenance of the intra-S and G2/M checkpoints<sup>135</sup>. This way, they enable the recruitment and action of the DNA repair mechanism, as well as its coordination with DNA replication and transcription processes<sup>135,147</sup>. Alternatively, if the DNA damage is too extensive to handle, they can promote cell senescence or apoptosis<sup>116,139</sup>.

Interestingly, these three kinase pathways are partially interconnected. For instance, many ATM substrates can also be phosphorylated by both ATR, in response to RS, and by DNA-PK, in cases such as H2AX phosphorylation<sup>135</sup>. Furthermore, in some cases, the ATM pathway acts upstream of ATR and promotes its recruitment, as is the case of the IR-damaged chromatin<sup>148</sup>.

In parallel, other important mechanisms act as DNA damage sensors. Due to its importance in this thesis project, we will highlight the case of poly(ADP-ribose) (PARP) enzymes<sup>149</sup>. PARP proteins are recruited to diverse types of DNA lesions (SSBs and DSBs) and catalyze the transference of poly(ADP-ribose) (PAR) to other proteins, as well as itself, in a process called PARylation<sup>150</sup>. This promotes the recruitment of different proteins to sites of DNA damage that cause several effects on DNA integrity and genome stability<sup>151</sup>. First, PARP promotes chromatin decompaction both by the direct action of the PARylation on the surrounding, as its negative charge causes the relaxation of chromatin<sup>150</sup>, and by the recruitment of remodeling factors<sup>152</sup>. Second, PARP is involved in the activation and recruitment of a variety of DNA damage response mechanisms, including SSB repair<sup>153</sup> and DSB repair<sup>154</sup>. Third, PARP activity is also associated with the DNA replication process and DNA replication forks. In this regard, it binds to different proteins involved in DNA replication<sup>155</sup>, and it has also been proven to get activated upon RS<sup>156</sup>.

### 3.2.4 Chromatin and DNA damage response.

Importantly, cellular response to DNA damage necessarily occurs in the context of an organized chromatin environment. Therefore, chromatin structure is highly reorganized in response to DNA damage. This facilitates a favorable environment for the accurate repair of DNA damage<sup>157</sup>. Numerous alterations of chromatin structure have been implicated in DNA Damage repair, including DNA methylation<sup>158</sup>, incorporation of histone variants such as H2AX and H2AZ<sup>159,160</sup> or histone PTMs<sup>161</sup>. Of note, after DNA damage, a cascade of histone PTMs, including phosphorylation, methylation, acetylation, and ubiquitylation is induced to open the chromatin environment and enable the assembly of mediator and effector proteins of DDR pathways<sup>161,162</sup>. For instance, phosphorylation of the H2AX histone variant ( $\gamma$ H2AX) occurs upon DSBs and is key in the sensing and activating of the DNA repair mechanisms<sup>160</sup>.

Interestingly, histone acetylation has been linked to DNA damage repair in the literature. Several histone acetyltransferases have been demonstrated to be implicated in DNA repair processes, such as Esa1<sup>163</sup>, Hat1<sup>164</sup>, and Gcn5<sup>165</sup>. Subsequently, it has been shown that acetylation levels are tightly controlled to regulate chromatin relaxation near DSB directly and to participate in the recruitment of nucleosome remodeling factors that also promote chromatin accessibility and permit DNA repair<sup>166</sup>. Furthermore, the histone acetylation can intervene in the DNA repair pathway choice. The histone acetylation marks, their corresponding acetyltransferases, and their involvement in the DNA damage response were collected by Aricthota *et al.*<sup>166</sup> in 2022 and can be found in **Table 2**.

**Table 2. List of acetyl-lysine modifications of histones with roles in DSB signaling and repair.**

Table adapted from Aricthota *et al.*<sup>166</sup>

Histone Acetylation	Acetyltransferase	Function in DDR
H1K85ac	PCAF	Decreases immediately post DNA damage. Promotes heterochromatin protein 1(HP1) recruitment leading to condensed chromatin
H2AK15ac	Tip60	Peaks at S/G2, reduced at sites specifically repaired by NHEJ. Tip60 dependent H2AK15ac regulates DSB repair pathway choice by inhibiting H2AK15Ub and binding of 53BP1 thus, promoting HR

H2AXK5ac	TIP60	Decreases the spread of $\gamma$ H2AX-P upon damage. Aids in NBS1 accumulation at the damaged regions via H2AX exchange, thus aiding in ATM signaling.
H2AXK36ac	p300/CBP	Constitutive acetylation, does not increase on radiation damage, however, promotes IR survival independently of $\gamma$ H2AX phosphorylation
H2BK120ac	SAGA acetyltransferase	Upon DSB induction H2BK120ub to H2BK120ac switch irrespective of the region of DSB. May help in nucleosome remodeling.
H3K9ac	GCN5, PCAF	Reduces upon DNA damage, helps in localization of Swi/SND complex to $\gamma$ H2AX containing nucleosomes. Obstructs ATM activation in stem cells leading to IR sensitivity.
H3K14ac	GCN5	Increases in response to DNA damage helps in localization of Swi/SND complex to $\gamma$ H2AX containing nucleosomes. Stimulated by HMGN1 and required for the activation of ATM.
H3K18ac	p300/CBP, GCN5	Recruitment of SWI/SNF and Ku at initial timepoints during G1 phase, later deacetylation by Sirt7 leads to loading of 53BP1 to facilitate effective NHEJ.
H3K56ac	p300/CBP	Both reduction and increase observed post DNA damage, deacetylated by Sirt6 and Sirt3 promotes NHEJ by recruiting SNF2H and 53BP1 to the DSB sites. Deactivates checkpoint to facilitate recovery and chromatin assembly.
H4K5ac, H4K8ac	Tip60-Trap	Repair by HR by facilitating recruitment of MDC1, BRCA1, 53BP1, and RAD51.
H4K12ac	p300/CBP	Recruitment of SWI/SNF complex, KU70/80, and repair by NHEJ. H4K12 was reduced at AsiSI-induced DSBs.
H4K16ac	Tip60-Trap MOF1	Biphasic response at the DSBs, facilitates both NHEJ and HR. Initial decrease and then increase at later timepoints. Abrogation of MDC1, 53BP1, and BRCA1 foci in the absence of MOF1.

### 3.2.5 DDR and NC

The information regarding DNA damage response pathways or RS in the context of NUT Carcinoma is scarce. However, there is a study in which a panel of NC cells was analyzed to study their molecular and genetic features. Through an NGS approach, they identified a recurring mutation in the DNA-helicase gene RECQL5 in 75% (9/12) of the cell lines studied. Furthermore, they also obtained mutation signature and network analyses consistent with a possible but not demonstrated general failure in DNA repair<sup>59</sup>. As this is an isolated study in the bibliography, further information and analysis need to be performed to better understand these results.

### 3.3 Replication stress as a source of DNA damage.

As discussed in previous sections, errors in the replication process are one of the main endogenous sources of DNA damage<sup>125,126</sup>. Therefore, its fidelity is instrumental in the maintenance of genome integrity. DNA replication is a multifaceted process involving the sequential activation of thousands of replication origins and the coordinated functioning of DNA polymerases, helicases, and other proteins forming the replisome at the replication forks<sup>167,168</sup>. Although the replication machinery is very accurate and different mechanisms are responsible for the correct replication process<sup>169</sup>, replication forks encounter obstacles along the DNA that disturb or impede the proper function of the DNA replication process, generating a state of RS in cells<sup>170</sup>. This can promote replication fork stalling and even collapse which can cause DNA damage and genome instability<sup>168,171</sup>.

#### 3.3.1 Mechanisms of replication fork rescue

RS, when detected by the cell machinery, induces several responses to stabilize, repair, and restart fork progression to ensure successful completion of the replication process<sup>168</sup>. First, the replication fork stalling is involved in the decoupling of replisome machinery, causing the exposure of ssDNA at forks<sup>172</sup>. As previously explained (see section **3.2.3. DNA damage sensors** of Introduction), ssDNA gets coated by RPA protein, and this activates the ATR pathway, which causes the arrest in the cell cycle<sup>145</sup> and the suppression of origin firing and RPA exhaustion<sup>173</sup> to facilitate the stabilization and restart of stalled replication forks<sup>174</sup>. It also regulates the activity of different fork repair or bypass mechanisms<sup>175</sup>.

ATR activation and the subsequent cell cycle arrest and fork stabilization are followed by the activation of mechanisms to remodel the stalled forks<sup>168</sup> (**Figure 19**). For instance, fork reversal is an important remodeling event in which forks are turned into four-way junction structures to slow down their velocity and facilitate the action of DNA damage repair or tolerance mechanisms<sup>176</sup>. Another mechanism to bypass fork stalling is repriming by PrimPol, a primase that generates *de novo* primers ahead of stalled forks, restarting the synthesis beyond the lesion<sup>177</sup>. These gaps can be further filled by DNA damage tolerance (DDT) mechanisms such as error-prone

translesion synthesis (TLS) or error-free template switching (TS)<sup>178</sup>. Alternatively, cells also modulate origin firing to ensure a successful replication. Origin firing is the event that initiates DNA synthesis at a specific genomic site during the DNA replication process. Cells account for many origins along their genomes, whose activation is tightly regulated to ensure a proper and accurate DNA replication that only occurs once per cell division<sup>179</sup>. Most of the replication origins spread along the genome are usually dormant. When the progression of replication forks is somehow impeded, cells can activate some dormant origins in the surrounding of the stalled fork to participate in the resolving process<sup>180</sup>.

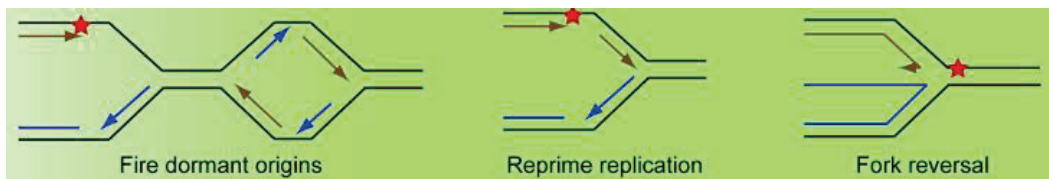


**Figure 19. Scheme of fork rescue mechanisms.**

Image from Zeman *et al.*<sup>170</sup>

In some cases, despite all the mechanisms above, if the RS persists or the RS response proteins are not functional, the replication fork fails to be restarted or bypassed, and eventually collapses<sup>170</sup>. Fork collapse is the unloading of the replisome from the genome and, as loading of new DNA helicases cannot occur once S phase has started to avoid re-replication<sup>181</sup>, it impedes a complete DNA replication, and causes generate genome instability and DSBs that can lead to mutations and abrogation of cell viability<sup>182</sup>. It has been demonstrated that this process of collapsing is accelerated in the context of ATR pathway deficiency<sup>183</sup>.

### 3.3.2 Sources of RS

Several endogenous and exogenous events can affect the correct development of fork progression during DNA replication and become a source of RS. Some of the main RS sources are depicted below.

Different events along DNA act as physical barriers that perturb the correct progression of the replication fork<sup>168,170,184</sup>. These physical barriers include DNA lesions and adducts from a wide variety of sources, such as UV, IR, ROS, or metabolites<sup>122,127</sup>; DNA secondary structures such as hairpins, cruciform structures, or G-quadruplexes<sup>185,186</sup>; or nicks, gaps, and stretches of ssDNA<sup>170</sup>.

Condensed chromatin can also act as a physical barrier that impedes fork progression and causes RS in cells<sup>187</sup>. Fork progression depends on chromatin remodelers to regulate the accessibility of nascent chromatin to recombination and repair factors<sup>188</sup>. For instance, when alterations in chromatin remodeling factors such as SWI/SNF complex occur, RS can arise<sup>189</sup>. In addition, epigenetic changes such as the incorporation of histone variants, DNA methylation, or histone modifications can also alter chromatin structure and accessibility, interfering with replication machinery, and causing fork stalling<sup>187</sup>. For instance, the loss of macro H2A deposition has been associated with an increase of H4K20me2 at stalled forks, causing a detrimental effect in fork protection<sup>190</sup>, and methylated H3K27 has been shown to be involved in the recruitment of MUS81 to stalled forks, an endonuclease which creates DSBs to facilitate HR-mediated fork restart<sup>191</sup>. Of note, histone acetylation has also been involved in replication fork protection, for example, HAT1 is involved in the protection of stalled forks from degradation, avoiding genome instability derived from RS<sup>192</sup>.

Additionally, the depletion of fundamental elements to conduct DNA replication, such as nucleotides, is also a source of RS. Although the nucleotide pool is tightly regulated, alterations have been reported to be associated with increased mutagenesis and genomic instability<sup>193</sup>. Furthermore, a decrease in the nucleotide pool can cause misincorporations during replication, generating DNA lesions that may be a source of RS in the subsequent cell cycle<sup>194</sup>. In line with this, mutations in any replisome

component can also contribute to a dysfunctional fork progression and, thus, RS status in cells<sup>168</sup>. For example, mutations in the catalytic subunit of DNA Polymerases such as POLD1 can lead to fork stalling and genome instability<sup>195</sup>. Furthermore, mutations in the minichromosome maintenance (MCM) helicase complex have also been demonstrated to cause fork stalling or collapse<sup>196</sup>.

Finally, it is worth highlighting the implication of transcription-replication conflicts (TRCs) as another important source of RS<sup>197</sup>. Transcription and replication machinery frequently compete for the same DNA template, which can lead to conflicts when they encounter each other. These collisions can have two orientations depending on the direction in which both replication and transcriptional machinery work: co-directional or head-on<sup>198</sup> (**Figure 20**). Although replication fork progression may be affected by collisions in both orientations, data suggest that the consequences of collisions are more dramatic in the head-on orientation<sup>199,200</sup>. Several features can interfere with and promote TRCs, including DNA supercoiling, secondary structures such as hairpins or G-quadruplexes, or RNA-DNA hybrids from between de nascent RNA and the homologous DNA<sup>197</sup>. In the following section, we will especially focus on RNA-DNA hybrids.

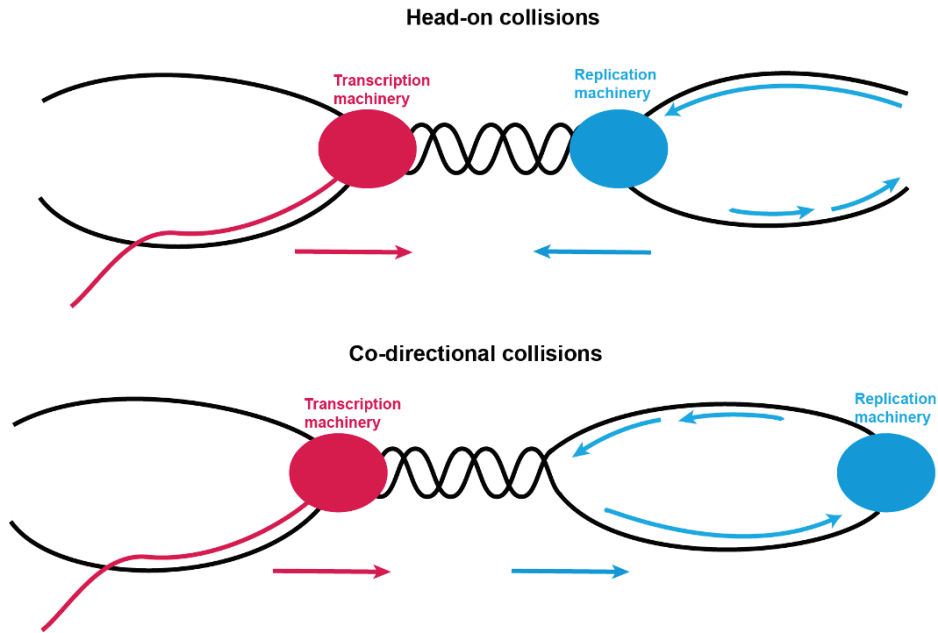


**Figure 20. Scheme of the different directionalities of TRCs.**

### 3.3.3 R-loops as a critical player in the RS

The RNA:DNA hybrids, when considered altogether with the displaced single-strand DNA, are called R-loops<sup>201</sup> (**Figure 21**). They form due to the hybridization of the nascent transcript emerging from the transcription machinery and the complementary DNA template<sup>202</sup>. Its accumulation due to TRC is associated with different events causing genome instability such as DNA damage<sup>203</sup> or transcription elongation defects<sup>204</sup>.

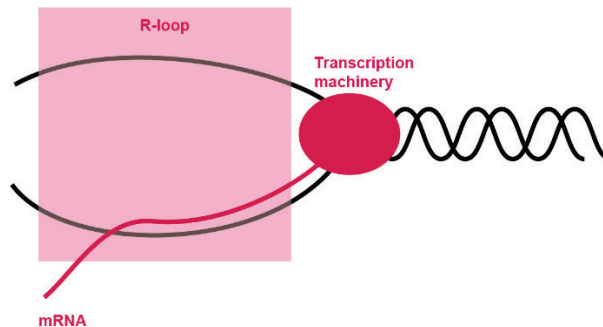


**Figure 21. Scheme of R-loop structure.**

Although considered mere accidental by-products of transcription malfunction for many years, it has recently increased the reported information claiming a class of R-loops with a critical role in a variety of biological processes<sup>202,205</sup> including gene regulation<sup>206,207</sup>, DNA repair<sup>208,209</sup> and chromatin structure<sup>205</sup>. Therefore, their formation, location, and removal must be tightly regulated to ensure cell viability and functionality, although little is known about the specific mechanisms involved<sup>202,210</sup>.

Three main ways have been found to avoid the detrimental accumulation of R-loops in cells<sup>211</sup>. First, prevention by proteins that bind to nascent RNA and avoid R-loop formation such as processing factors or topoisomerase 1<sup>212</sup>. Second, removal by nucleases such as RNase H1 (RNH1), an enzyme that specifically degrades RNA portion of RNA:DNA hybrids<sup>213</sup>. Third, repairing either the damage they generate or the source that causes them<sup>209,214</sup>.

#### 3.3.4 The bidirectional regulation between RS and chromatin structure.

Chromatin structure and DNA replication are connected to ensure the proper unpackage of DNA to enable replication, as well as the subsequent re-packaging<sup>215</sup>.

On the one hand, chromatin structure regulation plays a fundamental role in DNA replication. Thus, as previously discussed in depth, chromatin structure dysregulation such as chromatin remodelers<sup>189</sup>, histone variants incorporation<sup>190</sup>, or histone PTMs<sup>191,192</sup> can interfere with replication machinery, lead to replication stress, and fork stalling or collapse (see **3.3.2 Sources of RS** of Introduction).

Remarkably, the role of chromatin structure also affects R-loop homeostasis. For instance, the SWI/SNF chromatin remodeling complex has been demonstrated to participate in the resolution of R-loop from transcription-replication conflicts, as they suppress R-loop accumulation<sup>211</sup>. Furthermore, histone modifications, especially histone acetylation, are also implicated in R-loop prevention. For instance, Sin3A histone acetyltransferase has been demonstrated to interact with the RNA binding factor THO to suppress R-loops, and thus, DNA damage and replication stress<sup>216</sup>.

It is important to highlight the bi-directionality of the connection between RS and epigenetic regulation. Apart from the aforementioned implication of chromatin regulation in RS and R-loop accumulation, R-loop structures have been reported to affect epigenetic processes such as DNA methylation<sup>206,217</sup> or histone modification<sup>218</sup>. This way, R-loop structures participate in gene expression regulation and, therefore, cell behavior<sup>219</sup>. Furthermore, R-loops participate in transcription activation through the recruitment of chromatin remodeling factors and the modulation of the chromatin structure of promoters<sup>220</sup>. Ultimately, R-loops also intervene in chromatin condensation and heterochromatin formation<sup>221</sup>. Altogether, this evidence depicts the importance of R-loops in the regulation of gene expression through modulation of chromatin structure.

### **3. 4 The implication of RS in cancer.**

Genomic instability is a hallmark of cancer, contributing significantly to cancer initiation and progression<sup>222</sup>. It is a pan-cancer strategy to accumulate defects in the DDR pathways that enable tumor evolution and progression, as a certain degree of mutation accumulation confers key cancerous characteristics such as sustained proliferation by oncogene activation, evasion of tumor growth suppression, resistance to cell death, and promotion of invasion and metastasis<sup>223,224</sup>. Specifically, replication stress is a source of DNA alterations and genome instability. Therefore, it can significantly contribute to cancer progression<sup>170</sup>. Defects in the RS response pathways promote cancer progression. For instance, haploinsufficiency of CHK1, a member of the ATR pathway, contributes to tumorigenesis<sup>225</sup>. Additionally, other sources of replication stress can promote cancer development. For example, nucleotide deficiency has been demonstrated to promote genomic instability in the early stages of cancer development<sup>193</sup>.

In many cases, high RS observed in cancer cells occurs due to oncogene induction<sup>226</sup>. It promotes a hyperproliferative state by upregulating transcription factors that stimulate pro-proliferative gene transcription<sup>227</sup>. The increased transcription, together with the increased proliferation (and therefore, replication), is a source of RS. Furthermore, the hyper-replicative state can lead to the depletion of nucleotide pools<sup>193</sup>. Thus, the activation of

oncogenes, such as MYC<sup>228</sup> or Cyclin E<sup>229</sup> generate a state of RS, a hallmark of cancer<sup>227,230</sup>.

Due to their promotion of genome instability and RS, R-loop structures are potential drivers of cancer. Although further research is needed to uncover its specific role in cancer initiation, progression, and maintenance, several studies establish a connection between R-loop accumulation and cancer. For instance, *BRCA1* and *BRCA2* loss, which is a well-known event occurring in several cancer types such as breast and ovarian<sup>231</sup>, prostate<sup>232,233</sup> or pancreatic cancer<sup>233</sup>, is linked to an increased R-loop accumulation that causes DSBs<sup>234,235</sup>. Furthermore, some genes involved in the prevention of R-loop accumulation have been reported to be mutated in cancer contexts<sup>205</sup>. Nevertheless, the connection is still weak and indirect, and further investigation needs to be performed.

### 3.5 Targeting DDR as a therapeutical strategy in cancer

The accumulation of genome instability and the high RS observed in cancer cells are instrumental in the tumor evolution, acquisition of cancerous trades, and resistance to therapies. However, it also causes the dependency of cancer cells on different DDR pathways<sup>224</sup>. These vulnerabilities, being a differentiating factor between cancer and healthy cells, have emerged as an opportunity to develop cancer therapies based on DDR inhibitors (DDRi)<sup>129</sup>. To date, several DDRi targeting PARP, ATR, WEE1, ATM, or CHK1/2, have been developed<sup>236,237</sup>. PARP inhibitors (PARPi) are the first DDRi approved for their use in the clinical setting<sup>236,238</sup>. They are small molecules inhibiting PARP enzymes, that, as previously explained, play a critical role in DNA damage repair, particularly recognizing DNA lesions and recruiting the DNA repair machinery by adding PAR chains<sup>151</sup>. The rest of DDRi are currently going through different stages of clinical trials.

Initially, DDRi were explored to overcome chemotherapy and radiotherapy resistance, taking advantage of the synthetic lethality<sup>236</sup>. Synthetic lethality is a concept where the simultaneous disruption of two genes or pathways leads to cell death, while disruption of one alone does not<sup>239</sup>. Frequently, chemo- and radiotherapy resistance occurs due to DDR mutations that abrogate a specific DDR pathway<sup>240,241</sup>. In this context, compensatory mechanisms must

be activated, and this newly created vulnerability can be exploited<sup>236</sup>. In this regard, for instance, PARP inhibition has been demonstrated to modulate resistance to temozolomide in glioblastoma<sup>242</sup>. Nowadays, the use of DDRis in cancer is being expanded beyond chemo- and radiotherapy combinatorial treatment and resistance. However, synthetic lethality has been kept as the main strategy for their exploration and usage<sup>243</sup>. Of note, another example of synthetic lethality is the effect of PARP inhibitors in HR-deficient cell contexts. It has been demonstrated that the inhibition of PARP leads to the persistence of SSBs that subsequently turn into DSBs<sup>244</sup>. Those lesions are typically repaired by the HR mechanism. In the context of HR deficiency, the accumulation of DNA breaks due to PARPi will not be successfully overcome and, ultimately, that would lead to an abrogation of cell viability<sup>245,246</sup>. Furthermore, in recent years PARPi has demonstrated combinatorial efficacy with ATR inhibitors (ATRi) causing replication fork stalling and collapse in different cancer types<sup>247</sup>.

# HYPOTHESIS AND OBJECTIVES



The main objective of this thesis is to understand the molecular mechanism underlying NC oncogenesis and to identify targetable vulnerabilities that could be transferred to the clinics and ultimately impact NC patients' outcomes. Different strategies have been followed to achieve this.

Firstly, we hypothesized that the megadomains of acetylated histones, linked with BRD4-NUT fusion, might be associated with increased transcription in NC cells. This potential increase in transcription, coupled with the upregulation of pro-proliferative genes that could result in heightened replication, would lead to conflicts between transcription and replication processes within these cells. Consequently, these transcription-replication conflicts could cause an accumulation of R-loops and induce a high level of replication stress in NC cells. If this is the case, these cells must rely on factors involved in the RS response pathway, and certain DNA damage response inhibitors could decrease the viability of these cells (**Figure 22**).

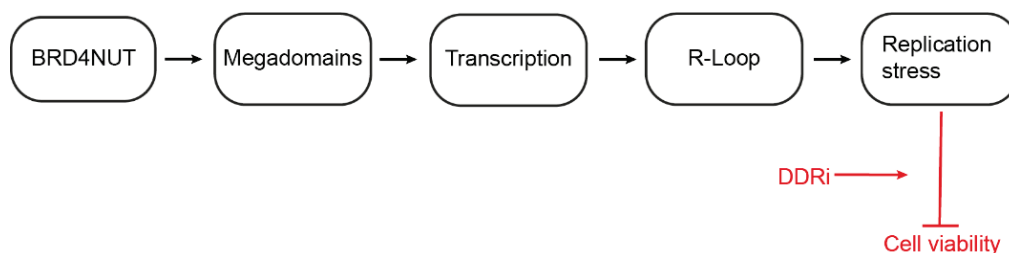


**Figure 22. Schematic representation of RS-focused hypothesis.**

Furthermore, considering the consistent impact of MYC overexpression as one of the few driving events in NC, we aimed to investigate the potential effects of MYC inhibition in NC models. We hypothesized that inhibiting MYC in NC cells would hinder their pro-proliferative and pro-apoptotic effects and impede the inhibition of cell differentiation. We have access to a promising novel MYC inhibitor called OMO-103 (Omomyc), which has completed phase 1 clinical trials with minimal toxicities and promising effects<sup>248</sup>. Currently, it is undergoing phase 2 clinical evaluation. Therefore, we aim to explore the effect of OMO-103 on NC cell's viability (**Figure 23**).

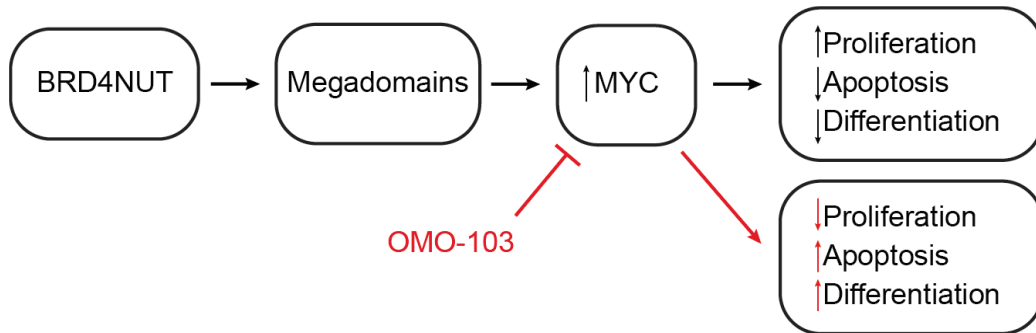


**Figure 23. Schematic representation of MYC-driven hypothesis.**

Moreover, we aim to broaden our understanding and investigate the effects of various drugs on this incurable and under-researched type of cancer. Given that the lungs are a prevalent site for NC, we hypothesized that chemotherapeutic agents currently approved for subtypes of lung cancer could be effective in treating NC.

Therefore, the specific objectives of this thesis are:

1. To study the impact of BRD4-NUT fusion on RS in NC cells.
  - 1.1. To understand whether the fusion protein is associated with RS in NC cells.
  - 1.2. To characterize the molecular mechanism underlying the potential link between BRD4-NUT fusion protein and RS in NC cells.
  - 1.3. To explore RS as a targetable vulnerability for NC treatment both *in vitro* and *in vivo*.
2. To study the effect of MYC inhibition in NC cells.
  - 2.1. To assess the sensitivity of NC cells to OMO-103 *in vitro* and *in vivo*.
  - 2.2. To characterize the phenotypic impact of OMO-103 in NC cells.
3. To explore the effect of chemotherapeutic agents approved for lung cancer in NC models.

# MATERIALS AND METHODS



## Cell lines and culture conditions

Four patient-derived NC cell lines were used: NC1015<sup>29</sup>, NC14169<sup>31</sup>, PER403<sup>1</sup>, and PER624<sup>249</sup>. All the molecular and clinical information published about the cell lines has been gathered in **Table 3**. In addition, the human embryonic kidney cell line HEK293T<sup>250</sup> was used to generate the inducible ectopic expression models.

**Table 3. Information about patient-derived samples.**

F: Female; M: male

Cell line	Sex	Age	Location	Translocation
PER403	F	11	Possible thymic	t(15;19) (q14;p13.1): BRD4-NUT (Exon 11:Exon 2)
PER624	F	16	Lung	t(6;19) (q13;p13.1): Cryptic BRD4-NUT (Exon15: Exon 2)
NC1015	M	na	Lung	t(15;19)BRD4-NUT
NC14169	na	na	na	t(15;19)BRD4-NUT

NC1015, NC14169, and HEK293T cells were maintained in Dulbecco's modified Eagle's medium (DMEM) (L0106-500, Biowest). PER403 and PER624 were cultured in Roswell Park Memorial Institute (RPMI) 1640 medium (L0501-500, Gibco). All of them were supplemented with 10% heat-inactivated fetal bovine serum (FBS) (10270106; Gibco), 2 mM L-glutamine (X0550-100, Biowest) and 1% penicillin-streptomycin (15140122, Gibco). Cell cultures were incubated at 37°C in 5% CO<sub>2</sub> and 95% humidity.

The ectopic overexpression (OE) models of green fluorescent protein (GFP), BRD4s, NUT, and BRD4-NUT were generated with the Tet-on system<sup>251</sup> in HEK293T cells. First, HEK293T cells were infected with the rtTA virus to generate a stable-expressing cell line maintained with 200ng/mL hygromycin selection (A2175,0020, Panreac). Then, HEK293T cells stably expressing rtTA were infected with constructs of GFP, BRD4s, NUT, or BRD4-NUT under the control of the Tet response element (TRE). After this second infection, cells were selected with 1 µg/mL puromycin (BP2956, Fisher Scientific). This system allows for the induction of the expression of the construct through the binding of doxycycline (an analog of tetracycline) to rtTA regions (**Figure 24**). Thus, cells were treated with doxycycline (HY-N0565B, MedChem) (0,1 µg/mL) to induce the expression of the constructs and collected 72 hours later.

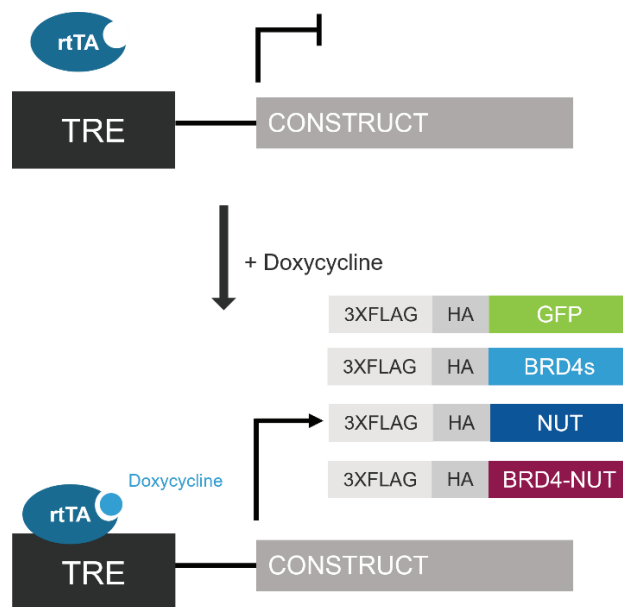


**Figure 24. Scheme of the OE constructs.**

The experiments used cell lines that did not exceed 15 passages after thawing. All cell lines were periodically tested for Mycoplasma contamination by PCR using the following primers:

Forward: 5' GGCGAATGGGTGAGTAACACG 3'

Reverse: 5' CGG ATA ACGCTTGCGACCTATG 3

## Drug treatments

Throughout the thesis project, various small molecules have been used as needed.

First, MZ1 (HY-107425, MedChemexpress) was used at 100nM for 4 hours to degrade the BRD4-NUT fusion protein. Based on the Proteolysis Targeted Chimeras (PROTAC) system, this small molecule is a heterobifunctional compound containing two ligands connected by a linker. One ligand binds BRD4, and the other brings it to the E3 ubiquitin ligase VHL, promoting the degradation via proteasome. In this way, MZ1 promotes the selective degradation of BRD4, and thus, the BRD4-NUT fusion expressed in NC cell lines potently and rapidly<sup>252</sup> (**Figure 25**).

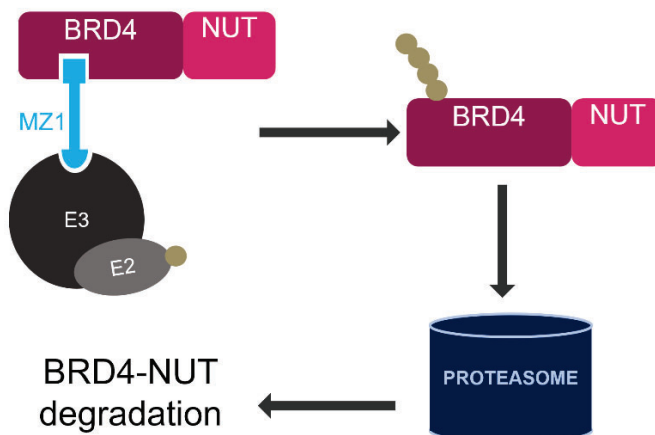


**Figure 25. Mechanism of action of MZ1.**

Similarly, a PROTAC system-based p300/CBP degrader named dCBP-1 (HY-134582, MedChemexpress) was used to degrade p300. In this case, one of the ligands of the heterobifunctional compound binds p300/CBP, and the other delivers it to the E3 ubiquitin ligase VHL, promoting the selective and potent degradation of p300<sup>253</sup> (**Figure 26**). When indicated, cells were treated with 1  $\mu$ M of dCBP-1 for durations between 2 and 24 hours. Finally, 4 hours was selected as the standard time point for further experiments.

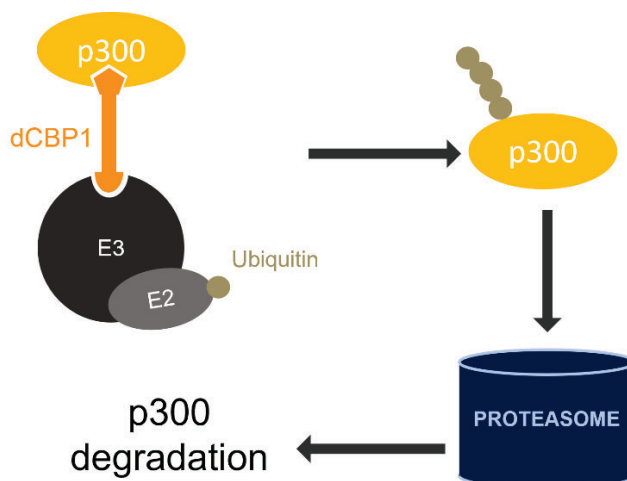


**Figure 26. Mechanism of action of dCBP-1.**

To inhibit RNA transcription, we used Actinomycin D (ActD) (A4262, Sigma-Aldrich). This molecule prevents the progression of the RNA polymerase by intercalating into DNA and forming a stable complex with it<sup>254</sup>. ActD was used, when indicated, at 500nM for 4 hours.

Additionally, a focused DDRi screening and a further IC<sub>50</sub> validation of several candidates were performed. The drugs used are listed in **Table 4**. All the stocks were prepared at 10mM and used as indicated in the Results section.

**Table 4. Table of DDRi for the focused screening.**

Category	Drug	Reference	Provider
DNA-Pki	KU-57788	HY-11006	MedChemexpress
	PIK-75	HY-13281	MedChemexpress
	AZD7648		Kindly provided by Violeta Serra's group
ATMi	KU-55933	HY-12016	MedChemexpress
	AZD0156		Kindly provided by Violeta Serra's group
ATRi	VE-821	HY-14731	MedChemexpress
	AZD6738/Celarasertib		HY-19323
WEE1i	AZD1775		Kindly provided by Violeta Serra's group
	PD0166285		Kindly provided by Violeta Serra's group
CDK1i	AZD-5438	HY-10012	MedChemexpress
	Dinaciclib		Kindly provided by Violeta Serra's group
CHK1i	CCT244747	HY-18175	MedChemexpress
	SCH900776	HY-15532	MedChemexpress
CHK2i	BML-277	HY-13946	MedChemexpress
PARPi	Olaparib	HY-10162	MedChemexpress
	Niraparib	HY-10619	MedChemexpress
	Talazoparib		Kindly provided by Violeta Serra's group
Topoisomerase II inhibitor	Doxorubicin	D1515	Merck Life Science
Alkylating agent	Temozolomide	S1237	Selleck Chemicals

To modulate MYC activity, we used an MYC inhibitor, OMO-103, developed and provided by Dr. Laura Soucek's group at VHIO. OMO-103 competitively

inhibits MYC activity by homodimerizing or heterodimerizing with MYC or MAX and thus displacing MYC-MAX functionally active heterodimer from its regulated regions<sup>255</sup> (**Figure 27**). Specific concentrations used to treat cells are specified in the Results sections.

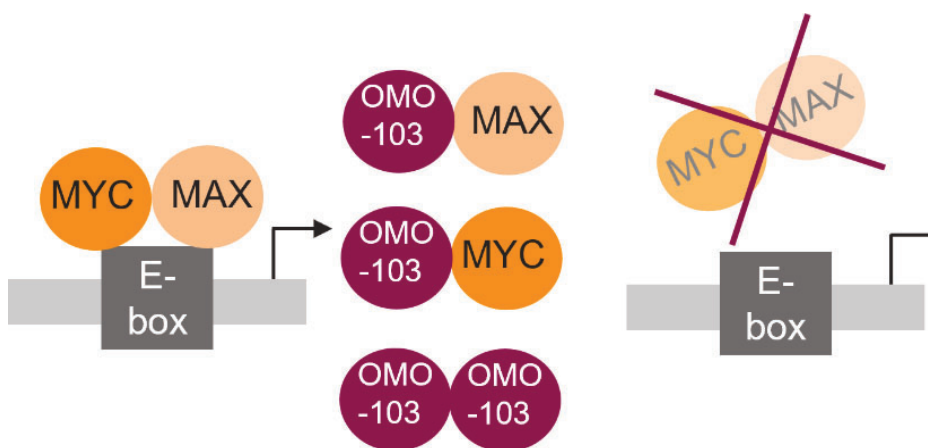


**Figure 27. Mechanism of action of OMO-103.**

Finally, two chemotherapeutic drugs were also tested: lurbinectedin (HY-16293, MedChemexpress), a drug that covalently binds to DNA, generating DNA adducts<sup>256</sup>, and irinotecan (HY-16562, MedChemexpress), a drug that inhibits topoisomerase I<sup>257</sup>.

## Patient samples information

Despite the scarce availability of samples, we obtained paraffin-embedded slides of 4 patients, whose clinical information on the collected patient samples is gathered in **Table 5**.

**Table 5. Patient information of paraffin samples.**

	Sex	Treatment	Tumor	Primary organ	Biopsy	Hospital
PATIENT 1	H	CC-90010 (BETi)	Primary	Lung	Lung	Hospital Vall d'Hebron
PATIENT 2	H	BET115521 (BETi)	NA	NA	NA	Hospital Virgen de la Macarena

PATIENT 3	H	BET115521 (BETi)	Primary	Lung	Lung	Hospital del Mar
PATIENT 4	H	CC-90010 (BETi)	Metastasis	Lung	Skin	Hospital Vall d'Hebron

Patient samples were obtained with informed written consent. The studies were conducted in accordance with the Declaration of Helsinki. Human samples were handled and processed following the institutional guidelines under protocols approved by the Institutional Review Boards (IRBs) at the Vall d'Hebron Hospital prior to tissue acquisition.

## Immunofluorescence

Immunofluorescence assays were performed to examine the proteins' localization, pattern, and intensity per nucleus of interest upon different experimental conditions.

Different amounts of cells were seeded on coverslips in a 24-multiwell plate: 50000 NC1015, 100000 PER403, 30000 NC14169, 30000 PER624, and 10000 for each OE cell line.

After the addition of the corresponding treatments, cells were fixed with 4% paraformaldehyde (PFA) (sc-281692, Santa Cruz Biotechnology) for 10 minutes at room temperature (RT), permeabilized with 0.3% Triton X-100 (93443, Sigma Aldrich) – phosphate-buffered saline (PBS) for 5 minutes and blocked with 1% bovine serum albumin (BSA) (A6588, Panreac Applichem) - PBS for 30 minutes at RT. Then, cells were incubated with the indicated primary antibodies (**Table 6**) overnight at 4°C. After three washes with PBS, cells were incubated with the conjugated secondary antibodies (**Table 6**) for 1 hour at RT covered from light. After three more washes with PBS, 0.5µg/mL of 4',6-Diamidino-2-phenylindole (DAPI) (D9542, Merck Life Science) was used for nuclear counterstaining. Finally, the coverslips were mounted on microscope slides using Fluoromount (0100-01, Southern Biotech).

In the specific case of RPA pS33 and S9.6 staining, cells were seeded on 1% gelatin-precoated coverslips (ES-006-B, Merck Life Science) and subjected to pre-extraction with CSK buffer (25mM Hepes pH 7.5, 50mM NaCl, 23mM MgCl, 300mM sucrose and 0.5% PBS-Triton X-100) for 3 or 9 minutes respectively before PFA fixation to eliminate the cytoplasm and facilitate nuclear staining and further analysis.

Of note, S9.6 recognizes RNA:DNA hybrids from R-loops structures and RNA:RNA hybrids<sup>258</sup>. To overcome this uncertainty, ribonuclease H1 (RNH1), able to specifically degrade R-loop structures<sup>211</sup>, was used as a negative control. Several coverslips were incubated with RNH1 (#M0297S, New England Biolabs) for 3 hours at 37°C after Triton incubation and before BSA blocking.

**Table 6. List of the antibodies used.**

Rb: Rabbit; Ms: Mouse. IF: Immunofluorescence; WB: Western blot.

Antigen	Host species	Application	Dilution	Reference
NUT	Rb	IF, WB	1:1000	3625S, Cell Signaling
pRPA S33	Rb	IF	1:500	A300-246A, Bethyl
pChk1 S317	Rb	WB	1:1000	2344T, Cell Signaling
Chk1	Ms	WB	1:1000	2360S, Cell Signaling
FLAG	Ms	IF	1:500	F3165, Sigma Aldrich
FLAG	Rb	WB	1:1000-5000	F7425, Sigma Aldrich
p300	Ms	IF	1:500	sc-48343, Santa Cruz Biotechnology
H3K27ac	Rb	IF	1:2000	Ab4729, Abcam
S9.6	Ms	IF	1:600	ENH001, Kerfast
BRCA2	Ms	WB	1:1000	OP95, Sigma Aldrich
γH2AX	Ms	IF	1:200	JBW301, Sigma Aldrich
RAD51	Rb	IF	1:2000	ab 133534, Abcam
cCaspase3	Rb	WB	1:1000	9664S, Cell Signaling
Involucrin	Ms	WB	1:1000	MS-126, Thermo Scientific
Tubulin	Ms	WB	1:1000-10000	T9026, Sigma Aldrich
H3	Rb	WB	1:1000-10000	ab1791, Abcam
Vinculin	Rb	WB	1:1000	ab129002, Abcam
Donkey Anti-Rabbit IgG (H+L), highly cross-adsorbed CF488A		IF	1:1000	BT-20015, Biotium
IgG (H+L) Highly Cross-Adsorbed Goat anti-Mouse, Alexa Fluor™ Plus 555		IF	1:1000	A32727, Invitrogen
Donkey Anti-Mouse IgG (H+L), highly cross-adsorbed CF488A		IF	1:1000	BT-20015, Biotium
Donkey Anti-Rabbit IgG (H+L) HRP		WB	1:1000-5000	711-035-152, Vitro
IgG (H+L) Cross-Adsorbed Goat anti-Mouse, HRP		WB	1:1000-5000	G21040, Invitrogen

CldU	Rat	DNA fiber assay	1:200	Ab6326, Abcam
IdU	Ms	DNA fiber assay	1:100	34758, Becton Dickinson
Donkey anti-Rat Cy3		DNA fiber assay	1:300	712-166-153, Jackson Immuno Research
Goat anti-Mouse Alexa Fluor 488		DNA fiber assay	1:300	A11001, Thermo Fisher Scientific

## Image analysis

Images obtained from Immunofluorescence or global transcription detection assays were captured using a Nikon C2+ confocal microscope and the NIS-Elements Advanced Research software with a CFI Plan Apochromat VC 60x/1.40 oil objective. Subsequent image analysis was performed using the Fiji ImageJ software. Nuclear regions were delimited with DAPI or Hoechst staining, and the total intensity of each stain was quantified within each nucleus. In all experiments, images were acquired considering a minimum of 90 cells per condition and replicate.

Data presentation and statistical analysis were performed using the GraphPad Prism 9 software, and the statistical significance of the data was determined by an ordinary one-way analysis of variance (ANOVA). Statistically significant differences are indicated with the p-value in every figure.

## Western blot.

Cell pellets obtained from different experimental conditions were washed with PBS to remove the residual culture medium.

### Standard WB protocol.

Cleaned cell pellets were lysed using 1% SDS lysis buffer (obtained from Cold Spring Harbor Protocols) containing 1% SDS, 50mM Tris-HCl pH8, 10mM EDTA pH8, and freshly added protease inhibitors (535140, Merck Life Science). Lysates were then sonicated using a Misonix s-3000-010 sonicator for 10 seconds at 1.5 potencies, and the amount of protein was quantified using the DC Protein Assay Reagents Package (#5000116, BioRad Laboratories). 15-40µg of protein were mixed with 6X loading buffer (250mM Tris-HCl pH 6.8, 10% SDS, 0.02% bromophenol blue, 50% glycerol, 20% β-mercaptoethanol) and boiled at 95°C for 5 minutes. Protein samples were resolved in SDS-PAGE gels (8-15% acrylamide) and ran in Tris-glycine-SDS (TGS) buffer (25mM Tris-OH pH 8.3, 192mM glycine and 5% SDS). Gels were then transferred to nitrocellulose membranes (1060002, Amersham) in transfer buffer (50mM Tris-OH, 396mM glycine, 0.1% SDS, and 20% methanol) for 60-120 minutes at 400mA. Membranes were blocked in 5% milk in TBS-T (25mM Tris-HCl pH 7.5, 137mM NaCl, and 0.1% Tween) for 30 minutes, and the indicated primary antibodies (**Table 6**) were incubated overnight at 4°C. After three washes of TBS-T, membranes were incubated for one hour at RT with horseradish peroxidase (HRP)-conjugated secondary antibodies (**Table 6**). Finally, after three washes, the membranes were developed with a substrate for HRP-enhanced chemiluminescence (ECL) (34580, Termofisher) or its extended duration version (34075, Termofisher), and protein bands were visualized in Amersham™ Imager 600 (GE Life Sciences).

### BRD4-NUT Western Blot

To precisely visualize the BRD4-NUT fusion protein, due to its large size, the standard WB protocol was adapted. A special lysis buffer, obtained from Rosencrance *et al.*<sup>107</sup> (10mM Tris-HCl pH 7.5, 150mM NaCl, 1mM EDTA, 1% SDS, and freshly added protease and phosphatase inhibitors (535140, Merck Life Science)), was used. Then, samples were boiled for 5 minutes at 95°C, avoiding the sonication step. The loading and running of the gel were

performed under standard conditions. However, the transference was performed using PVDF membranes (IPVH00010, Merck Life Science), previously activated by incubating for 15 seconds in methanol 100%, 2 minutes in water, and at least 5 minutes in a transfer buffer. Transference was performed at 40mA overnight. From this point, the rest of the protocol followed the standard setting.

## DNA fiber assay

DNA fiber assays, an important tool for monitoring DNA replication fork dynamics<sup>259</sup>, were performed in collaboration with Violeta Serra's laboratory at VHIO. PER403 and NC1015 were treated as indicated, and during the last part of the treatment, they were labeled with 30 $\mu$ M CldU for 25 minutes, washed with PBS three times, and exposed to 250 $\mu$ M IdU (maintaining the treatment) for 25 minutes. Then, cells were collected and resuspended in PBS. Subsequently, 2.5 $\mu$ L of the cell suspension was spotted on a positively charged slide (VWR) and mixed with 7 $\mu$ L lysis buffer (200mM Tris-HCl pH 7.4, 50mM EDTA, 0.5%SDS). Next, cells were incubated in lysis buffer horizontally for 8 minutes and tilted at  $\sim 45^\circ$ , allowing the drop to run by gravity. The DNA spreads were air-dried at RT, fixed in methanol/acetic acid (3:1) at RT for 10 minutes, and stored at 4°C overnight. Slides were rehydrated by rinsing with 1x PBS three times, DNA was denatured with 2.5 M HCl for 1 h at RT, and slides were washed four times with 1x PBS. Then, slides were blocked in 2% BSA in PBS with 0.1% Tween-20 (PBST) for 40 minutes in the dark at RT. Slides were stained with primary antibodies diluted in blocking buffer (**Table 6**) for 2 h at RT in the dark, washed three times with PBST, incubated with 2% PFA for 10 minutes, and rewashed three times with PBST. Next, slides were incubated with secondary antibodies diluted in blocking buffer (**Table 6**) for 1 h in the dark at RT and washed three times with PBST and once with blocking buffer. Then, slides were air-dried for 15 minutes and mounted with Aqua-poly/mount (50001, Ibbidi). Subsequently, they were conserved at 4°C in the dark until imaging. Finally, fibers were visualized and imaged using the Nikon Ti-2Eclipse fluorescent microscope at a 60x zoom. Images were analyzed in Image J (1.48v). Statistical analysis was carried out using GraphPad Prism.

## **Global transcription detection. EU assay.**

According to the manufacturer's instructions, nascent RNA synthesis was monitored using the Click-iT RNA Imaging Kit (C10329, Invitrogen). 50000 NC1015 and 100000 PER403 cells were seeded on coverslips in a 24-multiwell plate. After adding the appropriate treatments and 1 hour before cell collection, 1mM of 5-ethynyl uridine (EU), an analog of uridine, was added. Then, cells were fixed in 4% PFA (sc-281692, Santa Cruz Biotechnology) for 15 minutes and permeabilized with 0.5% Triton X-100 (93443, Silga Aldrich) - PBS for 15 minutes at RT. Cells were then incubated with the Click-iT reaction cocktail (Click-iT RNA reaction buffer, CuSO<sub>4</sub>, Alexa Fluor azide-488, and Click-iT reaction buffer additive) for 30 minutes at RT-covered from light. After one wash with the Click-iT reaction rinse buffer, cells were incubated for 15 minutes with 1:1000 of Hoechst 33342 dye as a nuclear counterstain. Finally, after two PBS washes, coverslips were mounted on microscope slides using fluoromount (0100-01, SouthernBiotech).

Labeled cells were analyzed, and images were captured using a Nikon C2+ Confocal Microscope and the NIS-Elements Advanced Research software with a CFI Plan Apochromat VC 60x/1.40 oil objective. Images were then analyzed according to specifications in the '

**Image analysis'** section of Materials and Methods.

## **Cell viability assay. MTT.**

The 3-(4,5-dimethylthiazol-2-yl)-2,5-diphenyltetrazolium bromide (MTT) assay was performed to assess cell viability in our cell models under different treatment conditions described in the Results section.

Different amounts of the four NC cells were seeded per well in 96-well plates. 1000 - 2000 cells for PER624, 2000 - 3000 cells for NC14169, 3000 - 5000 cells for PER403 and 3000 - 7000 cells for NC1015 cell line per well. Each cell line was seeded in quintuplicate for IC<sub>50</sub> calculation curves and triplicate for the DDRi focus screening. Cells were treated 18 hours after seeding according to the specific considerations of each experiment regarding concentration and duration of the treatment. At the endpoint of the treatment, MTT reagent (A2231, Panreach Aplichem) was added at a final concentration

of 0.03 mg/mL to the corresponding culture medium without FBS for 3 hours at 37°C, 5% CO<sub>2</sub>, and 95% humidity. Subsequently, the MTT-containing medium was removed, and cells were lysed in isopropanol to measure the absorbance of the insoluble resulting purple product formazan at 565nm with infinite M2000 Pro (Tecan) and Tecan i-control 1.11 software. Data management, presentation, and statistical analysis were performed using the GraphPad Prism 9 software.

## Apoptosis assay

The apoptotic population was assessed using Annexin V-FITC Apoptosis Detection Kit (88-8005-72, Thermo Scientific). 370000 - 500000 cells were seeded for PER624 and NC14169, and 750000 - 1000000 cells were seeded for PER403 and NC1015 in P60 dishes. Samples were treated under the indicated conditions for each experiment. Then, BD FACSCelesta™ Cell Analyzer was used, and data were analyzed using FlowJo software. Finally, Annexin V positive population was plotted. Statistical significance among the biological replicates was determined by an ordinary one-way ANOVA. Statistically significant differences are indicated by the p-value in every figure.

## HR reporter assay

To functionally assess HR capacity in NC cells, the PER624 cell line was transfected and selected with 1µg/mL puromycin (BP2956, Fisher Scientific) for the stable expression of the pHPRT-DRGFP vector<sup>260</sup> (#26476, Addgene). The vector contains an interrupted GFP gene sequence with a restriction site recognized by *SceI* restriction endonuclease. This approach allows the measurement of HR capacity by detecting the presence or absence of GFP expression upon the induction of DNA damage by *SceI* (see **Figure 49A**).

To have an HR deficient control in our experiment, a BRCA2KO clone was generated from PER624\_HR cells (see section of **Knockout cell generation** of Materials and Methods). Both PER624\_HR and PER624\_HR\_BRCA2KO cell lines were infected with a virus containing *SceI*-T2A-BFP construct (#32628, Addgene). This virus enables *SceI* expression in the cells and the monitoring of infection efficiency by a blue fluorescent protein (BFP) reporter. After *SceI*-induced double-strand DNA damage, HR-proficient cells will utilize

the complementary provided fragment of GFP, and the gene will thus be restored and expressed. In contrast, HR-deficient cells will repair the damage by other less precise methods, such as NEHJ, and the repair will not result in GFP expression (see **Figure 49A**).

GFP expression was analyzed using the BD FACSCelesta™ Cell Analyzer, and data was analyzed using FlowJo Software. An unpaired T-test determined statistical significance among the biological replicates. Statistically significant differences are indicated by the p-value in the figure.

## Knockout cell generation

As mentioned in the **HR reporter assay** section of Materials and Methods, the BRCA2KO cell line was generated from PER624\_HR cells to serve as an HR deficient control. CRISPR Cas9 technology was used.

First, PER624\_HR cell lines were transfected with a Cas9 + BRCA2sguide + GFP construct.

sgRNA sequence is the following: 5' AAACCATCTTATAATCAGC 3'

Seventy-two hours after transfection, cells were sorted to select GFP-positive ones. GFP-positive cells were seeded in very low confluence conditions to obtain individual colonies. When grown, clones were picked and placed in individual plate wells to amplify them. After amplification, the 60 picked clones were evaluated. First, a screening PCR was conducted. Primers were designed to include the sgRNA-targeted region in the amplification product to capture the potential alterations in the region of the gene.

Forward: 5' ACTGTTCTGGGTCACAAATTTG 3'

Reverse: 5' TCCCAGTCTACCATATTGCA 3'

From the PCR screening, the E8 clone was selected as a potentially successful candidate as it showed the most differential pattern of BRCA2 amplification compared to the parental cell line. Thus, TOPO cloning and further Sanger sequencing of the independent alleles were performed to compare allele sequences with the reference gene sequence.

## RAD51 assay

In collaboration with Violeta Serra's laboratory at the Vall d'Hebron Institute of Oncology (VHIO), the RAD51 score assay, a functional assay to study HR capacity developed by them<sup>261,262</sup>, was performed.

Two FFPE sections from each of our four paraffin-embedded NC patient samples (see section of '**Patient samples information**' of Material and Methods) were used for immunostaining and analysis of both RAD51 foci, the last effector of the HR pathway, and  $\gamma$ H2AX, a marker of DNA damage. Each biomarker was counterstained with geminin as a marker of the S/G2 cell cycle phase and DAPI. After performing the immunostaining according to the protocols described in the above publications, images were analyzed. At least 40 geminin-positive cells were analyzed per sample, and the  $\gamma$ H2AX score was used as quality control to ensure the presence of sufficient endogenous DNA damage to evaluate HR functionality (cut-off, 25% geminin-positive cells with  $\gamma$ H2AX foci). The RAD51 score was considered low or high based on the predefined cut-off of 10% geminin-positive cells with  $\geq 5$  RAD51 nuclear foci, meaning that samples with  $\geq 10\%$  geminin-positive cells with  $\geq 5$  RAD51 nuclear foci are considered HR proficient (HRP); and those samples with a score  $\leq 10\%$ , are considered HR deficient (HRD).

## Drug efficacy studies *in vivo*.

Different NC cell lines (PER403 or PER624, indicated in each case) were implanted subcutaneously in NOD-SCID mice. One million cells per flank were implanted. When tumors reached 100-200 mm<sup>3</sup> volume, mice were randomized and divided into different treatment groups. The various drugs, doses, and vehicles are indicated in **Table 7**. Tumor growth and mouse weight were measured two to three times per week, and treatment regimens are specified in the Results section. Tumor volume was calculated using the formula:  $V=(\text{length}\times\text{width}^2)/2$ .

**Table 7. List of drugs used *in vivo*.**

Drug	Dose	Vehicle	Reference/Provider
Olaparib	50mg/kg	10%DMSO, 10%Kleptose, 80%H2O	AZD2281, HY-10162, MedChemexpress
Ceralasertib	25mg/kg	10%DMSO, 40%propylene glycol, 50%H2O	AZD6738, HY-19323, MedChemexpress
OMO-103	50mg/kg	20mM Sodium acetate, 0,02% (w/v) polysorbate (Tween20), 200mM sorbitol	Provided by Laura Soucek's laboratory
Etoposide	4mg/kg	Saline solution	Provided by Vall d'Hebron Hospital
Cisplatin	1.5mg/kg	Saline solution	Provided by Vall d'Hebron Hospital

All animal procedures were approved by the Ethical Committee for the Use of Experimental Animals at the Vall d'Hebron Institute of Research (VHIR) and by the Catalan Government. According to protocols approved by the Ethical Committee for the Use of Experimental Animals (CEEA) at VHIO, mice were euthanized using CO<sub>2</sub> inhalation once tumors reached 1-1.5 cm<sup>3</sup>, or in case of severe weight loss or any other sign of discomfort. At the endpoint, tumors were harvested and formaldehyde-fixed and snap-frozen.

## **BrdU assay**

Cell cycle analysis was performed using BD Pharmingen™ BrdU Flow Kit (APC kit) (BDBiosciences #559619). 370000 cells were seeded for PER624 and NC14169, and 750000 cells were seeded for PER403 and NC1015 in P60 dishes. BD FACSCelesta™ Cell Analyzer was used, and data were analyzed using FlowJo software. Statistical significance among the biological replicates was determined by an ordinary one-way ANOVA. Statistically significant differences are indicated by the p-value in every figure.

## RNA sequencing

340000 cells of PER403 and NC14169 were seeded per MW6-well. After the treatment conditions described in the Results section, total RNA from NC cells was isolated using miRNeasy Mini Kit (Qiagen, Cat# 217004) following the manufacturer's protocol. Then, RNA was eluted in RNase-free water, and RNA quality and quantity were measured using the 4200 Tape Station System. RIN values of all samples were  $\geq 9.5$ . Subsequently, between 3-15 $\mu$ g per condition were sent, and library preparation was performed by BGI company following the BGI Optimal Dual-mode mRNA Library Prep Kit. Then, RNA sequencing was performed using the Novaseq platform with 150 bases paired-end reads. A total of 40 million clean reads were generated per sample.

Raw sequencing reads in the fastq files were processed through the nf-core/RNAseq pipeline<sup>263</sup> version 3.9. Differential gene expression analysis was assessed with voom+limma in the limma package version 3.54.0<sup>264</sup> using R version 4.2.2 and raw library size differences between samples were treated with the weighted trimmed mean method (TMM)<sup>265</sup> implemented in the edgeR package<sup>266</sup>. Then, the normalized counts were used in the unsupervised analysis and clusters.

For the differential expression analysis, raw counts were modeled using the Voom approach in the limma package. Corrections for multiple comparisons were performed using a false discovery rate (FDR)<sup>264</sup>, obtaining the adjusted p-values. Genes were considered to be differentially expressed between studied conditions if the adjusted p-value was  $< 0.05$  and the  $|\logFC| > 1$ .

Finally, pre-ranked GSEA<sup>267</sup> implemented in clusterProfiler<sup>268</sup> package version 4.6.0 was used to retrieve enriched functional pathways. The ranked list of genes was generated using the  $-\log(p\text{-value}) \cdot \text{signFC}$  for each gene from the statistics obtained in the DE analysis with limma<sup>264</sup>, and functional annotation was obtained based on the enrichment of gene sets belonging to gene set collections in Molecular Signatures Database (MSigDB) version 2023.

# RESULTS



## PART 1. The impact of BRD4-NUT fusion on RS in NC cells as a novel targetable vulnerability

### 1. BRD4-NUT fusion is involved in an increased RS in NC

#### 1.1. Modulation of the expression of BRD4-NUT fusion using degrader MZ1.

Cell models in which the fusion expression can be dynamically modulated were needed to elucidate the role of BRD4-NUT fusion protein and test its association with RS in NC. Thus, we utilized MZ1, a small molecule designed based on the PROTAC system, to degrade the BRD4-NUT fusion protein<sup>252</sup> (see section 'Drug treatments' of Materials and Methods).

According to the published literature<sup>107</sup>, we first treated NC cells with 100nM MZ1 for 4 hours, followed by the removal of the treatment for 24 hours, hereafter referred to as washout (WO) condition (**Figure 28A**). To monitor the expression of BRD4-NUT, immunofluorescence (IF) and western blot (WB) assays were conducted. Moreover, as the wildtype (WT) version of NUT protein is only expressed in the testis in normal conditions<sup>20</sup>, we could use NUT antibody to detect specifically BRD4-NUT fusion. We found that a 4-hour treatment of 100nM MZ1 resulted in a drastic decrease of BRD4-NUT fusion in 4 NC cell lines - PER403, PER624, NC1015, and NC14169 - as expected. However, after the MZ1 was removed for 24 hours, the BRD4-NUT fusion returned to 40%-160% compared to the untreated control condition (**Figure 28B, C**). Thus, this provides a consistent and dynamic strategy to modulate the BRD4-NUT fusion protein and study its effects on NC cells.

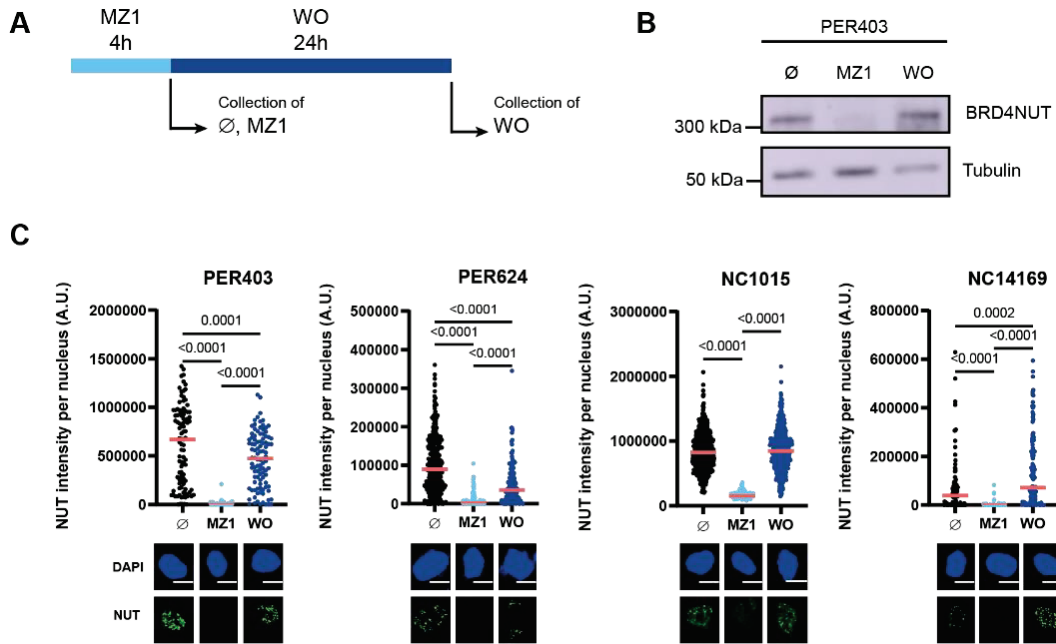


**Figure 28. MZ1 treatment led to the elimination of BRD4-NUT fusion, and the removal of MZ1 (WO) could restore its expression in NC cells.**

**A** Schematic representation of the treatment schedule. **B** Western blot analysis of BRD4-NUT protein in PER403 cell line after 4 hours' treatment (MZ1) and 24 hours' removal (WO). Tubulin was used as a loading control. Representative of two independent biological replicates is shown. **C** BRD4-NUT analysis by immunofluorescence with NUT antibody in 4 NC cell lines after MZ1, WO treatment. Quantification of the nuclear intensity of  $\geq 90$  cells per condition (above) and representative cells (below) were shown. Red lines represent the median values. Scale bar =  $50\mu\text{M}$ . Representatives of two independent biological replicates are shown. One-way ANOVA was used for statistical analysis.

1.2MZ1 treatment resulted in decreased expression of RS markers, and their recovery occurred upon MZ1 removal.

Based on the working hypothesis regarding the potential effect of BRD4-NUT fusion on the RS in NC cells (see **HYPOTHESIS AND OBJECTIVES**), we assessed the expression of the RS marker phosphorylated RPA at serine 33 (pRPA S33)<sup>269</sup> in NC cells, where BRD4-NUT expression was modulated via MZ1 treatment and removal (see section **1.1 Modulation of the expression of BRD4-NUT fusion using degrader MZ1**. of Results).

Using IF assays, we observed that even after 4 hours of treatment with 100nM MZ1, pRPA S33 significantly decreased in all four NC cell lines. Furthermore, pRPA S33 levels increased significantly 24 hours after MZ1 was removed (**Figure 29**).

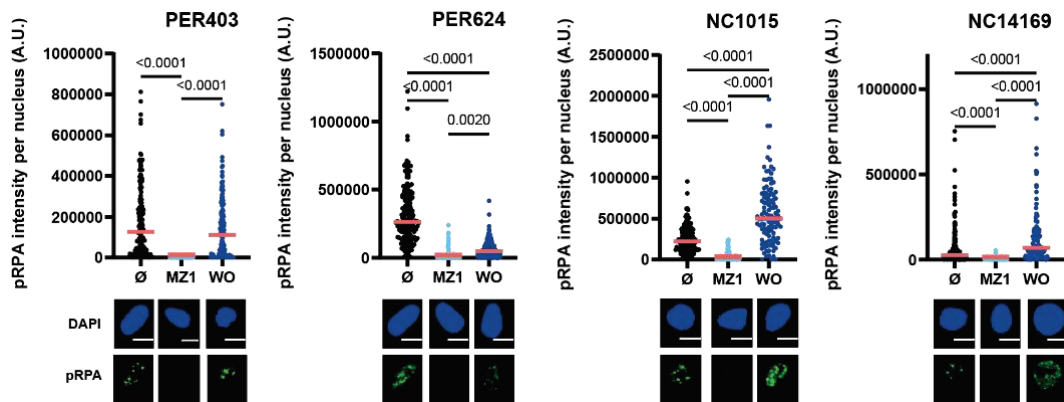


**Figure 29. MZ1 treatment decreased the presence of the RS marker pRPA S33, but its expression can be restored in WO conditions.**

pRPA S33 expression analysis by IF in 4 NC cell lines after 4 hours' MZ1 treatment (MZ1) and 24 hours' removal (WO). Quantification of the nuclear intensity of  $\geq 90$  cells per condition (above) and representative cells (below) were shown. Red lines represent the median values. Scale bar =  $50\mu\text{M}$ . Representatives of two independent biological assays were shown. One-way ANOVA was used for statistical analysis.

Overall, these data, together with the significant decrease in BRD4-NUT expression observed in NC cells following MZ1 treatment and its subsequent restoration upon removal of MZ1 treatment, indicate a potential involvement of BRD4-NUT in RS in NC cells.

### 1.3BRD4-NUT impacts on replication fork speed.

The DNA Fiber Assay is an important tool for understanding DNA replication stress, as it can be used to monitor DNA replication fork dynamics<sup>259</sup>. We performed the assay to study NC cell line replication velocity upon BRD4-NUT modulation using MZ1 treatment/removal scheme of treatment.

Interestingly, we observed a significant decrease in fork velocity with BRD4-NUT degradation by MZ1. Moreover, upon MZ1 removal, the original fork velocity was restored (**Figure 30**). These results indicate that BRD4-NUT fusion could play a role in the replication fork velocity, possibly linked to the increased RS status in NC cells.

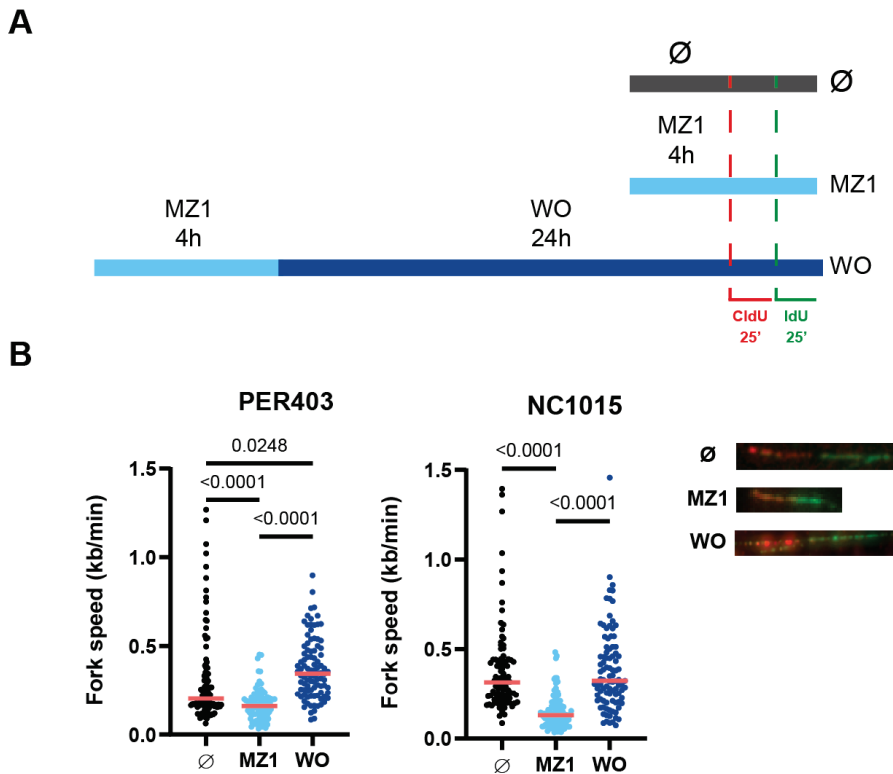


**Figure 30. MZ1 treatment can decrease the fork velocity, and it can be restored in WO conditions.**

**A** Schematic representation of the experimental schedule. **B** Fork velocity by sequential CldU/IdU incubation in 2 NC cell lines after 4 hours' MZ1 treatment (MZ1) and 24 hours' removal (WO). Quantification of the fiber length per minute of  $\geq 90$  cells per condition (left) and

representative fibers (right). Representative of two independent biological assays is shown. Red lines represent the median values. One-way ANOVA was used for statistical analysis.

## 2. The NUT moiety of the BRD4-NUT fusion affects the RS status in NC cells.

### 2.1. Generation and validation of ectopic expression models to study the involvement of BRD4-NUT fusion in RS.

Our results suggest that the BRD4-NUT fusion plays a role in the RS in NC cells. However, it is important to recognize that despite its rapid, potent, and reversible nature, the MZ1 degradation approach has a limitation. The small molecule MZ1 can degrade not only the BRD4-NUT fusion but also the BRD4 WT protein. To precisely determine the specific impact of the fusion and identify which moiety of the fusion protein contributes to the observed phenotype, we employed an inducible ectopic-expression strategy. We generated HEK293T cells expressing stably inducible GFP (as negative control), the BRD4 part of the fusion (corresponding to the BRD4 short isoform, BRD4s), the NUT moiety (representing nearly the full length of the NUT protein), and BRD4-NUT. Of note, these constructs were also tagged with 3X FLAG and HA to facilitate protein detection (see section ‘**Cell lines and culture conditions**’ of Materials and Methods).

We assessed these models and observed that doxycycline treatment effectively triggers transgene induction 72 hours after its addition to the cell culture (**Figure 31**). Interestingly, the BRD4-NUT protein displayed a foci-like pattern in immunofluorescence assays, reminiscent of the hyperacetylated megadomains observed in NC cells (**Figure 31**).

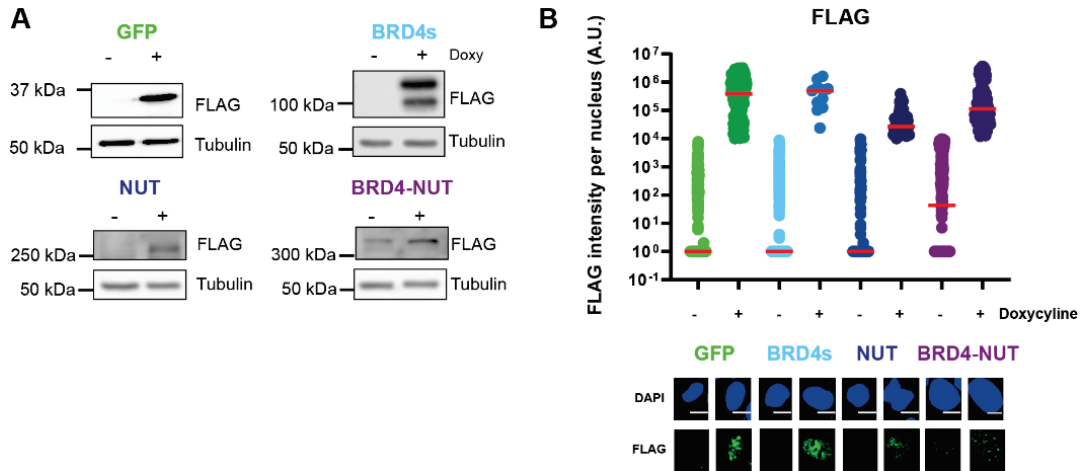


**Figure 31. Validation of cell lines expressing inducible forms of GFP, BRD4s, NUT, and BRD4-NUT.**

**A** Schematic representation of the transgene induction using doxycycline. **B** Western blot analysis of transgene expression using anti-FLAG antibody 72 hours after doxycycline addition. Tubulin was used as a loading control. **C** IF analysis of transgene expression using anti-FLAG antibody 72 hours after doxycycline addition. Quantification of the nuclear intensity of cells (above) and representative cells (below). Red lines represent the median values. Scale bar = 50 $\mu$ M.

Two significant aspects of the model warrant mention. Firstly, there might be a minor leakage in the expression of the constructs, which should not confound the results due to substantial enrichment in the doxycycline-treated conditions. Secondly, there is variability in the expression levels of the transgenes among the established cell lines, notably with lower expression of BRD4-NUT compared to others. This discrepancy was anticipated due to the BRD4-NUT construct encoding a notably large protein (>250 kDa), significantly impeding its stability. While it is crucial to consider this aspect throughout the result analysis, we have technically addressed it by establishing a positivity threshold and restricting the analysis to transgene-expressing cells in the IF analysis.

## 2.2. BRD4-NUT increases RS markers through the NUT moiety of the fusion.

With the established cell lines, we aimed to confirm the impact of the fusion protein on RS and identify which moiety of the fusion contributes to the RS phenotype.

We observed that ectopic expression of the BRD4-NUT fusion resulted in increased levels of RS markers pRPA S33 in IF assays (**Figure 32A**) and phosphorylated CHK1 (pCHK1) in Western blot analysis (**Figure 32B**). Importantly, it was found that the ectopic expression of the NUT moiety, but not the BRD4 moiety (BRD4s), led to the elevation of both RS marker expressions (**Figure 32A, B**). Taken together, these results demonstrate that BRD4-NUT fusion is able to induce the RS marker expression, and the NUT moiety of the oncogene fusion protein is associated with this phenotype.

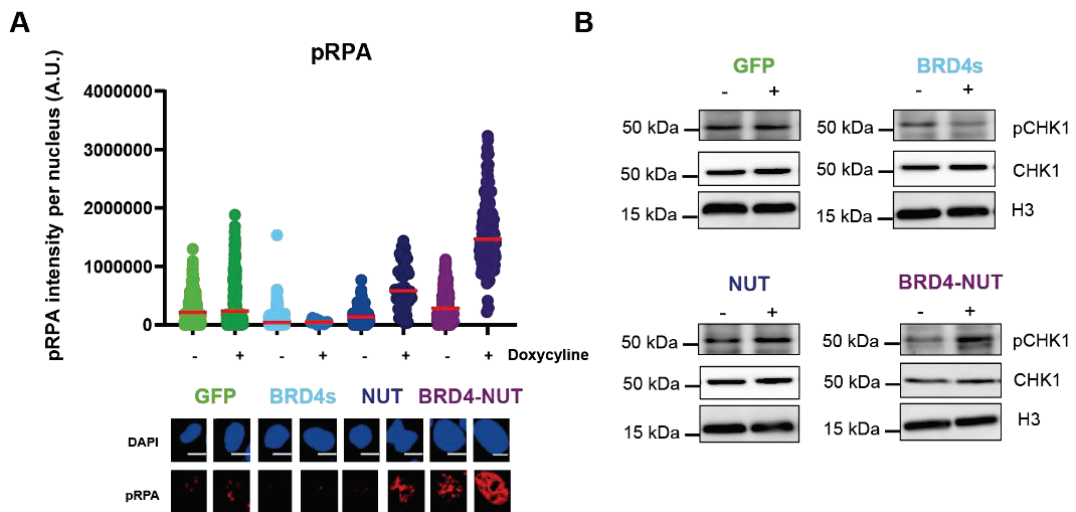


**Figure 32. Ectopic expression of BRD4-NUT and NUT moiety of the fusion can increase the expression of RS markers.**

**A** IF analysis of pRPA S33 expression 72 hours after doxycycline addition. pRPA staining was quantified in untreated cells with FLAG (transgene) intensity  $\leq 10000$  A.U. and in doxycycline-treated cells with FLAG (transgene) intensity  $\geq 10000$  A.U. Quantification of the nuclear intensity of cells (above) and representative cells (below). Scale bar =  $50\mu\text{M}$ . Red lines represent the median values. **B** Western blot analysis of RS marker pCHK1 S317 72 hours after doxycycline addition. Tubulin was used as a loading control. Representatives of two independent biological replicates are shown.

To summarize, our discoveries in the first two sections suggest a connection between BRD4-NUT and RS in NC, with the NUT moiety being the driving force behind this phenotype (**Figure 33**).

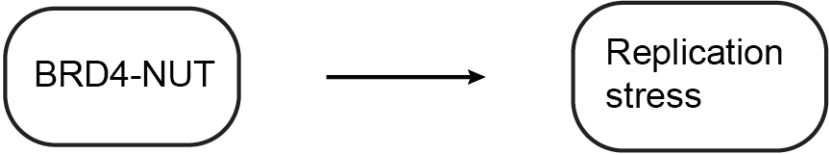


**Figure 33.** Schematic representation of the model (1).

### 3. p300 acetyltransferase and hyperacetylated chromatin megadomain formation are involved in BRD4-NUT fusion-induced RS in NC cells.

Previous studies have found that the BRD4-NUT fusion can interact with the acetyltransferase p300, leading to the formation of acetylation clusters known as megadomains throughout chromatin<sup>26</sup> (see section ‘1.2.2 Molecular mechanism behind NUT-fusion in NC.’ of Introduction). In this section, we aimed to investigate whether p300 is involved in BRD4-NUT fusion-induced RS in NC cells.

#### 3.1. BRD4-NUT degradation decreases the formation of megadomains in NC cell lines.

We first confirmed the requirement of the BRD4-NUT fusion for the formation of hyperacetylated chromatin megadomains. As expected, a significant decrease in megadomain presence was observed after 4 hours of MZ1 treatment, as detected using an H3K27ac-specific antibody. Notably, after 24 hours of MZ1 removal (WO condition), there was a notable increase in megadomain presence (**Figure 34**). Therefore, consistent with prior findings, BRD4-NUT can lead to megadomain formation.

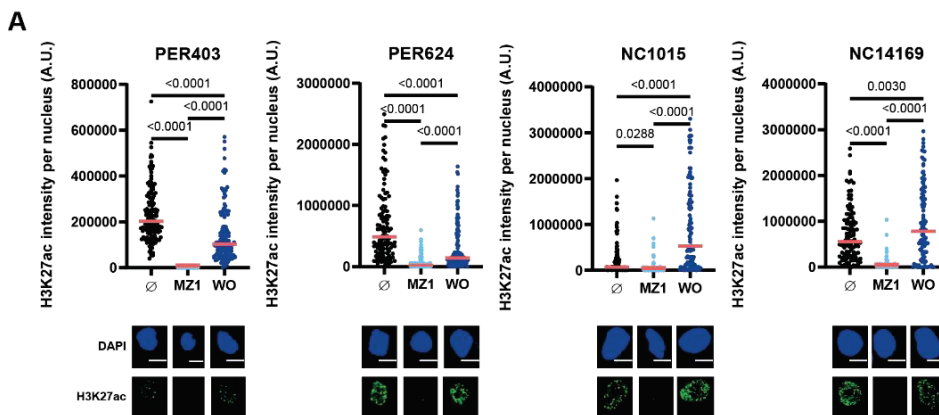


**Figure 34. Effects of BRD4-NUT degradation by MZ1 treatment on megadomain formation, reversed upon MZ1 removal.**

IF analysis of megadomain using H3K27ac specific antibody in 4 NC cell lines after 4 hours' MZ1 treatment (MZ1) and 24 hours' removal (WO). Quantification of the nuclear intensity of

≥90 cells per condition (above) and representative cells (below). Scale bar = 50μM. Red lines represent the median values. One-way ANOVA was used for statistical analysis.

### 3.2. p300 degradation with dCBP1 PROTAC degrader can lead to decreased hyperacetylated megadomain in NC cells.

To modulate the formation of hyperacetylated megadomains, we opted to alter the expression of the histone acetyltransferase p300 using a small molecule based on a PROTAC system, referred to as dCBP-1, which selectively degrades p300<sup>253</sup>.

NC cell lines were treated with 1μM of dCBP-1 for various durations spanning 2 to 24 hours. The presence of p300 and hyperacetylated megadomains (H3K27ac), was analyzed using IF assays. Results demonstrated a significant and fast depletion of p300 and megadomain upon dCBP-1 treatment (**Figure 35**). Furthermore, significant co-localization was observed between the stains of p300 and H3K27ac, providing further evidence for the presence of p300 within the H3K27ac-marked megadomains (**Figure 35C, F**). Based on this data, we selected the 4-hour treatment duration for further analysis.

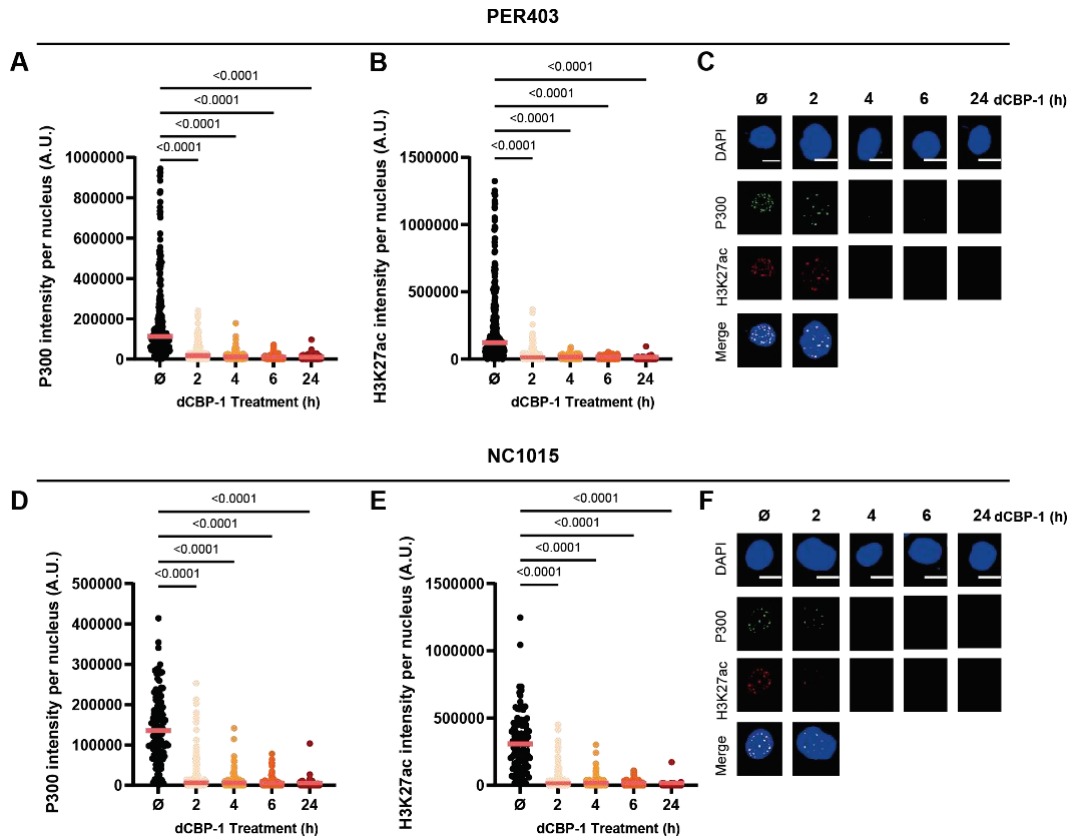


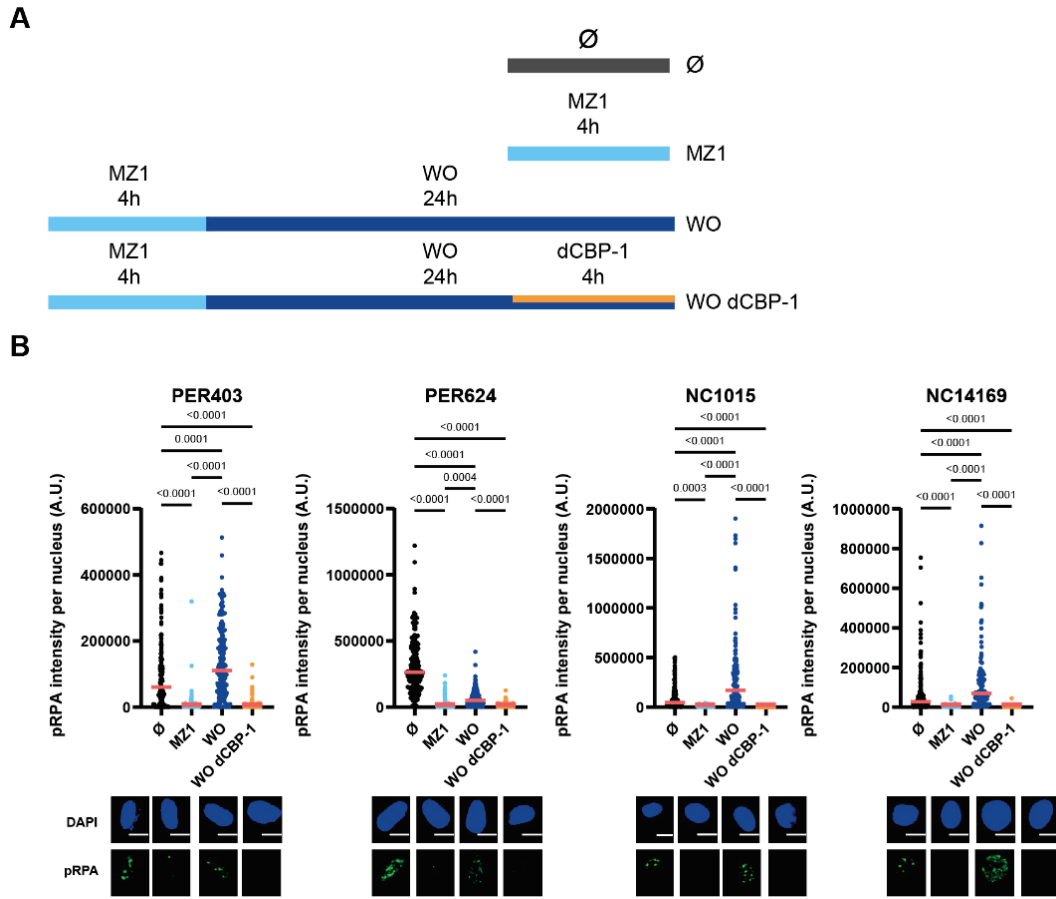
**Figure 35. dCBP-1 degrades p300 and decreases megadomains in NC cells.**

**A, D** p300 and **B, E** H3K27ac expression was analyzed by IF assays in PER403 and 1015 NC cell lines respectively, treated with dCBP-1 for 2, 4, 6, and 24 hours. Quantification of the nuclear intensity of  $\geq 90$  cells per condition. Red lines represent the median values. **C, F** Representative cells and colocalization (right). Scale bar =  $50\mu\text{M}$ . One-way ANOVA was used for statistical analysis.

### 3.3. p300 and associated megadomains are required for BRD4-NUT-induced RS in NC cells.

Having validated the tools above, we subjected NC cells to dCBP-1 treatment during the MZ1 washout phase (**Figure 36A**), during which increased BRD4-NUT expression was demonstrated to induce RS (**Figure 29**). As expected, MZ1 treatment resulted in decreased expression of the RS marker pRPA, and its expression increased after the removal of MZ1. Interestingly, during the washout phase (WO), the increase of the same RS marker associated with

BRD4-NUT recovery was completely hindered upon dCBP-1 treatment (**Figure 36B**).



Taken together, these data suggests that megadomains and their associated histone acetyltransferase p300 are required for BRD4-NUT-induced RS in NC cells (**Figure 37**).

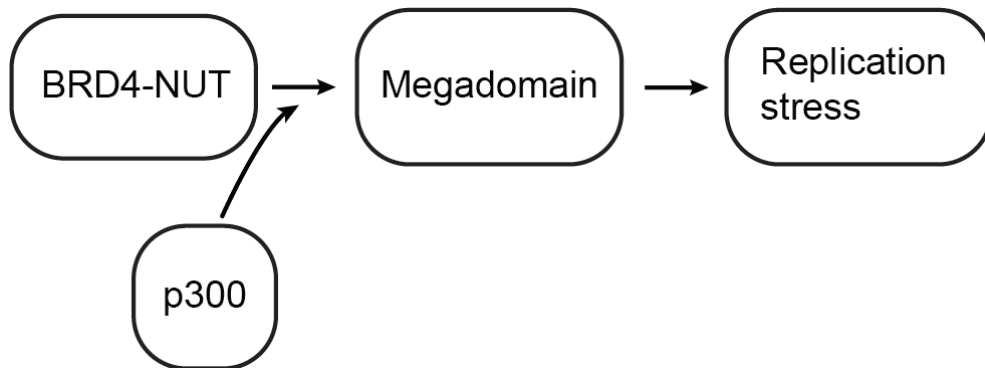


**Figure 37. Schematic representation of the model (2).**

#### 4. Transcription is required for BRD4-NUT-induced RS in NC cells.

Histone acetylation has been shown to be associated with open chromatin and directly linked to an active transcriptional state<sup>85</sup>. Transcription is a well-known source of RS<sup>227</sup>. Thus, we aimed to next investigate whether transcription is required for BRD4-NUT-induced RS.

##### 4.1. MZ1 treatment affects transcription levels, and this is recovered upon its removal.

To monitor transcription in cells, we employed an EU-labeling assay using Click-iT RNA Imaging techniques. This technique consists of incorporating EU, a modified uridine analog, into the newly synthesized RNA during active transcription and the subsequent detection using click chemistry to track and analyze transcriptional activity<sup>270</sup>.

Of note, we could observe a significant reduction of transcription upon MZ1 treatment. Furthermore, this decrease in the transcriptional activity was partially recovered upon the removal of MZ1 (**Figure 38**).

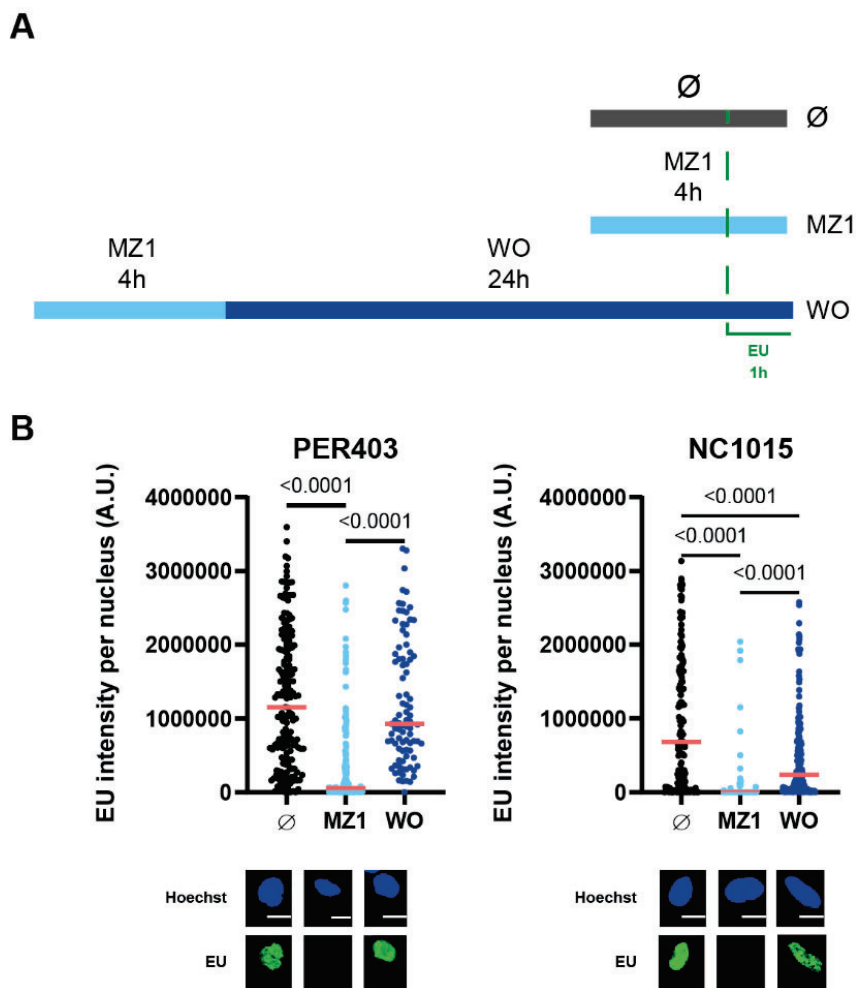


**Figure 38. Transcription is affected by MZ1 treatment and partially restored upon its removal.**

**A** Schematic representation of the treatment schedule. **B** EU staining as a marker of newly synthesized RNA, after 4 hours' MZ1 treatment (MZ1) and 24 hours' removal (WO). Quantification of the nuclear intensity of  $\geq 90$  cells per condition (above) and representative cells (below). Red lines represent the median values. Scale bar =  $50\mu\text{M}$ . Representative of two independent biological assays is shown. One-way ANOVA was used for statistical analysis.

4.2. p300 is required for the recovery in overall transcription observed upon BRD4-NUT restoration.

Next, we tested whether p300 and associated megadomains are required for BRD4-NUT-induced transcription. We exposed NC cells to p300 degradation by dCBP-1 treatment during MZ1 removal (WO) (**Figure 36A**). We found that although transcription was recovered upon WO, as expected, dCBP-1 treatment during that phase could abolish the transcription recovery in both PER403 and NC1015 NC cell lines (**Figure 39**).

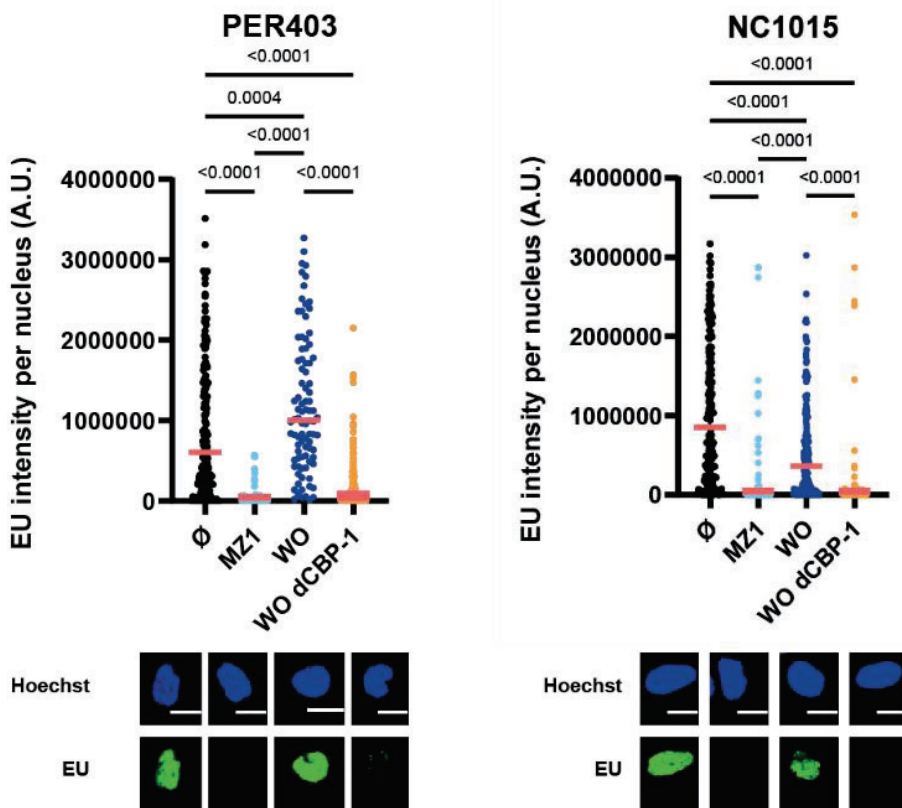


**Figure 39. Transcription recovery after the removal of MZ1 was abrogated upon dCBP-1 treatment.**

EU staining was analyzed as a marker of newly synthesized RNA in the conditions indicated in **Figure 36A**. Quantification of the nuclear intensity of  $\geq 90$  cells per condition (above) and representative cells (below). Red lines represent the median values. Scale bar =  $50\mu\text{M}$ . Representative of two independent biological assays is shown. One-way ANOVA was used for statistical analysis.

4.3. Transcription is required for the BRD4-NUT-induced RS in NC cells.

Next, we explored whether transcription is required for the BRD4-NUT-induced RS phenotype observed in NC cells.

To study this, we perturbed transcriptional activity using Actinomycin D (ActD), a well-known transcription inhibitor<sup>254</sup>. First, we confirmed that a treatment with 500nM ActD for 4 hours was sufficient to inhibit transcription in NC cell lines (**Figure 40A**). Then, we treated cells with ActD during the MZ1 removal phase and observed that the recovery of transcription, obtained upon MZ1 removal (WO), was significantly diminished following the inhibition of transcription by ActD (**Figure 40B**).

Under these experimental conditions, we analyzed the RS marker pRPA by IF in NC cell lines. Our results demonstrated that the increased RS marker pRPA expression observed upon MZ1 removal was abolished upon transcription inhibition by ActD treatment (**Figure 40C**).

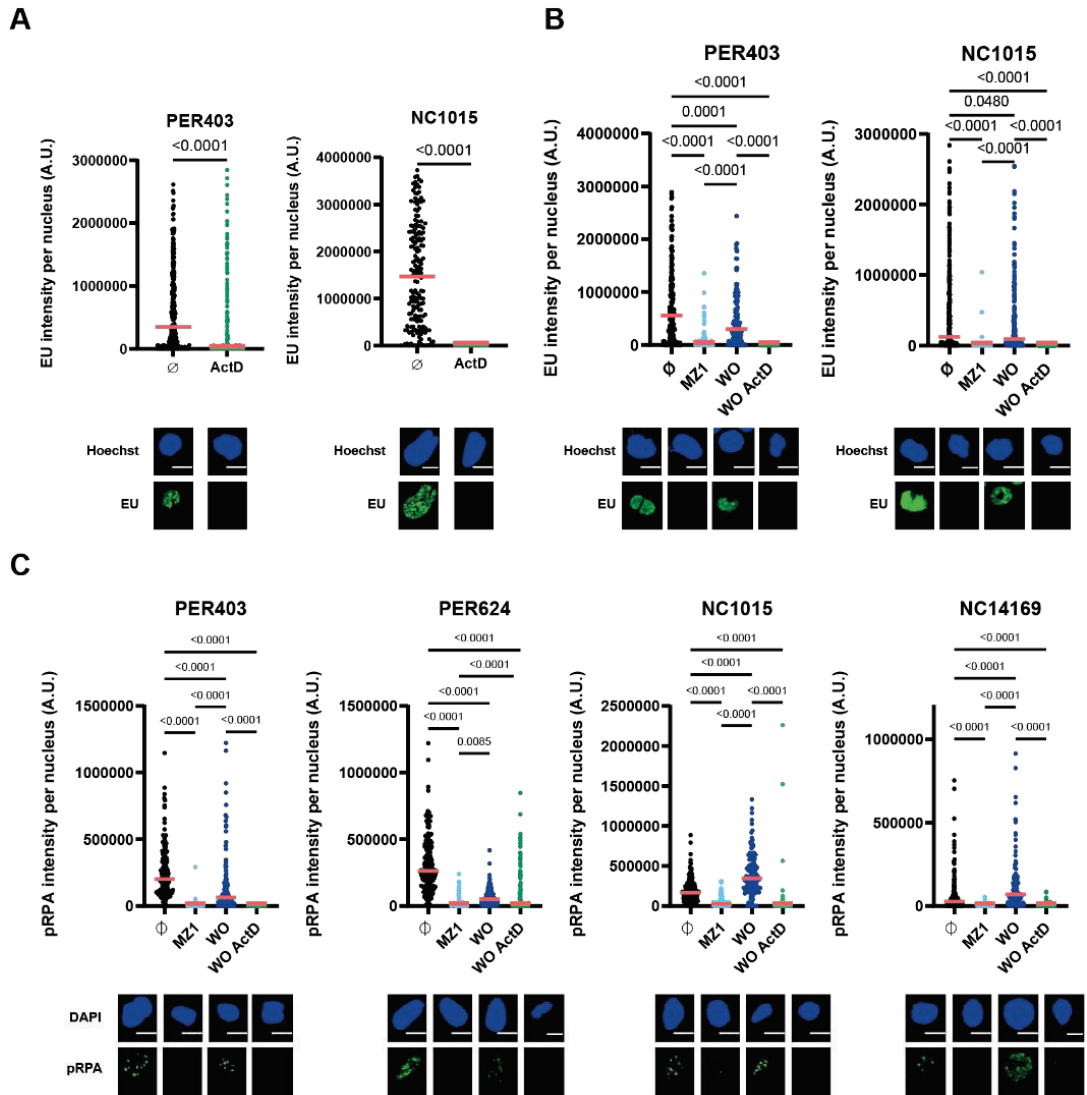


**Figure 40. Transcription modulation alters the BRD4-NUT-induced RS in NC cells.** EU staining, as a marker of newly synthesized RNA, was analyzed by IF after **A** 4 hours of Act D treatment or **B** 4 hours' MZ1 treatment (MZ1), 24 hours' removal (WO), and 4 hours' treatment of ActD during WO condition (similar *to Figure 36A*). **C** IF analysis of RS marker pRPA S33 in 4 NC cell lines treated with the same conditions as indicated in B. Quantification of the nuclear intensity of  $\geq 90$  cells per condition (above) and representative cells (below). Scale bar = 50 $\mu$ m. Red lines represent the median values. Representative of two independent biological assays is shown. For B and C, one-way ANOVA was used for statistical analysis. An unpaired t-test was performed for statistical analysis in A.

Taken together, these findings illustrate that the BRD4-NUT fusion, along with p300, enhances the overall transcriptional activity in NC cells, which is essential for the observed RS phenotype (**Figure 41**).

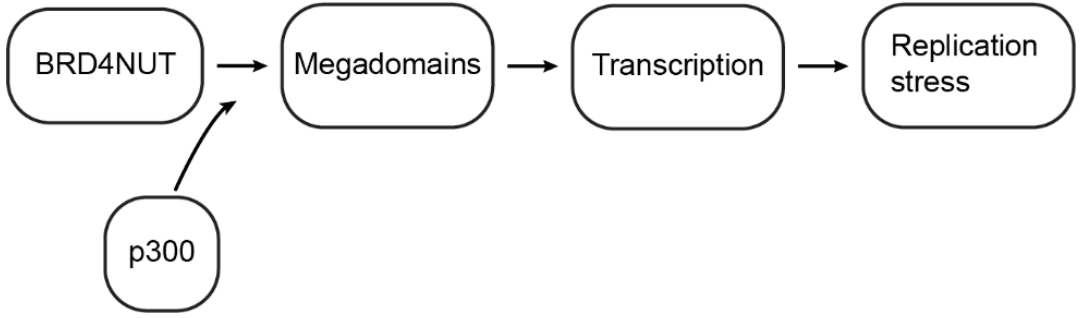


**Figure 41. Schematic representation of the model (3).**

## 5. R-loops are also involved in BRD4-NUT-induced RS in NC cells.

As previously discussed in the Introduction, elevated transcription can disrupt homeostasis and lead to the accumulation of R-loops, a well-known source of RS<sup>271</sup>.

R-loops are triploid structures formed by the nascent RNA hybridizing with the complementary DNA strand, together with the displaced single DNA strand<sup>202</sup>. They can be detected by the S9.6 antibody, which recognizes the secondary structure of R-loop<sup>249</sup>. Of note, there are mitochondrial R-loops in the cytoplasm<sup>272</sup>, which are irrelevant to the nuclear transcription process. To avoid the mitochondrial R-loop staining, we first eliminated the cytoplasm using CSK buffer before immunostaining (see section '**Immunofluorescence**' of Materials and Methods). Additionally, the S9.6 antibody can also recognize RNA-RNA hybrids<sup>258</sup>. For this, we used RNH1, an RNase enzyme capable of selectively degrading R-loop structures, as a negative control in S9.6 IF experiments<sup>211</sup>.

5.1. p300 and transcription are required for the BRD4-NUT-induced accumulation of R-loops in NC cells.

With the S9.6 antibody, we detected accumulations of R-loop structures in NC cells. Notably, treatment with RNH1 led to a significant decrease in S9.6 signals, confirming that the observed staining accurately reflects RNA-DNA hybrids and, consequently, R-loop levels (**Figure 42**).

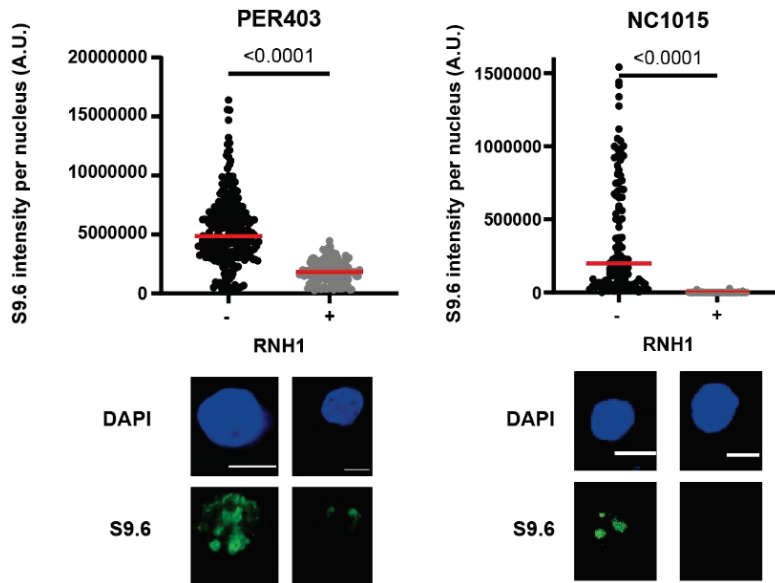


**Figure 42. S9.6 staining in NC cells.**

IF analysis of R-loops using S9.6 antibody and RNH1 treatment as a negative control in PER403 and NC1015 cell lines. Quantification of the nuclear intensity of  $\geq 90$  cells per condition was performed and representative cells are shown below. Red lines represent the median values. Scale bar =  $50\mu\text{M}$ . Representative of two independent biological assays is shown. An unpaired t-test was performed for statistical analysis.

Next, we investigated the impact of modulating fusion BRD4-NUT on the R-loop in NC cells. Our findings revealed pronounced S9.6 staining under basal conditions, which significantly decreased following MZ1 treatment and then recovered upon MZ1 removal (WO). Moreover, the restoration of S9.6 staining in the WO condition was hindered considerably by p300 degradation using dCBP-1 treatment or by transcription inhibition with ActD treatment (**Figure 43**).

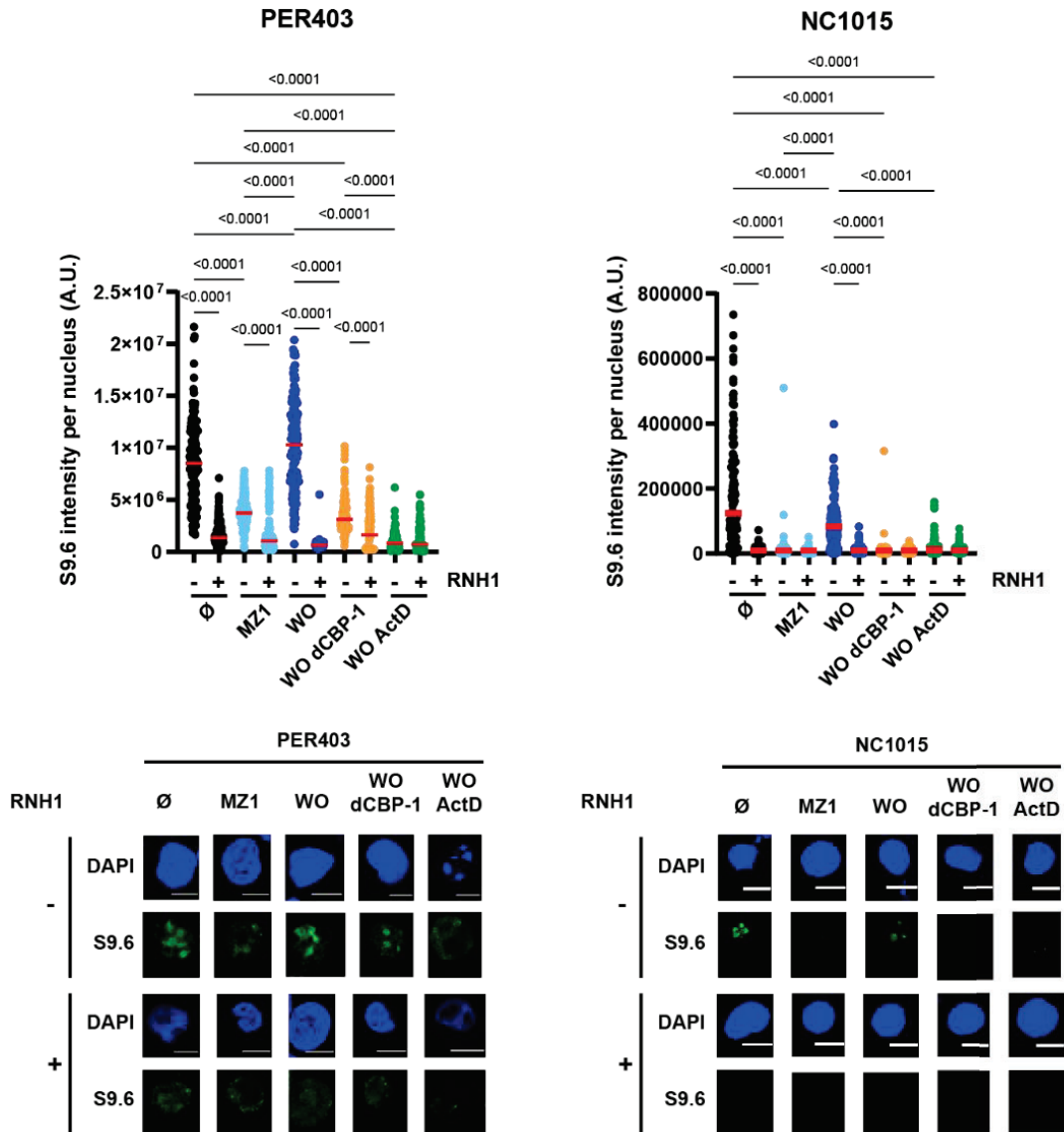


**Figure 43. p300 and transcription are required for NRD4-NUT-induced R-loops accumulation.**

IF analysis of R-loops using the S9.6 antibody in PER403 and NC1015 cell lines after 4 hours' MZ1 treatment (MZ1), 24 hours' MZ1 removal (WO), and 4 hours' treatment of either dCBP-1 or ActD during the WO condition. Quantification of the nuclear intensity of  $\geq 90$  cells per condition was performed and representative cells are shown below. Red lines represent the median values. Scale bar = 50 $\mu$ M. Representative of two independent biological assays is shown. One-way ANOVA was used for statistical analysis.

## 5.2. R-loop elimination by RNH1 abrogates BRD4-NUT-induced RS in NC cells.

Finally, we investigated whether these R-loops were involved in the BRD4-NUT-induced RS of NC cells. We observed a significant reduction in the expression of the RS marker pRPA following the elimination of R-loops through RNH1 incubation in NC cells (**Figure 44**). Furthermore, the recovery of pRPA levels upon WO was importantly diminished after RNH1 incubation (**Figure 44**).



## 6. Proposed model for the involvement of BRD4-NUT fusion in RS of NC cells.

Based on our findings, we propose a model where the BRD4-NUT fusion protein recruits p300 to chromatin, forming acetylation megadomains. These megadomains facilitate heightened transcriptional activity in NC cell lines and increased replication fork velocity. This elevated activity may trigger collisions between replication and transcriptional machinery, disrupting R-loop homeostasis and promoting their accumulation. Ultimately, this R-loop accumulation could be crucial in driving the high RS observed in NUT Carcinoma cells. Notably, as elaborated in subsequent sections, exploiting this newfound vulnerability may present a promising therapeutic strategy (**Figure 45**).

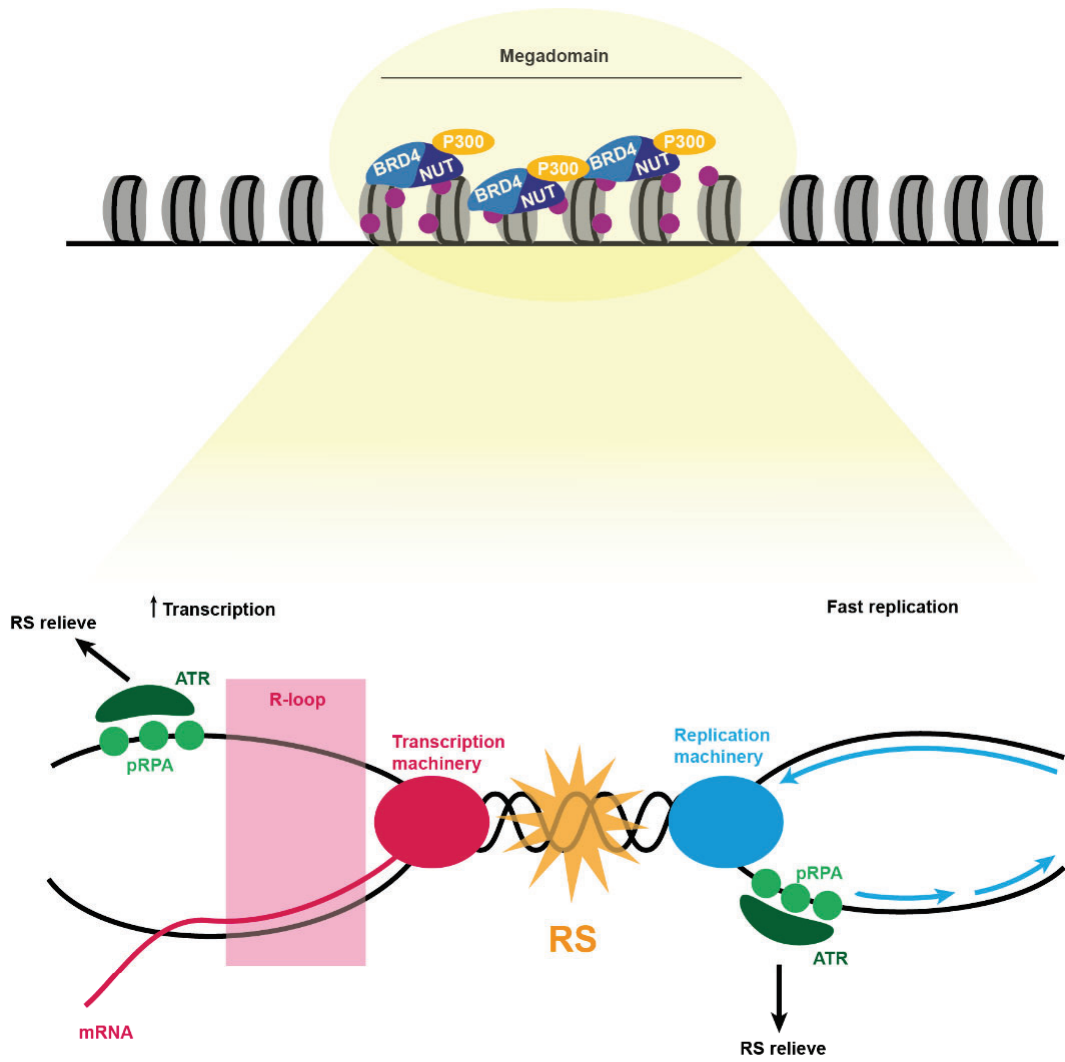


Figure 45. Scheme of the proposed model for the molecular mechanism.

## 7. NC cells exhibit sensitivity to a range of inhibitors that target factors implicated in the RS response pathways.

In the first section of this thesis, we uncovered a new and targetable feature of NC cells by establishing the association between BRD4-NUT and RS in NC cells. Subsequently, we investigated whether NC cells exhibit sensitivity to inhibitors of the DDR, given that a significant portion of these inhibitors are implicated in the RS response. This exploration aims to develop targeted strategies, considering that normal cells typically maintain low RS levels and do not heavily rely on factors involved in the RS response pathway for survival<sup>273</sup>.

7.1. A drug screening focused on DDRi revealed that NC cells are sensitive to inhibitors targeting factors involved in RS response pathways.

We first performed a focused drug screen testing a panel of 17 DDRi in our four patient-derived NC cell lines: PER403, PER624, NC1015, and NC14169. The DDRi-focused panel included inhibitors of DNA-PK, ATM, ATR, WEE1, CDK1, CHK1, CHK2 and PARP. Furthermore, doxorubicin and temozolomide were used as positive and negative controls, respectively. After three days of treatment, MTT assays were conducted to calculate the percentage of cell growth inhibition and thus detect potentially sensitive candidates.

As expected, both 10 $\mu$ M and 1 $\mu$ M treatments of doxorubicin led to high percentages of cell growth inhibition (**Figure 46**), whereas temozolomide treatments did not significantly affect NC cells' growth.

Upon 10 $\mu$ M treatment, the majority of drugs could lead to high percentages of cell growth inhibition in all four NC cell lines, except CHK2i (BML-277), ATMi (KU-55933), and DNA-PKi (AZD7648) (**Figure 46**). To identify the most sensitive candidates, we decreased concentration down to 1 $\mu$ M. Under this condition, we could observe that several drugs, including PARP inhibitors (PARPi) and molecules targeting the RS response pathway (ATR, CHK1, and WEE1 inhibitors), could significantly inhibit NC cell growth (**Figure 46**). These results demonstrated that these RS response proteins are required for NC cell survival.

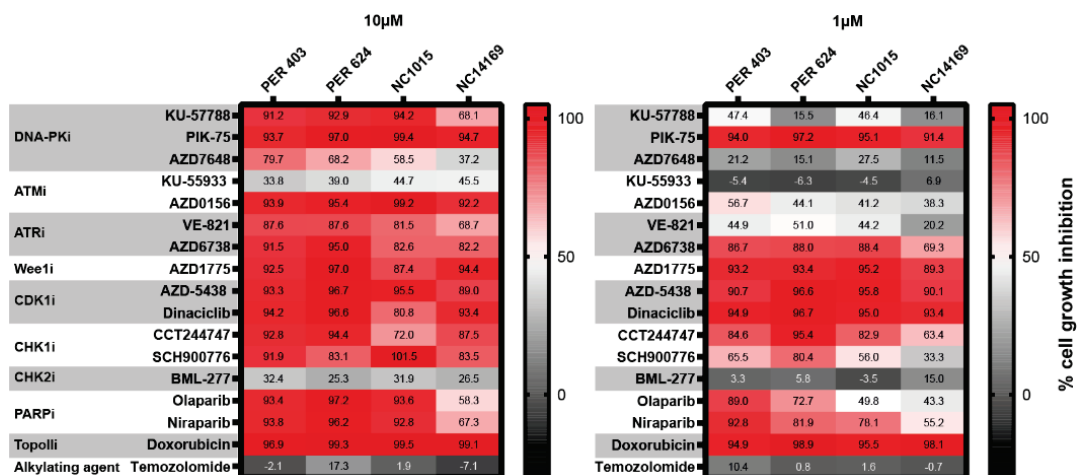


**Figure 46. A DDRi-focused drug screening evidenced several sensitive candidates in NC cells.**

Seventeen DDRi were tested in 4 NC cell lines with 1 or 10 µM for three days. Cell growth inhibition was calculated using untreated conditions as basal 100% control values. Values represented in the heatmap are the mean of three independent biological replicates.

The general sensitivity to RS response proteins, in contrast to other drugs involved in different DDR processes such as double-strand breaks through the ATM pathway, supports our previous data demonstrating the reliability of NC cells to RS response pathways.

### 7.2. The sensitivity of the selected drug candidates was confirmed through further validation.

From the initial screening results, eight potential candidates were selected for further validations, including two ATRi (VE821, AZD6738), two WEE1i (AZD1775, PD0166285), two CHK1i (CCT244747, SCH900776) and two PARPi (Olaparib, Talazoparib). We calculated the half-maximal inhibitory concentration (IC<sub>50</sub>) and found that most of the drugs tested showed IC<sub>50</sub> less than 1µM, suggesting an exquisite sensitivity of these drugs *in vitro* (**Figure 47**).

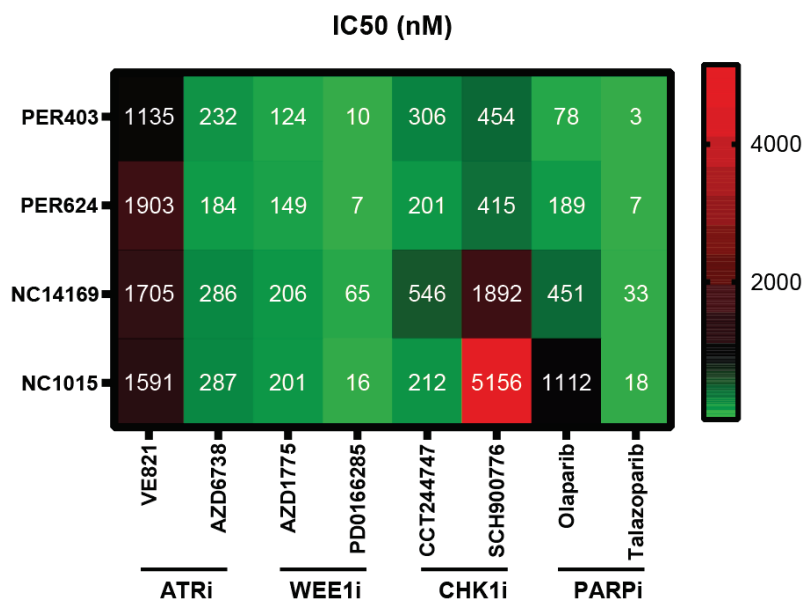


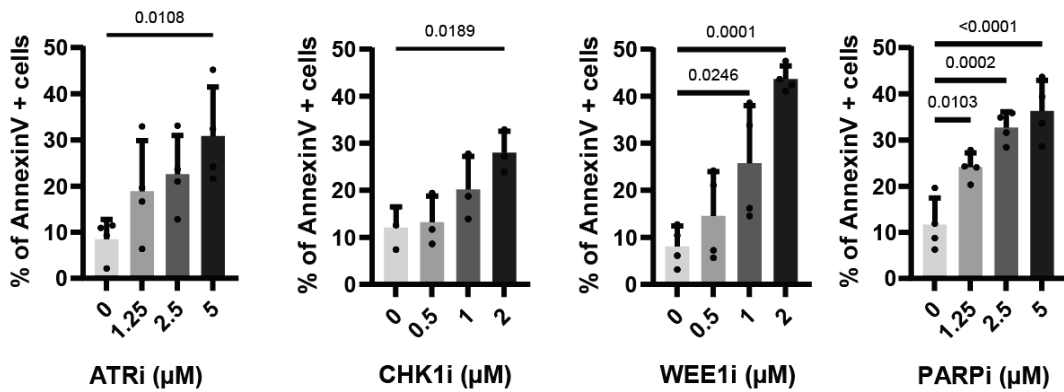
**Figure 47. IC<sub>50</sub> values of the selected candidate DDRi in NC cells.**

Heatmap representation of IC<sub>50</sub> values of a set of 8 potential DDRi in 4 NC cell lines upon three days of treatment. IC<sub>50</sub> values were calculated from three independent biological replicates.

### 7.3. Candidate drugs can induce apoptotic effects in NC cell lines.

To understand how the candidate drugs inhibit NC cell growth, we performed apoptosis assays using cell cytometry experiments to analyze Annexin V staining. PER403 and PER624 NC cell lines were treated for 48 hours with increasing concentrations of a representative inhibitor from each category: ATRi (AZD6738), CHK1i (CCT244747), WEE1i (AZD1775), and PARPi (olaparib). A dose-dependent increase in the percentage of Annexin V positive population was consistently observed across drug candidates in both cell lines (**Figure 48**), which demonstrated the capacity of these drugs to induce apoptosis in these cell lines and, thus, their cytotoxic effect.

## PER403



## PER624

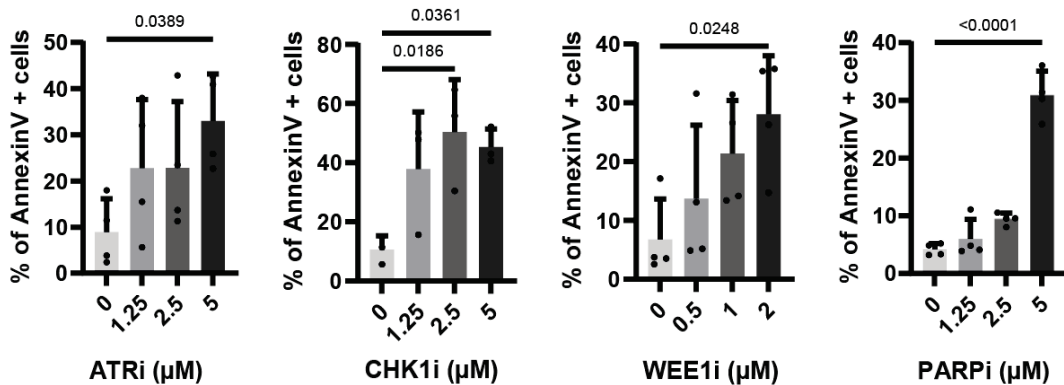


**Figure 48. Drug candidates induced apoptosis in NC cells. FACS analysis of apoptosis marker.**

Annexin V in *PER403* and *PER624* cell lines. 48 hours of increasing concentrations of different DDRi in two different NC cell lines. One-way ANOVA was used for statistical analysis.

In summary, NC cells exhibited significant sensitivity to a range of DDRi, including various components of the ATR pathway and PARP proteins, both critical in detecting and resolving RS. These findings align with earlier results indicating a heightened RS due to the BRD4-NUT fusion. Therefore, NC cells display a molecular trait that can be therapeutically exploited as a targetable vulnerability.

## 8. NC cell lines are not Homologous Recombination Deficient.

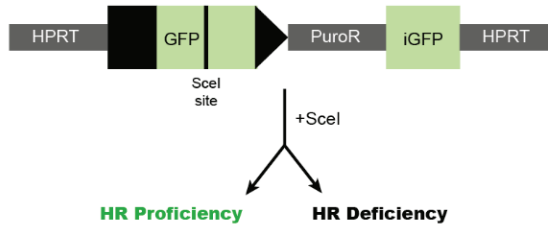
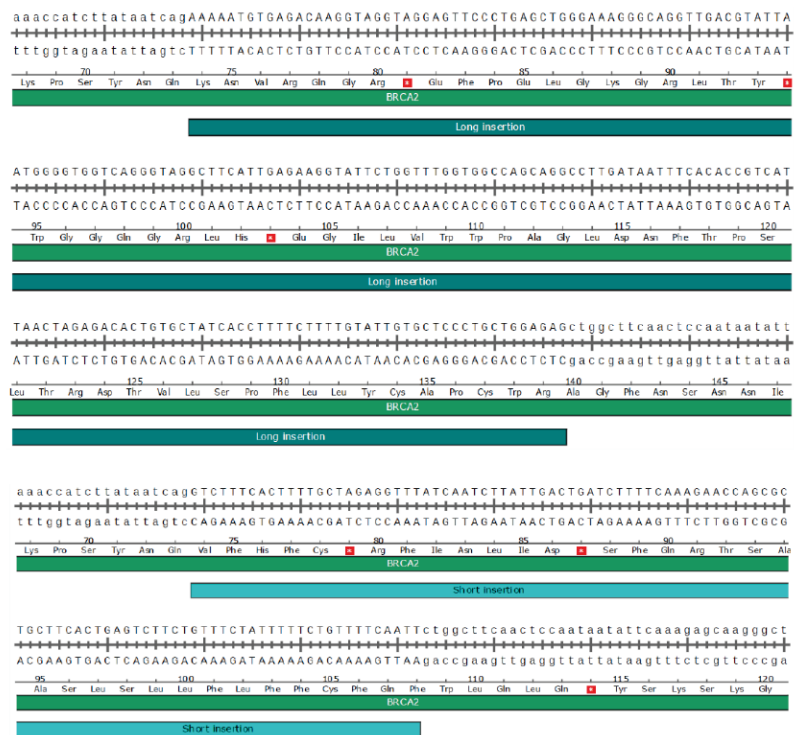
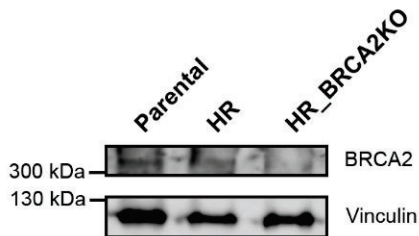
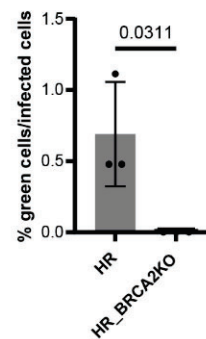
The literature reports an important link between alterations in DNA damage response, particularly Homologous Recombination Deficiency (HRD), and the sensitivity to PARPi and other DDRi in different cancer models<sup>129</sup>. To explore the possibility that NC has an HR deficiency that may explain its sensitivity to the DDRi mentioned above, we assessed the HR status of the NC model.

### 8.1. HR reporter assay shows HR proficiency in NC cells.

An HR reporter assay<sup>274</sup> was conducted to functionally evaluate the HR status of NC cells. The assay employs a pHPRT-DR-GFP vector, containing a GFP reporter gene flanked by homologous sequences to a target gene. Upon induction of double-strand DNA breaks using the *SceI* enzyme, cells with proficient HR repair mechanisms will repair the breaks using the homologous sequences, resulting in the expression of GFP. Therefore, the presence of GFP-positive cells indicates HR proficiency, providing a functional evaluation of HR capacity in the tested cells (**Figure 49A**).

As a positive control, we also generated a *BRCA2* knockout (KO) NC cell line (PER624) using CRISPR-Cas9 technology since *BRCA2* is required for HR repair and loss of *BRCA2* in cancer cells induces an HRD phenotype<sup>134</sup>. We confirmed through Sanger sequencing that the *BRCA2* KO cells displayed two different insertions that caused, in both cases, a disruption of the reading frame, resulting in biallelic truncation of the *BRCA2* locus (**Figure 49B**) and loss of protein expression (**Figure 49C**).

As expected, *BRCA2* KO cells did not show GFP expression after *SceI* treatment, indicating an HRD phenotype (**Figure 49D**). In contrast, the control cells showed GFP-positive cells upon the same treatment. Of note, it is important to consider that the efficacy of this method is limited, and our data follow the normal range of positivity obtained in different publications<sup>275,276</sup>. Thus, NC cell PER624 is HR proficient.

**A****B****C****D**

**Figure 49. NC cells PER624 is HR proficient.**

**A** Schematic representation of HR reporter assay mechanism. **B** Sequence of the two alleles of PER624\_HR\_BRCA2 KO clone showing two truncating insertions. **C** Western blot analysis of BRCA2 PER24 WT, HR, and HR\_BRCA2 KO cell lines. Vinculin is used as a loading control. **D** Percentage of GFP-positive cells analyzed by FACS to evaluate the HR status of PER624 HR and HR\_BRCA2 KO. An unpaired t-test was performed for statistical analysis.

8.2. NC cell lines and patient samples showed HR proficiency using RAD51-related functional assays.

To validate these results, IF assays of RAD51, a final effector of the HR pathway<sup>277</sup>, and  $\gamma$ H2AX, a marker of DNA damage<sup>160</sup> were performed. NC1015 cells were treated with a representative inhibitor from each category: ATRi (AZD6738), CHK1i (CCT244747), WEE1i (AZD1775), and PARPi (olaparib) for 24 hours, and both RAD51 and  $\gamma$ H2AX foci per nucleus were quantified.

Using a threshold of  $\geq 5$  foci per nucleus to consider positivity, we observed that all DDRi tested caused a significant increase of  $\gamma$ H2AX-positive cells, suggesting that these drugs can generate DNA damage in our cell model (**Figure 50A**). RAD51 positive cells were analyzed as functionally repairing cells among the  $\gamma$ H2AX positive cells. We observed a notably high percentage of RAD51 positive cells, capable of repairing DNA damage, among those affected (**Figure 50B**). This indicates that despite the capacity of DDR inhibitors to promote DNA damage in NC cells, these cells possess functional HR for repairing such damage.

Next, we used the RAD51 assay to evaluate the HR status of NC patients. The RAD51 assay serves as a surrogate measure of HR activity. It is currently used in the clinic to predict both clinical response and resistance to PARP inhibitors<sup>261,262</sup>. RAD51 assay analyzes nuclear staining of RAD51,  $\gamma$ H2AX, geminin, and DAPI (see section of '**RAD51 assay**' of Materials and Methods). Of note,  $\gamma$ H2AX was used to ensure the presence of sufficient endogenous DNA damage to evaluate HR functionality (cut-off, 25% geminin-positive cells with  $\gamma$ H2AX foci) (**Figure 50C**). Tumors with  $\geq 10\%$  of the geminin-positive tumor cells having  $\geq 5$  foci per nucleus of RAD51 were considered HRP. Four patient samples (see **Table 5**) were analyzed, and all of them showed HR proficiency, as all RAD51 scores were above the 10% threshold (**Figure 50D**).

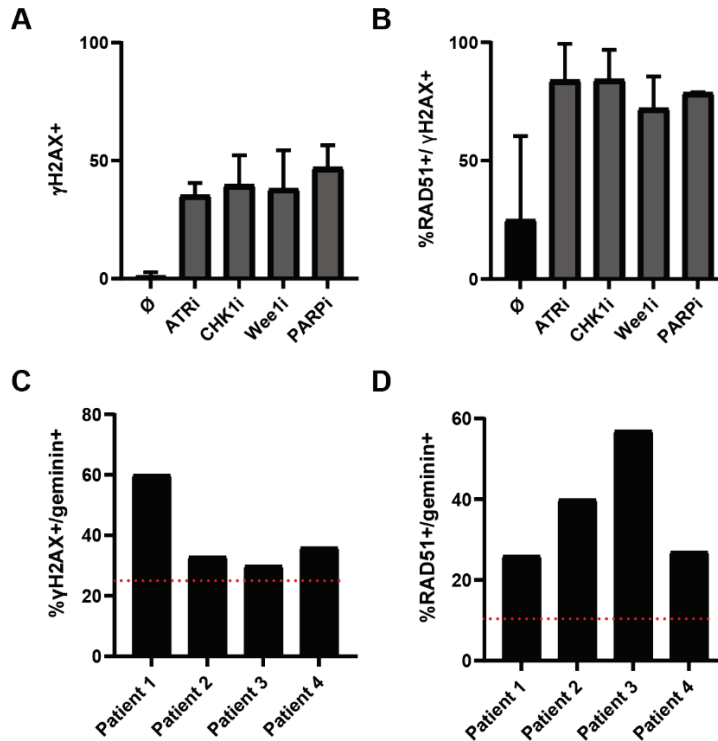


**Figure 50. NC cell lines and patient samples demonstrated HR proficiency using RAD51-related assays.**

**A** Quantification of  $\gamma$ H2AX positive cell lines ( $\geq 5$  foci per nucleus) upon different DDRi for 24 hours in NC1015 cells.  $\gamma$ H2AX was analyzed by IF. Representative of two independent biological assays is shown.  $\geq 90$  cells were quantified per condition. **B** Quantification of RAD51 positive cells ( $\geq 5$  foci per nucleus) among the  $\gamma$ H2AX positive ones. RAD51 and  $\gamma$ H2AX were analyzed by IF.  $\geq 90$  cells were quantified per condition. **C, D**  $\gamma$ H2AX (C), and RAD51 (D) scores were evaluated in 4 paraffin-embedded samples. The red line marks the threshold above which samples can be evaluated (C) or cataloged as HR proficient (D).

These data demonstrate that NC cells, unlike most PARP inhibitor-sensitive cancer models, do not exhibit signs of HRD. Consequently, HR capacity cannot account for the heightened sensitivity observed to PARP inhibitors, ATR inhibitors, CHK1 inhibitors, and WEE1 inhibitors.

## 9. The combined treatment of PARPi and ATRi significantly inhibits the growth of NC cells *in vivo*.

One of the main aims of this thesis is to unveil new therapeutic avenues for NC patients who currently lack treatment options. The novel insights gathered so far prompted us to investigate the impact of potential DDRi in an *in vivo* context. Given their advanced development and proximity to clinical application, we chose to prioritize PARP inhibitors, which have already received approval for various cancer types, such as subsets of breast, ovarian, prostate, and pancreatic cancers<sup>278</sup>. Additionally, we focused on ATR inhibitors, which have not yet been approved but are the subject of numerous advanced clinical trials<sup>279</sup>. Moreover, our focus on these two drugs is bolstered by recent publications in other cancer types demonstrating their promising effects in combination therapy<sup>280</sup>.

We first implanted PER624 cells subcutaneously into immunodeficient mice and evaluated tumor growth and mouse survival upon olaparib (PARPi), ceralasertib/AZD6738 (ATRi), or the combined treatment. Animals were weighed three times per week to monitor possible toxic effects that would affect the health or well-being of the animals. Mice weight showed minimal fold changes in vehicle and treatment groups (**Figure 51A**), confirming the lack of significant toxic effect in the treatment setting. In addition, tumor volume was measured three times per week. Results showed an important suppression of tumor growth upon ceralasertib that was not observed upon olaparib (**Figure 51B**). Furthermore, the combined treatment showed increased inhibition of tumor growth compared to ceralasertib monotherapy (**Figure 51B**). Importantly, we also found that although mouse survival was not improved upon olaparib treatment, ceralasertib could lead to increased survival, and the combination of olaparib and ceralasertib significantly increased the survival rate compared to monotherapy (**Figure 51C**).

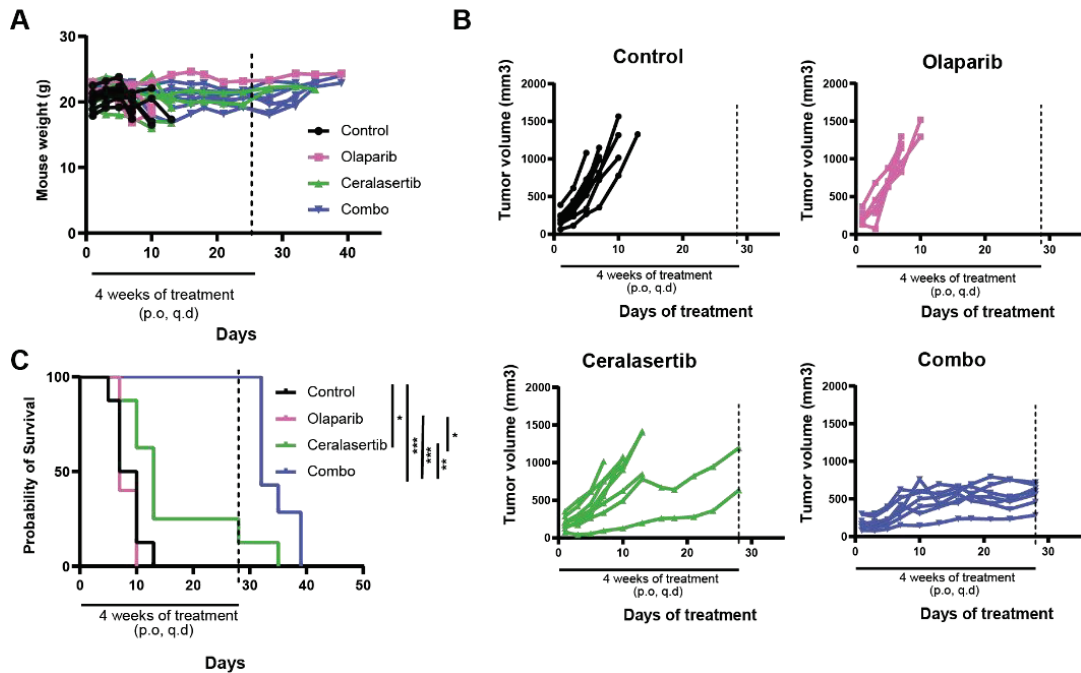


**Figure 51. PER624 xenografts show sensitivity to ATRi and PARPi combinatorial treatment.**

Mice implanted with PER624 cell subcutaneous xenografts (6-8 mice per group) were treated with vehicle, olaparib 50mg/kg orally 6 times per week, ceralasertib 25mg/kg orally 6 times per week, and the combined treatment between olaparib and ceralasertib. Each animal is independently represented in the graphs. **A** Mouse weight representation across different treatment groups. **B** Tumor growth representation across different treatment groups. **C** Survival rate of different treatment groups.

Moreover, we validated these findings by employing another NC cell line, PER403, with identical therapeutic protocols. Our results reaffirmed that the combined administration of ceralasertib and olaparib effectively inhibited tumor growth *in vivo* and extended the survival of xenograft-implanted mice (**Figure 52**).

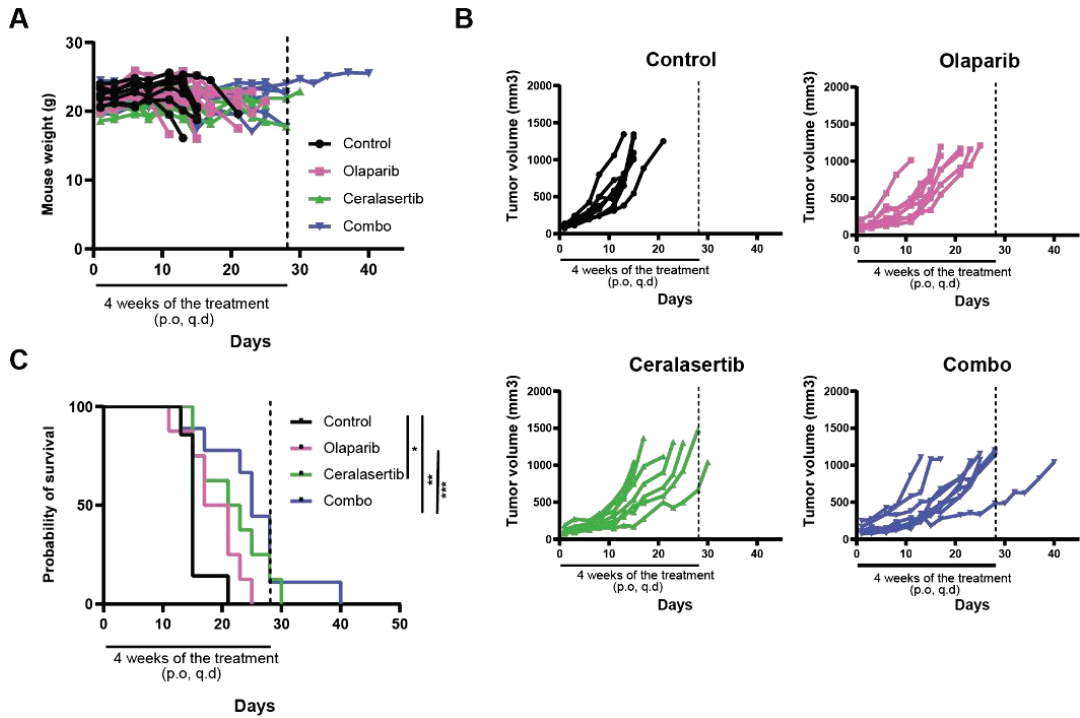


**Figure 52. PER403 xenografts show sensitivity to ATRi and PARPi combinatorial treatment.**

Mice implanted with PER403 cell subcutaneous xenografts (7-9 mice per group) were treated with vehicle, olaparib 50mg/kg orally 6 times per week, ceralasertib 25mg/kg orally 6 times per week, or combinatorial treatment. Each animal is independently represented in graphs. **A** Mouse weight representation across different treatment groups. **B** Tumor growth representation across different treatment groups. **C** Survival rate of different treatment groups.

These experiments provide compelling evidence that the combined therapy of olaparib and ceralasertib yields significant benefits in terms of inhibiting tumor growth and enhancing the survival of mice harboring NC xenografts. This promising outcome opens a new avenue for exploring novel therapeutic strategies for patients with NC, offering hope for improved outcomes in this patient population.

## PART 2. Targeting MYC as a novel therapeutic strategy for patients with NUT Carcinoma

In this second part of the thesis, we examined another molecular characteristic of NUT Carcinoma previously described: the consistent inclusion of the *MYC* gene within the megadomains and its resulting overexpression. As stated in the Introduction, megadomains of acetylation, driven by BRD4-NUT and p300, are consistently formed along the chromatin of NC cells, but with inconsistent localizations. However, it has been observed that the *MYC* locus is consistently found within these megadomains across various NC cell lines, with its expression being upregulated in a BRD4-NUT fusion-dependent manner<sup>29</sup>.

Given this observation, we sought to investigate the impact of inhibiting MYC in our cancer models. Specifically, we plan to study the effects of OMO-103. This MYC inhibitor has completed a phase I trial<sup>248</sup> and is currently undergoing a phase II clinical trial. We will evaluate whether OMO-103 is a promising new therapeutic approach for treating NC patients.

### **10. Novel MYC inhibitor OMO-103 showed remarkable sensitivity in NC cell lines.**

#### 10.1. NC cells are sensitive to OMO-103 *in vitro*.

First, we evaluated the sensitivity of our 4 NC cell lines to OMO-103 treatment. Through MTT assays, we determined that the IC<sub>50</sub> after 6 days of treatment, fell within the range of 1-9 μM (**Figure 53**). Compared to the IC<sub>50</sub> values reported for NSCLC cells and other cell types in similar *in vitro* experimental conditions<sup>281</sup>, the sensitivity of OMO-103 in NC cells appears notable.

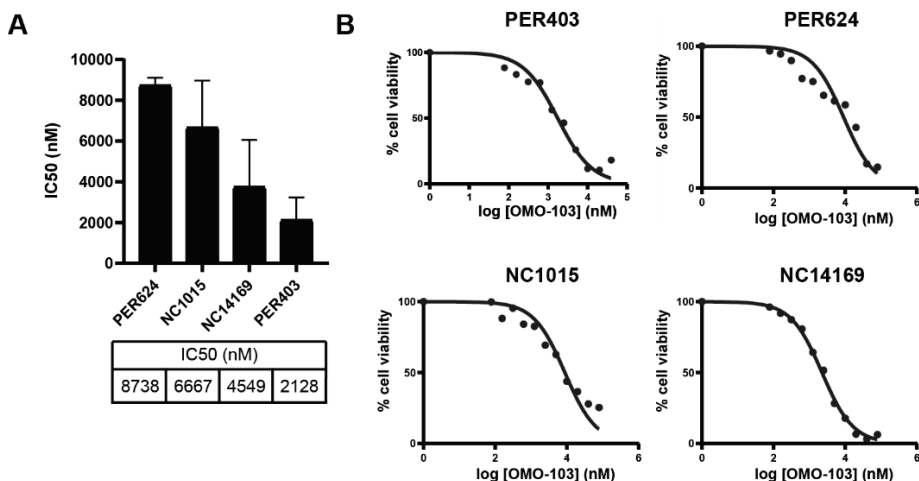


**Figure 53. NC cells are sensitive to OMO-103 *in vitro*.**

**A** IC<sub>50</sub> values for OMO-103 in 4 NC cell lines after six days of treatment using 2-4 independent biological replicates. **B** Representative growth inhibition curves of NC cell lines.

10.2. OMO-103 treatment *in vitro* enhances differentiation and induced apoptosis while halting the cell cycle progression in NC cell lines.

To explore whether OMO-103's impact on the viability of NC cells was due to its cytostatic or cytotoxic effects, we comprehensively characterized its effect on cell differentiation, apoptosis, and cell cycle progression.

We assessed the differentiation state of NC cells by examining levels of involucrin protein, a squamous differentiation marker, using Western blot analysis. Each of the four NC cell lines was treated with increasing concentrations of OMO-103 (5, 10, 20  $\mu$ M) for 48 hours. Our results revealed a consistent, dose-dependent increase in the differentiation marker across all cell lines (**Figure 54A**).

Subsequently, we aimed to determine whether OMO-103 also induced cell apoptosis, thereby exerting a cytotoxic effect. Employing the same experimental design, we treated the four NC cell lines with varying doses of OMO-103 (0, 5, 10, and 20  $\mu$ M) for 48 hours and analyzed levels of the apoptotic marker cleaved Caspase 3 (cCaspase3) via Western blot. Once again, we observed a dose-dependent elevation in cCaspase3 levels following OMO-103 treatment in all cell lines (**Figure 54B**). Additionally, we

assessed Annexin V protein expression on the cell surface via flow cytometry, another indicator of apoptosis. Consistent with previous findings, we detected a dose-dependent increase in the Annexin V-positive population across all cell lines upon MYC inhibition (**Figure 54C**).

Finally, we investigated the effect of MYC inhibition on cell cycle progression. To accomplish this, we analyzed BrdU and PI staining to identify and quantify cell cycle phases by FACS. Following treatment with varying concentrations of OMO-103 (0, 5, 10, and 20  $\mu$ M) for 48 hours, we observed a dose-dependent increase in the proportion of cells in the G1 phase, accompanied by a decrease in cells in the S phase. This indicated a predominant cell cycle arrest at the G1 phase (**Figure 54D**). As a positive control, we also included the treatment of 1  $\mu$ M JQ1, a well-established BET inhibitor known to induce cell cycle arrest in NC cells<sup>28</sup>.

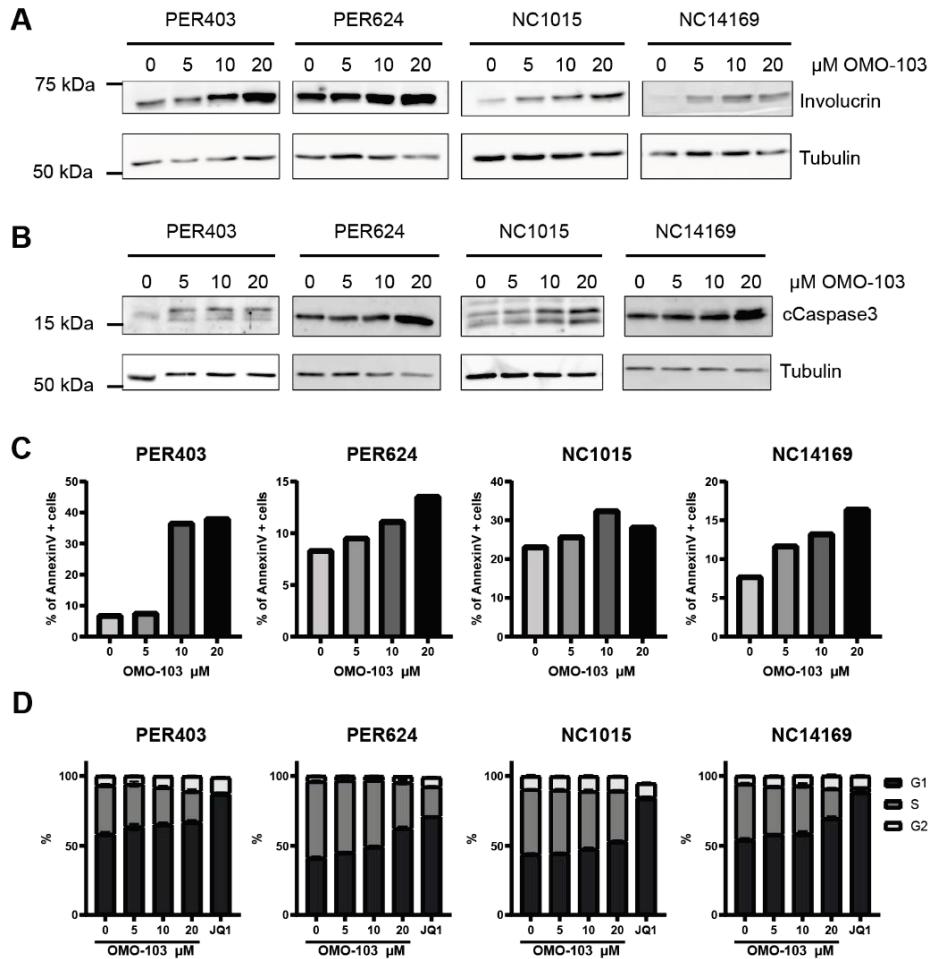


**Figure 54. OMO-103 induces differentiation, apoptosis, and cell cycle arrest in NC cells *in vitro*.**

Western blot analysis of Involucrin (**A**) and cCaspase3 (**B**) in the 4 NC cell lines upon increasing concentrations (0, 5, 10, 20  $\mu$ M) of OMO-103 treatment for 48 hours. Tubulin was used as a loading control. Representative of two independent biological assays is shown. **C** FACS analysis of Annexin V, a marker of apoptosis, in the 4 NC cell lines upon the treatment with increasing concentrations (0, 5, 10, 20  $\mu$ M) of OMO-103 for 48 hours. **D** Cell cycle analysis in the 4 NC cell lines upon the treatment with increasing concentrations (0, 5, 10, 20  $\mu$ M) of OMO-103 and 1  $\mu$ M JQ1 for 48 hours.

Overall, our findings demonstrate that OMO-103 *in vitro* treatment leads to enhanced differentiation, apoptosis, and cell cycle arrest, thus exhibiting both cytostatic and cytotoxic effects. These findings underscore its potential as a therapeutic agent for NUT Carcinoma.

## 11. Transcriptional analysis showed that OMO-103 treatment led to downregulating proliferation and cell cycle-related pathways.

In pursuit of a deeper understanding of the biological mechanism underlying MYC inhibition by the OMO-103 drug in NC cells, we subjected PER403 and NC14169 cell lines to treatment with 10  $\mu$ M of OMO-103 for 48 hours, followed by RNA sequencing analysis (**Figure 55A**). Examination of the differentially expressed genes (DEGs), with a cut-off of adjusted p-value (adj.P.Val)  $<0.05$  and log fold change (logFC)  $>1$ , revealed 125 upregulated and 222 downregulated genes in PER403 treated cells compared to untreated cells, and 104 upregulated and 70 downregulated genes in NC14169 treated cells compared to untreated cells (**Figure 55B**).

A functional analysis was conducted utilizing pre-ranked GSEA with the Hallmark collection from MSigDB. The results revealed an expected enrichment in DEGs associated with MYC target genes. Moreover, numerous pathways linked to proliferation and cell cycle advancement exhibited significant differential expression in both cell lines (**Figure 55C**).

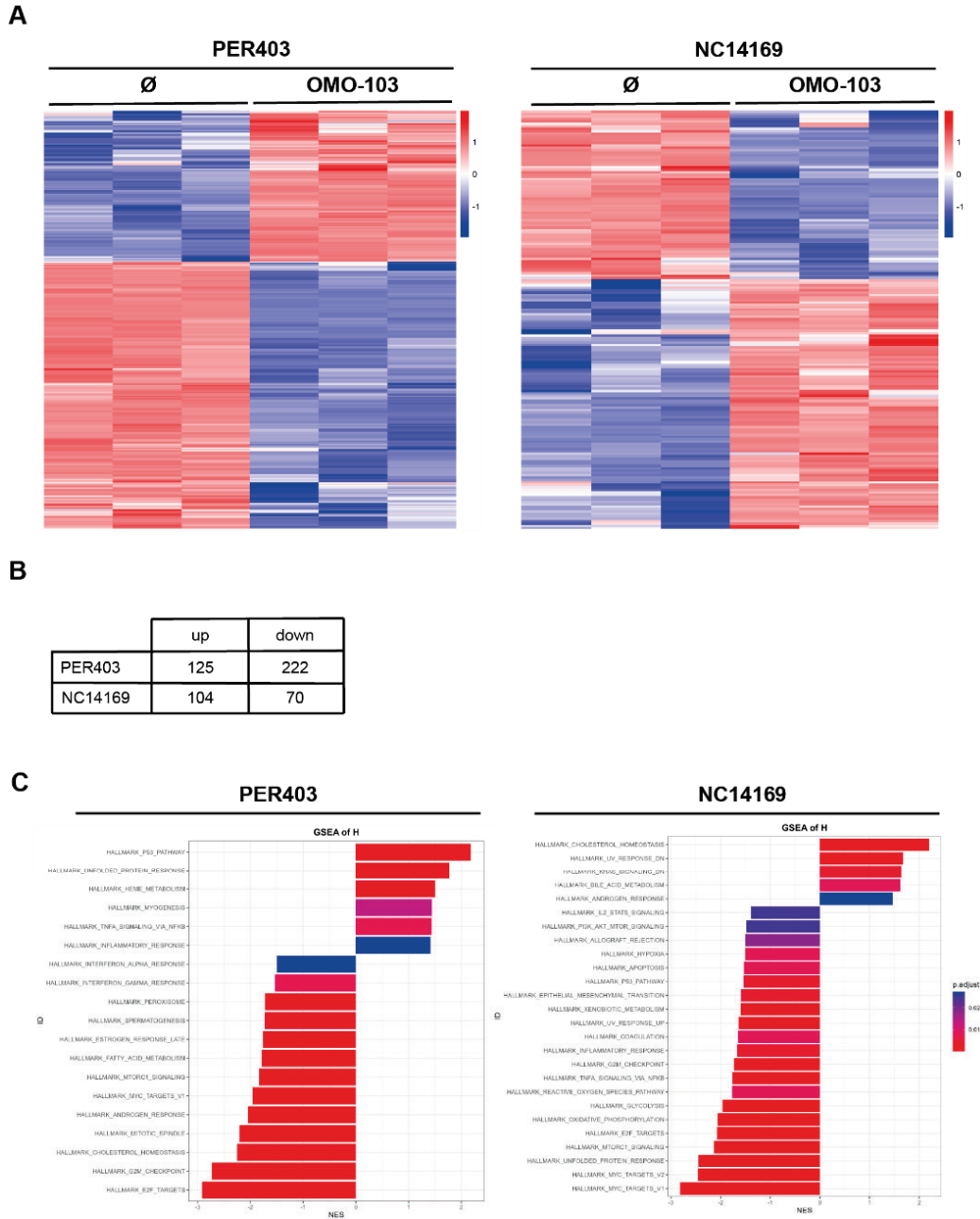


**Figure 55. OMO-103 treatment resulted in a downregulation of MYC signatures.**  
**A** Heatmap of significant differentially expressed genes in OMO-103 (10 $\mu$ M 48h) treated vs. untreated NC14169 and PER403 cell lines analyzed by RNA-seq. **B** Table of the number of differentially expressed genes (*adj.P.Val* <0.05,  $|\log_{FC}| >1$ ) per cell line **C** NES plot of significantly enriched terms (*adj.P.Val* <0.05) in OMO-103 (10 $\mu$ M 48h) treated vs. untreated NC14169 and PER403 cell lines representing the normalized enrichment score (NES).

## 12. OMO-103 can inhibit NC xenograft growth *in vivo*, particularly when combined with chemotherapy.

To validate these promising results in a more translational scenario, we evaluated the efficacy of OMO-103 in an *in vivo* setting. PER624 NC cells were subcutaneously implanted, and mice were treated with either a chemotherapy regimen of cisplatin and etoposide, OMO-103, or a combination of both. Notably, due to the rarity of NC and the current lack of clinical knowledge, there is no consensus about the standard of care chemotherapy regimen for NC patients. Nevertheless, the combination of cisplatin and etoposide has been reported as one of the most used regimens<sup>55</sup>.

The mice did not exhibit significant changes in weight across treatment conditions (**Figure 56A**). *In vivo*, OMO-103 effectively inhibited tumor growth, with more potent inhibition observed when administered in combination with a chemotherapy regimen (cisplatin and etoposide) (**Figure 56B**). mice bearing NC tumors showed significantly prolonged survival when treated with combination therapy compared to monotherapies (**Figure 56C**).

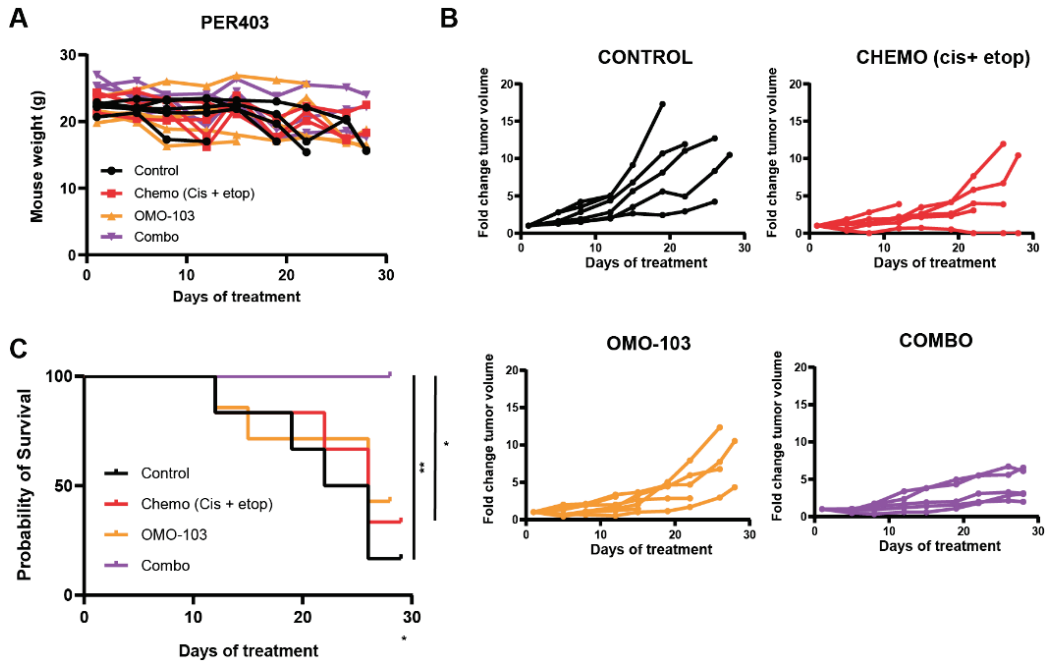


**Figure 56. The combination of OMO-103 and chemotherapy inhibited PER624 xenografts *in vivo*.**

Mice harboring PER624 subcutaneous xenografts (5-7 mice per group) were treated with vehicle, chemotherapy (cisplatin 1.5 mg/kg i.v. once per week; etoposide 4 mg/kg i.p. three times per week), OMO-103 (50mg/kg i.v. once per week), or combinatorial treatment. Each animal is independently represented in the graph. **A** Mouse weight representation of *the* different treatment groups. **B** Tumor growth of the various treatment groups. **C** Survival curves of *the* different treatment groups.

Altogether, this data provides promising perspectives about OMO-103 in terms of abrogation of cell growth with minor toxicities as a potential targeted therapy for the NC model.

## PART 3. Efficacy study of novel chemotherapy regimen for NC treatment.

In the last part of this thesis, we explored the potential utility of chemotherapeutic agents currently approved for subtypes of lung cancer. As explained in the introduction, tumors located in the thoracic region, particularly in the lungs, are the most prevalent among NC cases. Therefore, this approach has the potential to benefit a significant and clinically important subset of NC patients.

### **13. Lurbinectedin, an approved treatment for SCLC, demonstrated significant sensitivity in NC cells.**

Lurbinectedin is a chemotherapeutic drug approved for treating adults with metastatic small cell lung cancer (SCLC) who have experienced disease progression following platinum-based chemotherapy, as demonstrated in a successful phase 2 basket trial<sup>282</sup>. It functions by selectively inhibiting the active transcription of protein-coding genes, binding to promoters, and irreversibly halting transcription. Given that one of the oncogenic mechanisms of NUT Carcinoma involves high transcription, as discussed in **PART 1**. The impact of BRD4-NUT fusion on RS in NC cells as a novel targetable vulnerability of the Results, and that Lurbinectedin promotes fork stalling, leading to increased replication stress in a cellular model with already heightened replication stress, this drug holds potential for exerting a significant effect on NC cell viability.

We treated our four NC cell lines with escalating doses of Lurbinectedin for 72 hours and assessed cell viability using the MTT assay. The IC<sub>50</sub> values ranged from 40 to 180 pM (**Figure 57**), indicating remarkably high sensitivity of this cancer type to the chemotherapeutic agent, even at very low concentrations.

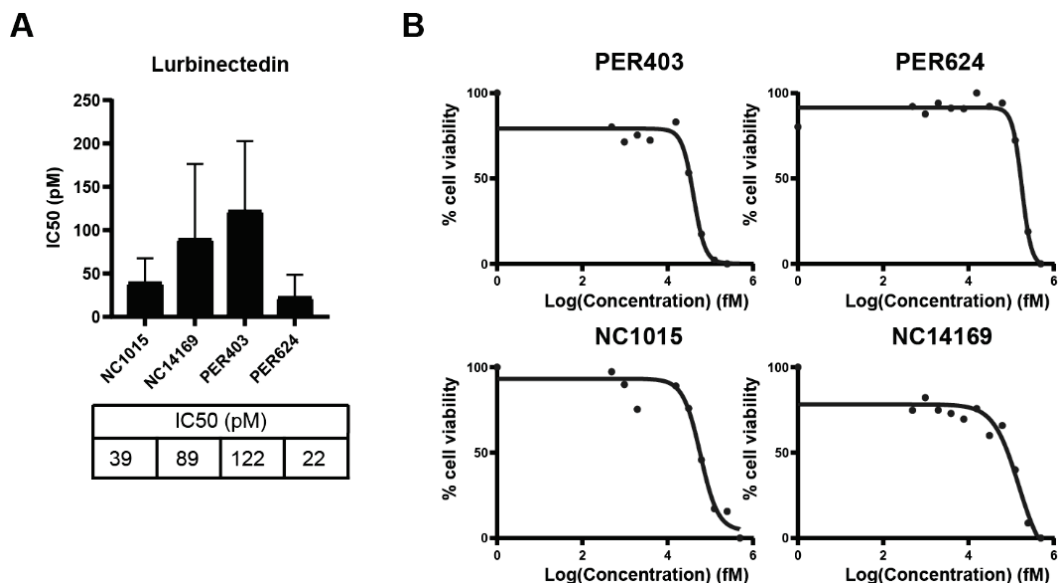


**Figure 57. NC cells are sensitive to lurbinectedin *in vitro*.**

**A** IC<sub>50</sub> values of Lurbinectedin in 4 NC cell lines upon three days of treatment. IC<sub>50</sub> values were calculated from 2-4 independent biological replicates. **B** Representative growth inhibition curves of NC cell lines.

#### 14. Irinotecan, an approved treatment for solid tumors, showed significant efficacy in NC cells.

In parallel, we evaluated another chemotherapeutic drug, irinotecan, in NC cell lines. Irinotecan, approved for treating various solid tumors, such as colorectal, ovarian, and small cell lung cancer<sup>283</sup>, is a small molecule that abrogates cell growth by inhibiting topoisomerase I. Given that topoisomerases play crucial roles in relieving DNA supercoiling generated by replication and transcription, we sought to evaluate the effect of irinotecan in our NC cell lines.

To do so, we exposed four NC cell lines to escalating concentrations of irinotecan for 72 hours to determine its IC<sub>50</sub> using an MTT assay. The IC<sub>50</sub> values were found to be in the nanomolar range (**Figure 58**), underscoring the sensitivity of NC cells to this drug.

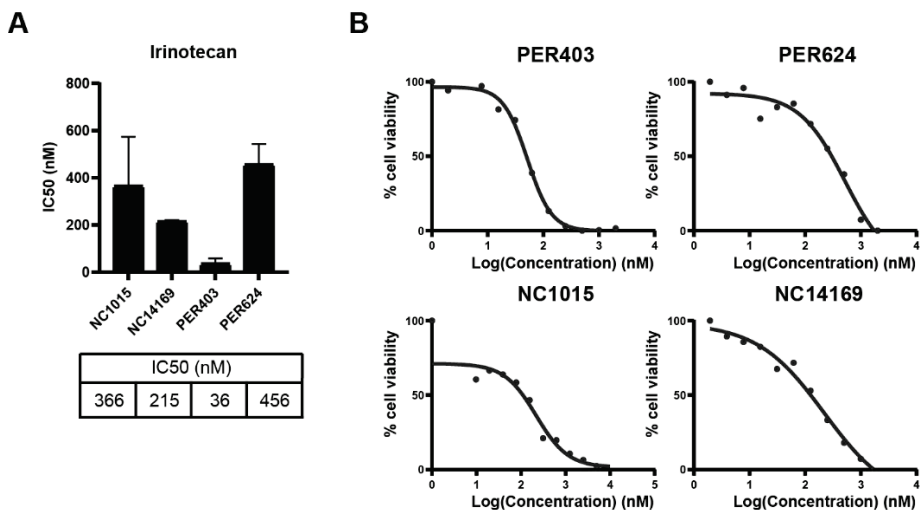


**Figure 58. NC cells are sensitive to irinotecan *in vitro*.**

**A** IC<sub>50</sub> values of irinotecan in 4 NC cell lines upon three days of treatment. IC<sub>50</sub> values were calculated from 2-4 independent biological replicates. **B** Representative growth inhibition curves of each of the NC cell lines.

In conclusion, these findings unveil potential therapeutic options that warrant further investigation *in vivo*. Moreover, rare cancers often encounter challenges in recruiting sufficient patients to establish clinical trials. Exploring the feasibility of integrating already approved drugs into the clinical management of these patients would greatly streamline the process and broaden the treatment horizons.

# DISCUSSION



In this thesis project, we have delved into the intricate molecular characterization of the rare cancer NUT Carcinoma (NC). We have found notable targetable vulnerabilities with potential implications for the clinical management of the disease. This section recapitulates the results attained throughout the project and discusses pivotal themes pertinent to our specialized field of study.

## 1. Addressing the complexities of research and advancement in treating rare cancers

NC is a sporadic cancer whose accurate incidence is currently unknown. This is, to a large extent, because of the lack of awareness in the clinical community. In general, rare cancers present challenges for diagnosis, treatment development, and clinical decision-making.

Of note, the RARECARE project, a collaborative European study, provides valuable insights into the epidemiological landscape of rare cancers and their impact on patient outcomes. According to this initiative, rare cancers, despite their rarity, collectively encompass nearly 200 distinct malignancies, constituting approximately one-quarter of all cancer diagnoses within the European Union<sup>284</sup>. Individuals afflicted with rare cancers often face disproportionately adverse prognoses compared to those with more prevalent malignancies. Consequently, a thorough exploration of these pathologies, coupled with advancements in diagnostic modalities and clinical management, holds promise for enhancing patient outcomes significantly. NC research could primarily benefit from this network.

The challenges inherent in rare cancer research extend to clinical drug development. Traditional clinical trials typically demand large patient cohorts, a criterion that proves daunting, if not impossible, for specific rare cancer subtypes. Consequently, fostering collaborative efforts across institutions and international boundaries, particularly in rare cancer therapeutics, is imperative to develop effective treatment strategies and conduct meaningful clinical trials. Moreover, conventional randomized controlled trial methodologies are being reevaluated within this context. Notably, Serrano *et al.* recently questioned the appropriateness of placebo-controlled trials as the gold standard for

assessing drug efficacy in rare cancers that, in many cases, lack a standard of care that can be used as a control arm<sup>285</sup>. Moreover, the utilization of placebos may sometimes pose risks for patients. As an alternative approach, the authors propose the implementation of synthetic control arms derived from meticulously curated, tumor-specific datasets. NC could adopt this strategy for further drug development.

## 2. Limitations of experimental models in NUT Carcinoma research

As mentioned above, studying rare cancers poses unique challenges due to their low occurrence rates and the limited understanding of their underlying molecular mechanisms. In such scenarios, the availability and suitability of appropriate models are crucial for advancing our knowledge and developing effective therapeutic approaches.

In this project, we utilized four patient-derived NC cell lines. Two originated from lung tissue, one from the thymus, and the fourth's origin remains unidentified (see **Table 3**). This selection partially mirrors the heterogeneity of tumor locations, with lung sites representing the most prevalent thoracic locations, thus closely resembling reality<sup>5,6</sup>.

Our NC cell lines exhibited the primary chromosomal rearrangement, resulting in the BRD4-NUT fusion protein. While three cell lines displayed the typical t(15;19) translocation generating BRD4-NUT<sup>1,29,31</sup>, the PER624 cell line exhibited a complex and uncommon karyotype, leading to the fusion of BRD4 exon 15 with NUT exon 2<sup>249</sup>. Although the literature offers limited NC-derived cell lines primarily harboring BRD4-NUT fusions, reports of two patient-derived cell lines expressing BRD3-NUT and NSD3-NUT fusions exist<sup>21,28</sup>.

We acknowledge that our experimental models lack representation of other NUT fusion partners such as BRD3 or NSD3. However, the identification of the BRD4-interacting complex involving BRD3, NSD3, or ZNF32<sup>26</sup> standardizes the molecular mechanism of all NC fusions. Thus, the mechanisms elucidated in this project can potentially be extrapolated to all

NUT fusion partners. Nevertheless, validating our findings in BRD3- or NSD3-NUT cell lines would strengthen our conclusions.

To better translate NC biological insights into clinical practice, models that more accurately mimic the intricate biological landscape of human NC tumors, such as patient-derived xenografts (PDXs), are critical. However, the low number of diagnosed patients and the challenges in obtaining tumor samples have hindered the success rate of PDX generation for NC tumors in our laboratory. Nevertheless, ongoing collaborative efforts aim to validate our promising *in vivo* results in successfully generated PDX models.

Crucially, the recent development of a genetically engineered mouse model (GEMM) for NC has confirmed the strong capacity of BRD4-NUT fusion protein to induce the malignant transformation of squamous progenitor cells into NC. This advancement holds excellent promise for substantially improving our comprehension of NC oncogenesis, disease progression, and metastasis<sup>15,34</sup>.

### 3. Strategies for modulating BRD4-NUT expression in NC cells.

Gain and loss-of-function strategies are imperative for investigating a protein's biological role. In this project, modulation of the BRD4-NUT fusion protein has played a crucial role in elucidating its molecular mechanism and its impact on the behavior and identity of NC cells.

On the one hand, we successfully developed an inducible OE model to better understand the role of the BRD4-NUT fusion and its BRD4 and NUT components. Despite observing variations in construct expression levels, the results remained unbiased. The BRD4-NUT fusion OE model exhibited lower expression levels compared to the rest, likely due to the protein's large size. Nonetheless, the cell line overexpressing BRD4-NUT demonstrated a more pronounced phenotypic effect, displaying increased expression of various RS markers such as pRPA or pChk1. This suggests that despite its lower expression than counterparts such as BRD4s or NUT, the BRD4-NUT OE cell line can cause the most significant phenotype.

On the other hand, to eliminate the BRD4-NUT fusion, the use of siRNAs or shRNAs targeting the NUT moiety could be beneficial. However, these approaches typically necessitate an extended time window, usually around 72 hours, for an effective elimination of the fusion protein. This extended period could potentially lead to cellular adaptation, confounding the results.

Therefore, we adopted a fast degradation approach to examine changes in NC cells upon the elimination of the BRD4-NUT fusion protein. Small molecules that selectively and rapidly target our protein of interest are crucial for studying immediate phenotypic consequences. However, the limited availability of specific small molecules targeting our fusion of interest restricted our tool selection. Currently, there are no specific inhibitors or degraders of NUT. Thus, we opted for MZ1, a small molecule based on the PROTACs system that selectively degrades BRD4 over BRD3 or BRD2, and, consequently, the BRD4-NUT fusion protein within 4 hours. It's worth noting that this approach does not rule out the potential phenotypic effects of concurrent degradation of wild-type BRD4. Nevertheless, results from the OE model demonstrated that the increased RS phenotype depends on NUT, with a non-significant role of BRD4 modulation implying a significant impact of BRD4-NUT degradation over BRD4 WT in the RS phenotype upon MZ1 treatment.

Despite the absence of existing small molecules specifically degrading NUT and thus the fusion protein, employing the auxin-inducible degron system could serve as a further step to validate our findings<sup>286</sup>.

#### 4. Epigenetic-driven cancers: understanding the impact of BRD4 in cancer development and progression.

As discussed in the introduction, epigenetic dysregulation can significantly contribute to cancer development, maintenance, or progression by causing rapid and dynamic changes in chromatin structure and transcriptional landscape. NUT Carcinoma is an example of an epigenetic-driven cancer type, where the BRD4-NUT fusion triggers mechanisms that profoundly alter chromatin acetylation distribution across the chromatin, affecting cellular behavior. Similar epigenetic dysregulations are observed in other cancer

types. For instance, Acute Myeloid Leukemia (AML) harbors mutations in genes encoding epigenetic regulators such as DNMT3A, TET2, or IDH1/2, resulting in abnormal DNA methylation patterns<sup>287</sup>. Additionally, subtypes of lung or breast cancers exhibit epigenetic dysregulations involving aberrant DNA methylation<sup>288</sup>, histone modification patterns<sup>289</sup>, or the chromatin repressive factor EZH2<sup>290</sup>.

BRD4 is widely acknowledged for its pivotal role in regulating super-enhancers and oncogene expression<sup>98</sup>. It identifies acetylated sites in chromatin through its bromodomains and interacts with hyperacetylated histone regions, such as enhancers, or megadomains in the case of NC. Subsequently, it can recruit the Mediator complex, facilitating the assembly of the transcription machinery and stabilizing various transcription factors. This accumulation of transcriptionally active regulatory elements promotes gene transcription<sup>98</sup>. Notably, BRD4 demonstrates selectivity towards cancer-related genes such as *MYC*<sup>291</sup>.

Recent studies have revealed additional roles of BRD4 in cancer, extending beyond transcriptional regulation. It has been identified as a guardian of genome stability, influencing DNA damage checkpoint activation and repair<sup>292–295</sup>. Therefore, BRD4 isn't solely reliant on its conventional transcriptional activity, but it also acts as a platform between histone modifications and components of the DNA repair machinery, facilitating DNA damage checkpoint activation.

The *BRD4* gene encodes two main isoforms, BRD4 long (BRD4l) and short (BRD4s) (see **Figure 12**), with different domain compositions and some differential roles. BRD4l promotes RNA elongation through interaction with P-TEFb through its C-terminal domain, absent in BRD4s, and both isoforms facilitate transcription by associating with the transcriptional co-factor MED1 and forming condensates of high densities of transcriptional proteins<sup>99,296</sup>. Additionally, BRD4l has a HAT domain capable of catalyzing histone acetylation<sup>100</sup>. In the case of NC, the p300 recruitment by the NUT moiety of the fusion bypasses the lack of HAT activity of the BRD4s isoform included in the fusion. Despite being less expressed, BRD4s exhibit a higher affinity to histone modifications and a greater capacity to organize transcription factors, likely resulting in its significant predominance in the phenotype of NC

cells<sup>99,296</sup>. Of note, emerging data suggest contradictory functions of BRD4s and BRD4l isoforms in cancer, with BRD4s demonstrating an oncogenic role in breast cancer studies while BRD4l exhibits tumor-suppressive behavior<sup>101</sup>.

## 5. Targeting replication stress in NUT Carcinoma.

This thesis project explores a novel role of the BRD4-NUT fusion protein in NUT Carcinoma. With our data, we proposed a model in which BRD4-NUT triggers the formation of megadomains in a p300-dependent manner, leading to an overall increase in the transcription rate and replication fork speed. Additionally, our experiments with BRD4-NUT expression modulation revealed the accumulation of R-loop in NC, driven by increased transcription mediated by BRD4-NUT and p300. We propose that this accumulation of R-loops is a key factor contributing to the RS observed in NC cells (**Figure 45**). These results indicate that while the BRD4-NUT fusion protein promotes an oncogenic state by upregulating transcription of pro-proliferative genes and downregulating transcription of pro-differentiation genes (as mentioned in the Introduction), it also induces replication stress.

Cancer cells often heavily depend on specific signaling pathways to fuel their aggressive proliferative property, a phenomenon known as pathway addiction<sup>297</sup>. This addiction to specific signaling pathways is a crucial aspect of cancer biology and has significant implications for cancer therapy development<sup>298</sup>. By targeting particular pathways that cancer cells rely on, we can potentially inhibit their viability and achieve therapeutic benefits. Notably, such targeted treatments often exhibit selective toxicity towards cancer cells addicted to these pathways compared to healthy tissues. Our findings suggest that NC cells rely on the replication stress response pathways, and we aimed to explore this dependency for therapeutic intervention.

After identifying this newfound vulnerability, we investigated the sensitivity of NC cells to various drugs targeting DNA damage response (DDR) pathways. Consistent with earlier findings indicating a heightened RS status in NC cells, inhibitors of the ATR pathway (including ATR, WEE1, and CHK1 inhibitors) and PARP showed the most significant impact on NC cell viability. Conversely, small molecules targeting other DDR pathways like DNA-PK or ATM, which are involved in resolving different types of DNA damage, did not produce a

comparable effect. This supports the notion that NC cells exhibit oncogenic addiction to pathways involved in resolving replication stress, particularly the ATR pathway.

Genome instability is a well-established hallmark of cancer<sup>223</sup>. Transcription-replication conflicts (TRCs) emerge as significant sources of genome instability, influenced by various cellular factors, such as heightened transcriptional activity, aberrant DNA replication, altered epigenetic modifications, and oncogene activation<sup>197,202,227</sup>. In NC cells, we observed alterations in all these factors. Firstly, the presence of the BRD4-NUT fusion protein elevates overall transcription levels. Secondly, our DNA fiber assay results indicate a BRD4-NUT fusion-dependent dysregulation of DNA replication, as evidenced by decreased replication velocity upon BRD4-NUT degradation, with velocity restoration upon BRD4-NUT expression recovery. Notably, although replication stress is often linked to slower or stalled replication forks, recent evidence suggests that faster forks, as observed here, can also lead to RS<sup>171</sup>. Thirdly, there is a notable alteration in epigenetic modifications, with the BRD4-NUT fusion protein promoting the formation of megadomains that alter histone acetylation along the chromatin. Fourthly, consistent upregulation of the oncogene MYC has been observed in NC cells<sup>29</sup>. Collectively, these findings suggest the presence of TRCs in NC cells, which are known to promote R-loop accumulation, as a significant source of RS, also considered a hallmark of cancer<sup>171,202</sup>.

Additionally, it's worth noting that *RECQL5* is among the few genes found to be consistently mutated in NC cells<sup>59</sup>. *RECQL5* is a DNA helicase that prevents TRCs by associating with both transcription and replication machinery, thus limiting their occurrence. Furthermore, *RECQL5* seems to play a role in preventing the formation of RNA-DNA hybrids<sup>197</sup>. Therefore, further investigation is warranted to explore the potential connection between accumulated RS and R-loops in NC cells and the consistent mutation in the *RECQL5* gene.

An apparent discrepancy arises when comparing our findings with previous studies regarding the role of BRD4 in regulating RS. In 2018, a study by Zhang *et al.* reported that eliminating BRD4 with the BET inhibitor JQ1 significantly increased various RS markers, such as pCHK1 (S317)<sup>295</sup>. Similarly, a 2020

study by Lam *et al.* observed that the loss of BRD4 by JQ1 led to the accumulation of R-loops and collisions of the replication machinery, resulting in RS and DNA damage<sup>299</sup>. However, despite these apparently conflicting results, closer scrutiny reveals meaningful differences between our study and previous ones. Firstly, the studies referenced used commonly employed cancer cell lines such as U2OS (osteosarcoma), OVCAR3 (ovarian cancer), HeLa (cervical cancer), and HCT116 (colon cancer). In contrast, our study focuses on NUT carcinoma, driven by the BRD4-NUT fusion, a distinct model from these cell lines. Secondly, as previously mentioned, the BRD4l and BRD4s isoforms often demonstrate opposing effects in tumor cells. BRD4l is more frequently expressed in general terms. However, the BRD4-NUT fusion protein contains BRD4s isoform. It is possible that in this specific NC cell context, due to the aforementioned higher affinity of BRD4s to histone modifications, the presence of BRD4-NUT fusion proteins might displace BRD4l from the acetylated sites. Furthermore, when comparing these contradictory results, it is fundamental to highlight the fact that, in NUT Carcinoma, the replication stress (RS) phenotype is dependent on the NUT moiety rather than BRD4, further distinguishing our model.

Finally, while our research has demonstrated the role of BRD4-NUT fusion proteins in the RS phenotype of NC cells, there remains a need to delve deeper into understanding the intricate relationship between megadomains, R-loops, and their functional outcomes. To address this, our next step involves conducting Chromatin Immunoprecipitation (ChIP)-sequencing experiments to precisely map the localization of BRD4-NUT fusion proteins and megadomains within the chromatin. Additionally, we will also perform DNA-RNA immunoprecipitation (DRIP)-sequencing assays to delineate the distribution of R-loops across the chromatin. Subsequently, we will rigorously analyze the obtained data to gain deeper insights into the potential genome-wide localizations of the fusion protein, megadomains, and R-loops. This comprehensive analysis will enable us to elucidate the functional implications of these interactions and better explain the phenotype.

## 6. The effect of PARP inhibitors beyond Homologous Recombination deficiency.

As previously discussed, NC cells displayed pronounced sensitivity to ATR pathway inhibitors, such as ATR, CHK1, or WEE1, aligning with their elevated replication stress and suggesting reliance on the ATR pathway for resolution. NC cells exhibited notable sensitivity to PARPis in our DDR inhibitor screening. These drugs target PARP proteins, primarily known for their role in single-strand break (SSB) DNA repair, but also crucial in various cellular functions, including chromatin modulation and response to replication stress<sup>300</sup>.

Initially, PARP inhibitors were found to be efficacious in treating ovarian cancer with BRCA1/2 deficiencies, leading to FDA approval for this indication. The traditional understanding of PARPi sensitivity involves synthetic lethality. In this model, PARPis blocks SSB repair, hindering the BER pathway, and thereby converting SSBs to double-strand breaks (DSBs). In contexts of homologous recombination deficiency (HRD), such as BRCA mutated cases, these DSBs cannot be efficiently repaired, resulting in an accumulation of DNA damage and, ultimately, cell death<sup>244,246</sup>. Subsequently, PARP inhibitors have received approval for their use in various HRD contexts beyond ovarian cancer, including breast, prostate, and pancreatic cancer<sup>236</sup>.

For many years, PARP inhibitors were commonly believed to be effective only in scenarios characterized by HRD. To explore this assumption, we conducted experiments to assess the HR capacity in our NC cell lines. Surprisingly, our findings revealed no evidence of HRD in NC cells. This observation aligns with reports indicating sensitivity to PARP inhibitors in non-HRD models. For instance, Ewing Sarcoma, another rare cancer driven by a fusion protein, has been shown to exhibit sensitivity to PARP inhibition due to the interaction between PARP and its fusion protein, which plays a critical role in maintaining genome stability<sup>301</sup>. Additionally, PARP inhibitors have demonstrated efficacy in triple-negative breast cancer (TNBC) with proficient HR (HRP). In this scenario, mutations in the PTEN gene lead to chromosomal instability and sensitize cells to PARPis in a replication-dependent manner<sup>302</sup>.

Recent research has revealed that PARP1 is involved in the protein-protein interaction network associated with R-loops. In this context, PARP1 binds to R-loops, associates with sites of R-loop formation, and activates its catalytic activity<sup>303</sup>. This finding supports the hypothesis that NUT Carcinoma cells experience elevated replication stress levels but have developed mechanisms to resolve it and survive. However, inhibiting either the ATR or PARP pathways, which are crucial for alleviating RS, entirely and rapidly abolishes their viability. Notably, the investigation of combinatorial treatment in this study also revealed an enhanced effect *in vivo*.

Taken together, the NUT Carcinoma model contributes to the growing body of evidence showing that PARP inhibitors impact cell viability in non-HRD contexts and underscores the involvement of PARP in the response to replication stress.

## 7. The emerging role of *MYC* oncogene in NUT Carcinoma.

The fusion protein BRD4-NUT consistently upregulates *MYC* expression across various NUT Carcinoma cell lines, serving as a driving mechanism of NC oncogenesis by promoting a pro-proliferative and undifferentiated state<sup>29</sup>. Given the high variability and lack of common targets among the studied NC cell lines and the absence of consistent mutations in their genomic landscape, we sought to investigate this consistent characteristic as a potential targeted therapeutic strategy.

*MYC* is a pivotal regulator and transcription factor for tumor development and maintenance. It governs cell proliferation, growth, metabolism, apoptosis, and immune suppression<sup>111</sup>. Amplification or dysregulation of the *MYC* oncogene is prevalent in most human cancers. However, *MYC* has long been deemed challenging to target therapeutically for several reasons. Firstly, *MYC* is vital in healthy cells, and complete inhibition may lead to adverse effects. Secondly, its nuclear localization poses challenges for drug development due to issues with penetrance. Thirdly, the redundant functions of *MYC* family members, including c-*MYC*, L-*MYC*, and N-*MYC*, necessitate simultaneous inhibition.

Fourthly, its intrinsically disordered structure and lack of an enzymatic catalytic site require non-canonical molecule designs<sup>281</sup>.

However, Dr. Laura Soucek's team has developed a 91-amino acid mini-protein called OMO-103, which inhibits MYC function. OMO-103 acts as a dominant negative molecule for MYC by displacing it from its target genes and binding to E-boxes of the DNA as an inactive competitor, forming either a homodimer or a heterodimer with MYC itself or its partner MAX<sup>281</sup> (**Figure 27**). OMO-103 has demonstrated efficacy in several cancer models, including non-small cell lung cancer (NSCLC)<sup>281</sup>, breast cancer<sup>304</sup>, and melanoma<sup>305</sup>. Moreover, it has completed a phase 1 clinical trial in advanced solid tumors, demonstrating minor toxicities, establishing a recommended dose for phase 2 trials, and showing preliminary signs of efficacy<sup>248</sup>. Currently, a phase 2 clinical trial is being conducted.

Our findings reveal that NC cells exhibit a notably high sensitivity to OMO-103, surpassing that observed in other cancer models such as NSCLC<sup>281</sup>. Additionally, OMO-103 treatment induces cytotoxic and cytostatic effects in NC cells, triggering apoptosis, promoting cell differentiation, and halting the cell cycle. Moreover, NC xenografts display sensitivity to OMO-103, particularly when combined with chemotherapy, without significant toxicities. It is worth noting that optimizing the treatment regimen for OMO-103 could potentially enhance its effectiveness as monotherapy. While the current treatment scheme follows the standard protocol for other cancer models, the aggressive and rapid nature of NUT Carcinoma suggests that increasing the dosing frequency may inhibit tumor growth to a greater extent.

The promising results regarding MYC targeting in this MYC-dependent cancer model, coupled with the positive outcomes of the phase 1 clinical trial, present an opportunity to explore the clinical benefits of this therapeutic approach for NC patients.

## 8. A possible connection between RS and MYC in NC oncogenesis.

BRD4 and MYC, individually, serve as master regulators in cell biology and are implicated in various diseases, including cancer<sup>306</sup>. Both proteins are

ubiquitous and influence critical cellular processes such as growth, development, stress responses, and metabolism. Moreover, they participate in pivotal nuclear events like chromatin remodeling, super-enhancer function, transcriptional regulation, condensate formation, and extrachromosomal DNA (ecDNA) hub assembly<sup>306</sup> (**Figure 59**).

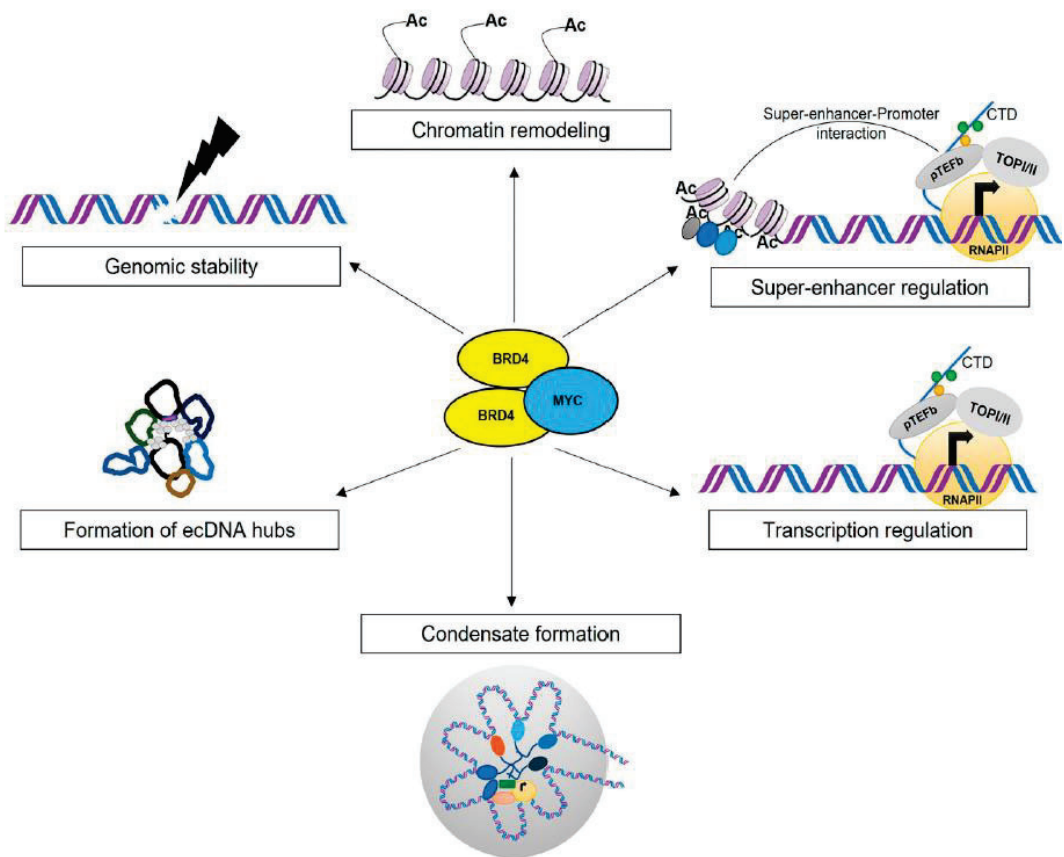


**Figure 59. BRD4 and MYC roles in nuclear processes.**  
From Kotekar *et al.*<sup>306</sup>

Interestingly, previous work has linked the regulation of MYC, both transcriptionally and post-transcriptionally, to BRD4 function<sup>306</sup>. At the transcriptional level, BRD4 binds to the MYC promoter and its adjacent super-enhancer region, exerting regulatory control over its transcription. Inhibition of BRD4 by JQ1 has decreased MYC expression<sup>307</sup>. Consequently, BRD4

inhibition has long been considered a clinical strategy for indirectly modulating MYC expression, with observed clinical benefits in specific contexts such as a subtype of lung adenocarcinoma<sup>281,308</sup>. Moreover, BRD4 and MYC are interconnected at a post-transcriptional level as well. For example, Devaiah *et al.* demonstrated that BRD4 phosphorylates MYC at Thr58, leading to its ubiquitination and subsequent degradation. Additionally, MYC can bind to BRD4 and inhibit BRD4's histone acetyltransferase (HAT) activity through a conformational change, thereby establishing a negative feedback loop that regulates its expression<sup>309</sup>.

As a new layer of overlapping complexity, MYC overexpression can be considered a source of RS, in addition to the already discussed accumulation of megadomains of acetylation, causing a hypertranscriptional state. MYC acts as a global transcriptional amplifier, increasing the overall activation of promoters and leading to a hyper-transcription in cancer cells<sup>310</sup>. As explained in the introduction, this increased transcription is a source of RS in cells.

Moreover, the function of MYC extends beyond transcriptional regulation, as it has also been implicated in other processes such as nuclear organization, replication stress response, and R-loop regulation. MYC protein relieves torsional stress caused by active transcription, prevents collisions between transcription DNA replication machinery, resolves R-loops, and participates in the repair of DNA damage by interacting with topoisomerases as well as DNA repair and RNA processing factors<sup>311</sup>. Therefore, MYC's oncogene function intrinsically increases RS in cells, but, in parallel, it participates in various mechanisms to resolve it.

In conclusion, there is a possibility that both parts of this thesis are two partial explanations of the same phenomena (**Figure 60**). BRD4-NUT fusion confers an oncogenic role in NC cells by completely remodeling the histone acetylation and the formation of megadomains. These megadomains promote an incremented proliferative and undifferentiated state, which is essential (but probably not only) driven by the hyperactivation of the *MYC* locus included in these megadomains. As a consequence of this oncogenic strategy, a general hyper-transcription causes an increased RS status in the NC cells through the

accumulation of unresolved R-loops. As an adaptation mechanism, NC cells depend on RS-releasing mechanisms, including ATR, PARP, and MYC. Therefore, inhibiting any of these key survival pathways in NC cells causes an abrogation of cell viability and a subsequent reduction of tumor growth.

To investigate this interconnection further, an analysis of different RS and R-loops markers such as pRPA or pChk1 and S9.6 and DNA fiber assays should be performed under MYC inhibition with OMO-103. Furthermore, the combinatorial ATR and MYC inhibition treatment should be explored in NC xenografts and PDXs.

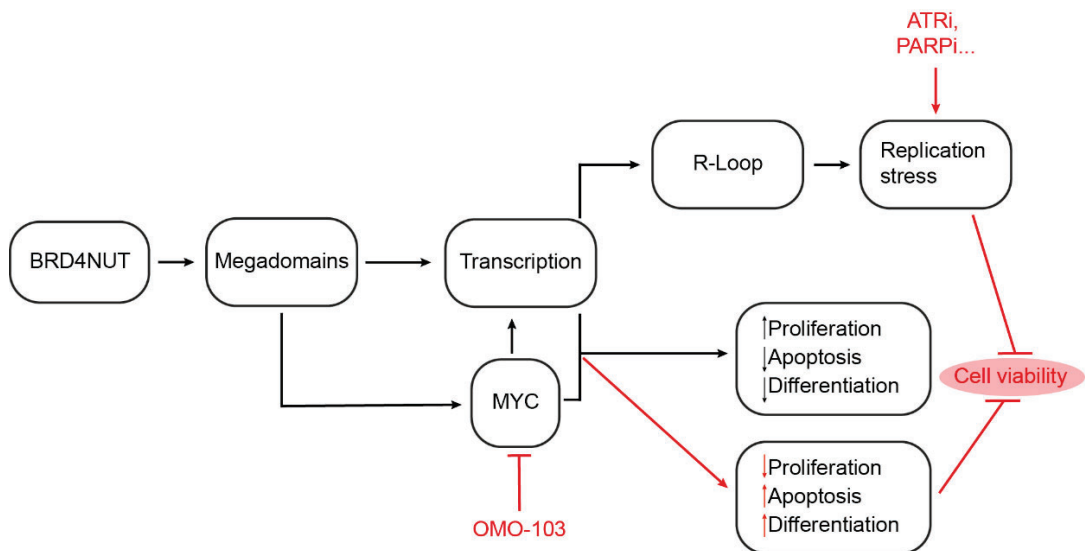


**Figure 60. Scheme of the potential connection between RS and MYC in NC.**

# CONCLUSIONS



1. BRD4-NUT is linked to RS markers in NC cells.
2. The NUT moiety of the fusion protein is associated with the RS phenotype in NC cells.
3. BRD4-NUT fusion expression also impacts the replication fork speed.
4. The histone acetyltransferase p300 and megadomains are required for BRD4-NUT fusion-induced RS in NC cells.
5. Transcription is required for BRD4-NUT fusion-induced RS in NC cells.
6. There is an accumulation of R-loops in NC cells, and R-loops are also required for BRD4-NUT-induced RS in NC cells.
7. NC cells are sensitive to inhibitors targeting RS response proteins, including PARPi, ATRi, CHK1i, and WEE1i.
8. NC cell lines and patient samples are absent of Homologous Recombination deficiency.
9. The combination treatment of olaparib and ceralasertib demonstrates significant benefits by effectively restraining tumor growth *in vivo* and improving the survival rate of mice carrying NC xenografts.
10. NC cell lines exhibit remarkable sensitivity to the MYC inhibitor OMO-103, which induces differentiation, apoptosis, and cell cycle arrest *in vitro* and manifests both cytotoxic and cytostatic effects.

11. Treatment with OMO-103 inhibits the growth of NC cells *in vivo*, particularly when combined with a chemotherapy regimen comprising cisplatin and etoposide.
  
12. NC cell lines demonstrate sensitivity to lurbinectedin and irinotecan *in vitro*.

# REFERENCES



1. Kees, U. R., Mulcahy, M. T. & Willoughby, M. L. N. Intrathoracic Carcinoma in an 11-Year-Old Girl Showing a Translocation t(15;19). *J. Pediatr. Hematol. Oncol.* **13**, 459–464 (1991).
2. Kubonishi, I., Takehara, N. & Iwata, J. Novel t(15;19)(q15;p13) chromosome abnormality in a thymic carcinoma. *Cancer Res.* **51**, 3327–3328 (1991).
3. French, C. A. *et al.* BRD4-NUT Fusion Oncogene: A Novel Mechanism in Aggressive Carcinoma 1. *Cancer Research.* **63**, 304-307 (2003)
4. French, C. A. *et al.* Report of the First International Symposium on NUT Carcinoma. *Clin. Cancer Res.* **28**, 2493–2505 (2022).
5. Chau, N. G. *et al.* An anatomical site and genetic-based prognostic model for patients with nuclear protein in testis (NUT) midline carcinoma: Analysis of 124 patients. *JNCI Cancer Spectr.* **4**, 1–9 (2021).
6. Giridhar, P., Mallick, S., Kashyap, L. & Rath, G. K. Patterns of care and impact of prognostic factors in the outcome of NUT midline carcinoma: a systematic review and individual patient data analysis of 119 cases. *Eur. Arch. Oto-Rhino-Laryngology* **275**, 815–821 (2018).
7. Zhang, K. *et al.* A sinonasal NUT midline carcinoma in an 84-year-old man undergoing radiation and proton therapy . *Clin. Case Reports* **11**, 1–4 (2023).
8. Bauer, D. E. *et al.* Clinicopathologic features and long-term outcomes of NUT midline carcinoma. *Clin. Cancer Res.* **18**, 5773–5779 (2012).
9. Haack, H. *et al.* Diagnosis of NUT midline carcinoma using a NUT-specific monoclonal antibody. *Am. J. Surg. Pathol.* **33**, 984–991 (2009).
10. French, C. A. *et al.* Midline carcinoma of children and young adults with NUT rearrangement. *J. Clin. Oncol.* **22**, 4135–4139 (2004).
11. Shehata, B. M. *et al.* NUT midline carcinoma in a newborn with multiorgan disseminated tumor and a 2-year-old with a pancreatic/hepatic primary. *Pediatr. Dev. Pathol.* **13**, 481–485 (2010).
12. Lemelle, L. *et al.* NUT carcinoma in children and adults: A multicenter retrospective study. *Pediatr. Blood Cancer* **64**, 1–9 (2017).
13. Dickson, B. C. *et al.* NUTM1 Gene Fusions Characterize a Subset of Undifferentiated Soft Tissue and Visceral Tumors. *Am. J. Surg. Pathol.* **42**, 636–645 (2018).
14. Mertens, F., Wiebe, T., Adlercreutz, C., Mandahl, N. & French, C. A. Successful treatment of a child with t(15;19)-positive tumor. *Pediatr. Blood Cancer* **49**, 1015–1017 (2006).
15. Durall, R. T. *et al.* The BRD4-NUT Fusion Alone Drives Malignant Transformation of NUT Carcinoma. *Cancer Res.* **83**, 3846–3860 (2023).
16. Serritella, A. V. *et al.* Retrospective analysis of NUT carcinoma: The Northwestern experience. *J. Clin. Oncol.* **41**, e18096–e18096 (2023).
17. Lee, J. K. *et al.* Complex chromosomal rearrangements by single catastrophic pathogenesis in NUT midline carcinoma. *Ann. Oncol.* **28**, 890–897 (2017).
18. Evans, A. G. *et al.* Pathologic characteristics of nut midline carcinoma arising in

- the mediastinum. *Am. J. Surg. Pathol.* **36**, 1222–1227 (2012).
19. Bishop, J. A. & Westra, W. H. NUT midline carcinomas of the sinonasal tract. *Am J Surg Pathol.* **36**, 1216–1221 (2012).
  20. Shiota, H. *et al.* Nut Directs p300-Dependent, Genome-Wide H4 Hyperacetylation in Male Germ Cells. *Cell Rep.* **24**, 3477–3487 (2018).
  21. French, C. A. *et al.* NSD3-NUT fusion oncoprotein in NUT midline carcinoma: Implications for a novel oncogenic mechanism. *Cancer Discov.* **4**, 929–941 (2014).
  22. Shiota, H. *et al.* ‘Z4’ complex member fusions in nut carcinoma: Implications for a novel oncogenic mechanism. *Mol. Cancer Res.* **16**, 1826–1833 (2018).
  23. Wu, S. J. *et al.* Novel BRD2::NUTM1 Fusion in NUT Carcinoma With Exceptional Response to Chemotherapy: A Case Report. *JTO Clin. Res. Reports* **5**, 100625 - 100629 (2024).
  24. Moreno, V., Saluja, K. & Pina-Oviedo, S. NUT Carcinoma: Clinicopathologic Features, Molecular Genetics and Epigenetics. *Front. Oncol.* **12**, 1–10 (2022).
  25. Reynoird, N. *et al.* Oncogenesis by sequestration of CBP/p300 in transcriptionally inactive hyperacetylated chromatin domains. *EMBO J.* **29**, 2943–2952 (2010).
  26. Alekseyenko, A. A. *et al.* Ectopic protein interactions within BRD4-chromatin complexes drive oncogenic megadomain formation in NUT midline carcinoma. *Proc. Natl. Acad. Sci. U. S. A.* **114**, E4184–E4192 (2017).
  27. Alekseyenko, A. A. *et al.* The oncogenic BRD4-NUT chromatin regulator drives aberrant transcription within large topological domains. (2015)
  28. French, C. A. *et al.* BRD-NUT oncoproteins: A family of closely related nuclear proteins that block epithelial differentiation and maintain the growth of carcinoma cells. *Oncogene* **27**, 2237–2242 (2008).
  29. Grayson, A. R. *et al.* MYC, a downstream target of BRD-NUT, is necessary and sufficient for the blockade of differentiation in NUT midline carcinoma. *Oncogene* **33**, 1736–1742 (2014).
  30. Alekseyenko, A. A. *et al.* The oncogenic BRD4-NUT chromatin regulator drives aberrant transcription within large topological domains. *Genes Dev.* **29**, 1507–1523 (2015).
  31. Wang, R. *et al.* Activation of SOX2 expression by BRD4-NUT oncogenic fusion drives neoplastic transformation in NUT midline carcinoma. *Cancer Res.* **74**, 3332–3343 (2014).
  32. Alekseyenko, A. A. *et al.* Cell state-dependent chromatin targeting in NUT carcinoma. *Genetics* **224**, 1–9 (2023).
  33. Eagen, K. P. & French, C. A. Supercharging BRD4 with NUT in carcinoma. *Oncogene* **40**, 1396–1408 (2021).
  34. Zheng, D. *et al.* BRD4-NUTm1 fusion gene initiates NUT carcinoma in vivo. *bioRxiv* (2023).
  35. French, C. A. NUT Carcinoma: Clinicopathologic features, pathogenesis, and

- treatment. *Pathol. Int.* **68**, 583–595 (2018).
36. Lauer, U. M., Hinterleitner, M., Horger, M., Ohnesorge, P. V. & Zender, L. NUT Carcinoma—An Underdiagnosed Malignancy. *Front. Oncol.* **12**, 1–11 (2022).
  37. Solomon, L. W., Magliocca, K. R., Cohen, C. & Müller, S. Retrospective analysis of nuclear protein in testis (NUT) midline carcinoma in the upper aerodigestive tract and mediastinum. *Oral Surg. Oral Med. Oral Pathol. Oral Radiol.* **119**, 213–220 (2015).
  38. McEvoy, C. R., Fox, S. B. & Prall, O. W. J. Emerging entities in NUTM1-rearranged neoplasms. *Genes Chromosom. Cancer* **59**, 375–385 (2020).
  39. Charlab, R. & Racz, R. The expanding universe of NUTM1 fusions in pediatric cancer. *Clin. Transl. Sci.* **16**, 1331–1339 (2023).
  40. Diolaiti, D. *et al.* A recurrent novel MGA-NUTM1 fusion identifies a new subtype of high-grade spindle cell sarcoma. *Cold Spring Harb. Mol. Case Stud.* **4**, 1–16 (2018).
  41. Schaefer, I. M. *et al.* CIC-NUTM1 fusion: A case which expands the spectrum of NUT-rearranged epithelioid malignancies. *Genes Chromosom. Cancer* **57**, 446–451 (2018).
  42. Yang, S. *et al.* CIC-NUTM1 Sarcomas Affecting the Spine: A Subset of CIC-Rearranged Sarcomas Commonly Present in the Axial Skeleton. *Arch. Pathol. Lab. Med.* **146**, 735–741 (2022).
  43. Boer, J. M. *et al.* Favorable outcome of NUTM1-rearranged infant and pediatric B cell precursor acute lymphoblastic leukemia in a collaborative international study. *Leukemia* **35**, 2978–2982 (2021).
  44. Chau, N. G. *et al.* Intensive treatment and survival outcomes in NUT midline carcinoma of the head and neck. *Cancer* **122**, 3632–3640 (2016).
  45. Luo, J. *et al.* Initial Chemotherapy for Locally Advanced and Metastatic NUT Carcinoma. *J. Thorac. Oncol.* (2024)
  46. Wang, S. *et al.* Advances in the pathogenesis and treatment of nut carcinoma: A narrative review. *Transl. Cancer Res.* **9**, 6505–6515 (2020).
  47. Maher, O. M., Christensen, A. M., Yedururi, S., Bell, D. & Tarek, N. Histone deacetylase inhibitor for NUT Midline Carcinoma. *Pediatr. Blood Cancer* **62**, 715–717 (2015).
  48. Filippakopoulos, P. *et al.* Selective inhibition of BET bromodomains. *Nature* **468**, 1067–1073 (2010).
  49. Piha-Paul, S. A. *et al.* Phase 1 study of molibresib (GSK525762), a bromodomain and extra-terminal domain protein inhibitor, in NUT carcinoma and other solid tumors. *JNCI Cancer Spectr.* **4**, 1–9 (2020).
  50. Shapiro, G. I. *et al.* A Phase 1 study of RO6870810, a novel bromodomain and extra-terminal protein inhibitor, in patients with NUT carcinoma, other solid tumours, or diffuse large B-cell lymphoma. *Br. J. Cancer* **124**, 744–753 (2021).
  51. Ameratunga, M. *et al.* First-in-human Phase 1 open label study of the BET inhibitor ODM-207 in patients with selected solid tumours. *Br. J. Cancer* **123**,

- 1730–1736 (2020).
52. Hilton, J. *et al.* Initial results from a phase I/IIa trial evaluating BMS-986158, an inhibitor of the bromodomain and extra-terminal (BET) proteins, in patients (pts) with advanced cancer. *Ann. Oncol.* **29**, viii134 (2018).
  53. Tontsch-Grunt, U. *et al.* Therapeutic impact of BET inhibitor BI 894999 treatment: backtranslation from the clinic. *Br. J. Cancer* **127**, 577–586 (2022).
  54. Romero, F. A. *et al.* GNE-781, A Highly Advanced Potent and Selective Bromodomain Inhibitor of Cyclic Adenosine Monophosphate Response Element Binding Protein, Binding Protein (CBP). *J. Med. Chem.* **60**, 9162–9183 (2017).
  55. Morrison-Smith, C. D. *et al.* Combined targeting of the BRD4-NUT-p300 axis in NUT midline carcinoma by dual selective bromodomain inhibitor, NEO2734. *Mol. Cancer Ther.* **19**, 1406–1414 (2020).
  56. Shiota, H. *et al.* Chemical screen identifies diverse and novel histone deacetylase inhibitors as repressors of nut function: Implications for NUT carcinoma pathogenesis and treatment. *Mol. Cancer Res.* **19**, 1818–1830 (2021).
  57. Schwartz, B. E. *et al.* Differentiation of NUT midline carcinoma by epigenomic reprogramming. *Cancer Res.* **71**, 2686–2696 (2011).
  58. Knight, A., Karapetyan, L. & Kirkwood, J. M. Immunotherapy in Melanoma: Recent Advances and Future Directions. *Cancers (Basel)*. **15**, 1–18 (2023).
  59. Stirnweiss, A., Oommen, J., Kotecha, R. S., Kees, U. R. & Beesley, A. H. Molecular-genetic profiling and high-throughput in vitro drug screening in NUT midline carcinoma - an aggressive and fatal disease. **8**, 112313–112329 (2017).
  60. Davis, A., Mahar, A., Wong, K., Barnett, M. & Kao, S. Prolonged Disease Control on Nivolumab for Primary Pulmonary NUT Carcinoma. *Clin. Lung Cancer* **22**, e665–e667 (2021).
  61. Chen, M., Chen, X., Zhang, Y., Wang, W. & Jiang, L. Clinical and molecular features of pulmonary NUT carcinoma characterizes diverse responses to immunotherapy, with a pathologic complete response case. *J. Cancer Res. Clin. Oncol.* **149**, 6361–6370 (2023).
  62. Kornberg, R. D. Chromatin Structure : A Repeating Unit of Histones and DNA. *Science* **184**, 868–871 (1974).
  63. McGinty, R. K. & Tan, S. Nucleosome structure and function. *Chem. Rev.* **115**, 2255–2273 (2015).
  64. Misteli, T. The Self-Organizing Genome: Principles of Genome Architecture and Function. *Cell* **183**, 28–45 (2020).
  65. Dixon, J. R. *et al.* Topological domains in mammalian genomes identified by analysis of chromatin interactions. *Nature* **485**, 376–380 (2012).
  66. Lieberman-aiden, E. *et al.* Comprehensive mapping of long-range interactions reveals folding principles of the Human Genome. **326**, 289–294 (2009).
  67. Sanyal, A., Baù, D., Martí-Renom, M. A. & Dekker, J. Chromatin globules: A

- common motif of higher order chromosome structure? *Curr. Opin. Cell Biol.* **23**, 325–331 (2011).
68. Cremer, T. & Cremer, M. Chromosome territories. *Cold Spring Harb. Perspect. Biol.* **2**, 1–24 (2010).
  69. Millán-Zambrano, G., Burton, A., Bannister, A. J. & Schneider, R. Histone post-translational modifications — cause and consequence of genome function. *Nat. Rev. Genet.* **23**, 563–580 (2022).
  70. van Steensel, B. & Furlong, E. E. M. The role of transcription in shaping the spatial organization of the genome. *Nat. Rev. Mol. Cell Biol.* **20**, 327–337 (2019).
  71. Taberlay, P. C. *et al.* Three-dimensional disorganization of the cancer genome occurs coincident with long-range genetic and epigenetic alterations. *Genome Res.* **26**, 719–731 (2016).
  72. Moore, L. D., Le, T. & Fan, G. DNA methylation and its basic function. *Neuropsychopharmacology* **38**, 23–38 (2013).
  73. Clapier, C. R. & Cairns, B. R. The biology of chromatin remodeling complexes. *Annu. Rev. Biochem.* **78**, 273–304 (2009).
  74. Cutter, A. & Hayes, J. J. A brief review of nucleosome structure. *FEBS Lett.* **589**, 2914–2922 (2015).
  75. Bannister, A. J. & Kouzarides, T. Regulation of chromatin by histone modifications. *Cell Res.* **21**, 381–395 (2011).
  76. Hebbes, T. R., Thorne, A. W. & Crane-Robinson, C. A direct link between core histone acetylation and transcriptionally active chromatin. *EMBO J.* **7**, 1395–1402 (1988).
  77. Vakoc, C. R., Sachdeva, M. M., Wang, H. & Blobel, G. A. Profile of Histone Lysine Methylation across Transcribed Mammalian Chromatin. *Mol. Cell. Biol.* **26**, 9185–9195 (2006).
  78. Black, J. C., Van Rechem, C. & Whetstine, J. R. Histone Lysine Methylation Dynamics: Establishment, Regulation, and Biological Impact. *Mol. Cell* **48**, 491–507 (2012).
  79. Rossetto, D. *et al.* Histone phosphorylation. A chromatin modification involved in diverse nuclear events Histone phosphorylation. *Epigenetics* **7**, 1098–1108 (2012).
  80. Gillette, T. G. & Hill, J. A. Readers, writers and erasers: Chromatin as the whiteboard of heart disease. *Circ Res.* **116**, 1245–1253 (2015).
  81. Zhang, T., Cooper, S. & Brockdorff, N. The interplay of histone modifications – writers that read. *EMBO Rep.* **16**, 1467–1481 (2015).
  82. Falkenberg, K. J. & Johnstone, R. W. Histone deacetylases and their inhibitors in cancer, neurological diseases and immune disorders. *Nat. Rev. Drug Discov.* **13**, 673–691 (2014).
  83. Allfrey, V. G., Mirsky, A. E., Anderson, D. L., Appelman, E. H. & Malm, J. G. Structural Modifications of Histones and their Possible Role in the Regulation of RNA Synthesis. 27–29 (1964).

84. Eberharter, A. & Becker, P. B. Histone acetylation: A switch between repressive and permissive chromatin. Second in review on chromatin dynamics. *EMBO Rep.* **3**, 224–229 (2002).
85. Verdin, E. & Ott, M. 50 years of protein acetylation: From gene regulation to epigenetics, metabolism and beyond. *Nat. Rev. Mol. Cell Biol.* **16**, 258–264 (2015).
86. Wang, Y. *et al.* Dysregulation of histone acetyltransferases and deacetylases in cardiovascular diseases. *Oxid. Med. Cell. Longev.* **2014**, (2014).
87. Yang, X. J. & Seto, E. HATs and HDACs: From structure, function and regulation to novel strategies for therapy and prevention. *Oncogene* **26**, 5310–5318 (2007).
88. Wang, J. *et al.* HAT- and HDAC-Targeted Protein Acetylation in the Occurrence and Treatment of Epilepsy. *Biomedicines* **11**, 1–26 (2023).
89. Lundblad, J. R., Kwok, R. P. S., Laurence, M. E., Harter, M. L. & Goodman, R. H. Adenoviral E1A-associated protein p300 as a functional homologue of the transcriptional co-activator CBP. *Nature* **374**, (1995).
90. Liao, Z. W. *et al.* High expression of p300 is linked to aggressive features and poor prognosis of Nasopharyngeal Carcinoma. *J. Transl. Med.* **10**, 1–8 (2012).
91. Castillo, J. *et al.* CBP/p300 drives the differentiation of regulatory T cells through transcriptional and non-transcriptional mechanisms. *Cancer Res.* **79**, 3916–3927 (2019).
92. Gou, P. & Zhang, W. Protein lysine acetyltransferase CBP/p300: A promising target for small molecules in cancer treatment. *Biomed. Pharmacother.* **171**, 116130 (2024).
93. Dyson, H. J. & Wright, P. E. Role of intrinsic protein disorder in the function and interactions of the transcriptional coactivators CREB-binding Protein (CBP) and p300. *J. Biol. Chem.* **291**, 6714–6722 (2016).
94. Gallinari, P., Di Marco, S., Jones, P., Pallaoro, M. & Steinkühler, C. HDACs, histone deacetylation and gene transcription: From molecular biology to cancer therapeutics. *Cell Res.* **17**, 195–211 (2007).
95. Cheung, K. L., Kim, C. & Zhou, M. M. The Functions of BET Proteins in Gene Transcription of Biology and Diseases. *Front. Mol. Biosci.* **8**, 1–15 (2021).
96. Hargreaves, D. C., Horng, T. & Medzhitov, R. Control of Inducible Gene Expression by Signal-Dependent Transcriptional Elongation. *Cell* **138**, 129–145 (2009).
97. Liu, W. *et al.* Brd4 and JMJD6-associated anti-pause enhancers in regulation of transcriptional pause release. *Cell* **155**, 1581–1595 (2013).
98. Donati, B., Lorenzini, E. & Ciarrocchi, A. BRD4 and Cancer: Going beyond transcriptional regulation. *Mol. Cancer* **17**, 1–13 (2018).
99. Drumond-Bock, A. L. & Bieniasz, M. The role of distinct BRD4 isoforms and their contribution to high-grade serous ovarian carcinoma pathogenesis. *Mol. Cancer* **20**, 1–15 (2021).
100. Devaiah, B. N. *et al.* BRD4 is a histone acetyltransferase that evicts

- nucleosomes from chromatin. *Nat. Struct. Mol. Biol.* **23**, 540–548 (2016).
101. Wu, S. Y. *et al.* Opposing Functions of BRD4 Isoforms in Breast Cancer. *Mol. Cell* **78**, 1114–1132.e10 (2020).
  102. Valencia, A. M. & Kadoch, C. Chromatin regulatory mechanisms and therapeutic opportunities in cancer. *Nat. Cell Biol.* **21**, 152–161 (2019).
  103. You, J. S. & Jones, P. A. Cancer Genetics and Epigenetics: Two Sides of the Same Coin? *Cancer Cell* **22**, 9–20 (2012).
  104. Audia, J. E. & Campbell, R. M. Histone modifications and cancer. *Cold Spring Harb. Perspect. Biol.* **8**, 1–31 (2016).
  105. Kosno, M., Currie, S. L., Kumar, A., Xing, C. & Rosen, M. K. Molecular features driving condensate formation and gene expression by the BRD4-NUT fusion oncoprotein are overlapping but distinct. *Sci. Rep.* **13**, 1–20 (2023).
  106. Yu, D. *et al.* Structural mechanism of BRD4-NUT and p300 bipartite interaction in propagating aberrant gene transcription in chromatin in NUT carcinoma. *Nat. Commun.* **14**, 1–16 (2023).
  107. Rosencrance, C. D. *et al.* Chromatin Hyperacetylation Impacts Chromosome Folding by Forming a Nuclear Subcompartment. *Mol. Cell* **78**, 112–126.e12 (2020).
  108. Yang, A. *et al.* P63, a P53 Homolog At 3Q27-29, Encodes Multiple Products With Transactivating, Death-Inducing, and Dominant-Negative Activities. *Mol. Cell* **2**, 305–316 (1998).
  109. Ramsey, M. R. *et al.* FGFR2 signaling underlies p63 oncogenic function in squamous cell carcinoma. *J. Clin. Invest.* **123**, 3525–3538 (2013).
  110. Novak, D. *et al.* SOX2 in development and cancer biology. *Semin. Cancer Biol.* **67**, 74–82 (2020).
  111. Dhanasekaran, R. *et al.* The MYC oncogene — the grand orchestrator of cancer growth and immune evasion. *Nat. Rev. Clin. Oncol.* **19**, 23–36 (2022).
  112. Huang, Y. *et al.* EZH2 Cooperates with BRD4-NUT to Drive NUT Carcinoma Growth by Silencing Key Tumor Suppressor Genes. *Cancer Res.* **83**, 3956–3973 (2023).
  113. Sun, S., Yu, F., Xu, D., Zheng, H. & Li, M. EZH2, a prominent orchestrator of genetic and epigenetic regulation of solid tumor microenvironment and immunotherapy. *BBA Rev. Cancer* **1877**, 188700 (2022).
  114. Burgess, J. T. *et al.* The Therapeutic Potential of DNA Damage Repair Pathways and Genomic Stability in Lung Cancer. *Front. Oncol.* **10**, 1–14 (2020).
  115. Ma, Q. *et al.* Increased chromosomal instability characterizes metastatic renal cell carcinoma. *Transl. Oncol.* **14**, 100929 (2021).
  116. Giglia-Mari, G., Zotter, A. & Vermeulen, W. DNA damage response. *Cold Spring Harb. Perspect. Biol.* **3**, 1–19 (2011).
  117. Huang, R. & Zhou, P. K. *DNA damage repair: historical perspectives, mechanistic pathways and clinical translation for targeted cancer therapy.* *Signal Transduction and Targeted Therapy* vol. 6 (Springer US, 2021).

118. Jackson, S. P. & Bartek, J. The DNA-damage response in human biology and disease. *Nature* **461**, 1071–1078 (2009).
119. Hoeijmakers, J. H. J. DNA Damage, Aging, and Cancer. 1475–1485 (2009).
120. Goshal, G. & Chen, J. DNA damage tolerance: a double-edged sword guarding the genome. *Transl Cancer Res.* **2**, 107–129 (2013).
121. Chatterjee, N. & Walker, G. C. Mechanisms of DNA damage, repair, and mutagenesis. *Environ. Mol. Mutagen.* **58**, 235–263 (2017).
122. Kim, S. I., Jin, S. G. & Pfeifer, G. P. Formation of cyclobutane pyrimidine dimers at dipyrimidines containing 5-hydroxymethylcytosine. *Photochem. Photobiol. Sci.* **12**, 1409–1415 (2013).
123. Borrego-Soto, G., Ortiz-López, R. & Rojas-Martínez, A. Ionizing radiation-induced DNA injury and damage detection in patients with breast cancer. *Genet. Mol. Biol.* **38**, 420–432 (2015).
124. Waters, M. D., Stack, H. F. & Jackson, M. A. Genetic toxicology data in the evaluation of potential human environmental carcinogens. *Mutat. Res. - Rev. Mutat. Res.* **437**, 21–49 (1999).
125. Kunkel, T. A. Evolving Views of DNA Replication ( In ) Fidelity OVERLAPPING FUNCTIONS. *cold Spring Harb. Lab. Press* **LXXIV**, 1–11 (2009).
126. Calzada, A., Hodgson, B., Kanemaki, M., Bueno, A. & Labib, K. Molecular anatomy and regulation of a stable replisome at a paused eukaryotic DNA replication fork. *Genes Dev.* **19**, 1905–1919 (2005).
127. Ravanat, J.-L., Cadet, J. & Douki, T. Oxidatively Generated DNA Lesions as Potential Biomarkers of In Vivo Oxidative Stress. *Curr. Mol. Med.* **12**, 655–671 (2012).
128. Lindahl, T. Instability and decay of the primary structure of DNA. *Nature* **362**, 709–715 (1993).
129. O'Connor, M. J. Targeting the DNA damage response in cancer. *Mol. Cell* **60**, 547–560 (2015).
130. Krokan, H. E. & Bjoras, M. Chapter 06: Base Excision Repair. *Cold Spring Harb Perspect Biol.* **5**, a012583 (2013).
131. Petrusheva, I. O., Evdokimov, A. N. & Lavrik, O. I. Molecular mechanism of global genome nucleotide excision repair. *Acta Naturae* **6**, 23–34 (2014).
132. Jiricny, J. The multifaceted mismatch-repair system. *Nat. Rev. Mol. Cell Biol.* **7**, 335–346 (2006).
133. Radhakrishnan, S. K., Jette, N. & Lees-Miller, S. P. Non-homologous end joining: Emerging themes and unanswered questions. *DNA Repair (Amst).* **17**, 2–8 (2014).
134. Moynahan, M. E. & Jasin, M. Mitotic homologous recombination maintains genomic stability and suppresses tumorigenesis. *Nat. Rev. Mol. Cell Biol.* **11**, 196–207 (2010).
135. Blackford, A. N. & Jackson, S. P. ATM, ATR, and DNA-PK: The Trinity at the Heart of the DNA Damage Response. *Mol. Cell* **66**, 801–817 (2017).

136. Damia, G. Targeting DNA-PK in cancer. *Mutat. Res. - Fundam. Mol. Mech. Mutagen.* **821**, 111692 (2020).
137. Jette, N. & Lees-Miller, S. P. The DNA-dependent protein kinase: a multifunctional protein kinase with roles in DNA double strand break repair and mitosis. *Prog Biophys Mol Biol* **117**, 194–205 (2015).
138. Scully, R. & Xie, A. Double strand break repair functions of histone H2AX. *Mutat. Res. - Fundam. Mol. Mech. Mutagen.* **750**, 5–14 (2013).
139. Shiloh, Y. & Ziv, Y. The ATM protein kinase: Regulating the cellular response to genotoxic stress, and more. *Nat. Rev. Mol. Cell Biol.* **14**, 197–210 (2013).
140. Zou, L. & Elledge, S. J. Sensing DNA damage through ATRIP recognition of RPA-ssDNA complexes. *Science (80-. )*. **300**, 1542–1548 (2003).
141. Kumagai, A., Lee, J., Yoo, H. Y. & Dunphy, W. G. TopBP1 activates the ATR-ATRIP complex. *Cell* **124**, 943–955 (2006).
142. Haahr, P. *et al.* Activation of the ATR kinase by the RPA-binding protein ETAA1. *Nat. Cell Biol.* **18**, 1196–1207 (2016).
143. Guo, Z., Kumagai, A., Wang, S. X. & Dunphy, W. G. Requirement for Atr in phosphorylation of Chk1 and cell cycle regulation in response to DNA replication blocks and UV-damaged DNA in *Xenopus* egg extracts. *Genes Dev.* **14**, 2745–2756 (2000).
144. Boubberhan, S. *et al.* The evolving role of DNA damage response in overcoming therapeutic resistance in ovarian cancer. *Cancer Drug Resist.* **6**, 345–357 (2023).
145. Ruiz, S. *et al.* A Genome-wide CRISPR Screen Identifies CDC25A as a Determinant of Sensitivity to ATR Inhibitors. *Mol. Cell* **62**, 307–313 (2016).
146. Cortez, D. Preventing replication fork collapse to maintain genome integrity. *DNA Repair (Amst)*. **32**, 149–157 (2015).
147. Abraham, R. T. Cell cycle checkpoint signaling through the ATR and ATM kinases. *Genes Dev.* **15**, 2177–2196 (2001).
148. Cuadrado, M. *et al.* ATM regulates ATR chromatin loading in response to DNA double-strand breaks. *J. Exp. Med.* **203**, 297–303 (2006).
149. Amé, J. C., Spenlehauer, C. & De Murcia, G. The PARP superfamily. *BioEssays* **26**, 882–893 (2004).
150. D'Amours, D., Desnoyers, S., D'Silva, I. & Poirier, G. G. Poly(ADP-ribosylation) reactions in the regulation of nuclear functions. *Biochem. J.* **342**, 249–268 (1999).
151. Ray Chaudhuri, A. & Nussenzweig, A. The multifaceted roles of PARP1 in DNA repair and chromatin remodelling. *Nat. Rev. Mol. Cell Biol.* **18**, 610–621 (2017).
152. Ahel, D. *et al.* Poly(ADP-ribose)-dependent regulation of DNA repair by the chromatin remodeling enzyme ALC1. *Science (80-. )*. **325**, 1240–1243 (2009).
153. Fisher, A. E. O., Hochegger, H., Takeda, S. & Caldecott, K. W. Poly(ADP-Ribose) Polymerase 1 Accelerates Single-Strand Break Repair in Concert with Poly(ADP-Ribose) Glycohydrolase. *Mol. Cell. Biol.* **27**, 5597–5605 (2007).

154. Ali, A. A. E. *et al.* The zinc-finger domains of PARP1 cooperate to recognize DNA strand breaks. *Nat. Struct. Mol. Biol.* **19**, 685–692 (2012).
155. Dantzer, F., Nasheuer, H. P., Vonesch, J. L., De Murcia, G. & Ménissier-De Murcia, J. Functional association of poly(ADP-ribose) polymerase with DNA polymerase  $\alpha$ -primase complex: A link between DNA strand break detection and DNA replication. *Nucleic Acids Res.* **26**, 1891–1898 (1998).
156. Bryant, H. E. *et al.* PARP is activated at stalled forks to mediate Mre11-dependent replication restart and recombination. *EMBO J.* **28**, 2601–2615 (2009).
157. Escargueil, A. E., Soares, D. G., Salvador, M., Larsen, A. K. & Henriques, J. A. P. What histone code for DNA repair? *Mutat. Res. - Rev. Mutat. Res.* **658**, 259–270 (2008).
158. Russo, G. *et al.* DNA damage and Repair Modify DNA methylation and Chromatin Domain of the Targeted Locus: Mechanism of allele methylation polymorphism. *Sci. Rep.* **6**, 1–14 (2016).
159. Xu, Y. *et al.* H2AZ controls DSB repair. **48**, 723–733 (2012).
160. Fernandez-Capetillo, O., Lee, A., Nussenzweig, M. & Nussenzweig, A. H2AX: the histone guardian of the genome. *DNA Repair (Amst.)* **3**, 959–967 (2004).
161. Clouaire, T. *et al.* Comprehensive Mapping of Histone Modifications at DNA Double-Strand Breaks Deciphers Repair Pathway Chromatin Signatures. *Mol. Cell* **72**, 250–262.e6 (2018).
162. Sharma, A. K. & Hendzel, M. J. The relationship between histone posttranslational modification and DNA damage signaling and repair. *Int. J. Radiat. Biol.* **95**, 382–393 (2019).
163. Bird, A. W. *et al.* Acetylation of histone H4 by Esa1 is required for DNA double-strand break repair. *Nature* **419**, 411–415 (2002).
164. Qin, S. & Parthun, M. R. Histone H3 and the Histone Acetyltransferase Hat1p Contribute to DNA Double-Strand Break Repair. *Mol. Cell. Biol.* **22**, 8353–8365 (2002).
165. Tamburini, B. A. & Tyler, J. K. Localized Histone Acetylation and Deacetylation Triggered by the Homologous Recombination Pathway of Double-Strand DNA Repair. *Mol. Cell. Biol.* **25**, 4903–4913 (2005).
166. Arichthota, S., Rana, P. P. & Haldar, D. Histone acetylation dynamics in repair of DNA double-strand breaks. *Front. Genet.* **13**, 1–16 (2022).
167. Burgers, P. M. J. & Kunkel, T. A. Eukaryotic DNA replication fork. *Annu. Rev. Biochem.* **86**, 417–438 (2017).
168. Saxena, S. & Zou, L. Hallmarks of DNA replication stress. *Mol. Cell* **82**, 2298–2314 (2022).
169. Bębenek, A. & Ziuzia-Graczyk, I. Fidelity of DNA replication—a matter of proofreading. *Curr. Genet.* **64**, 985–996 (2018).
170. Zeman, M. K. & Cimprich, K. A. Causes and consequences of replication stress. *Nat. Cell Biol.* **16**, 2–9 (2014).

171. Lin, Y.-L. & Pasero, P. Replication stress: from chromatin to immunity and beyond. *Genet. Dev.* **71**, 136–142 (2021).
172. Byun, T. S., Pacek, M., Yee, M. C., Walter, J. C. & Cimprich, K. A. Functional uncoupling of MCM helicase and DNA polymerase activities activates the ATR-dependent checkpoint. *Genes Dev.* **19**, 1040–1052 (2005).
173. Toledo, L. I. *et al.* ATR prohibits replication catastrophe by preventing global exhaustion of RPA. *Cell* **155**, 1088 (2013).
174. De Piccoli, G. *et al.* Replisome Stability at Defective DNA Replication Forks Is Independent of S Phase Checkpoint Kinases. *Mol. Cell* **45**, 696–704 (2012).
175. Dungrawala, H. *et al.* The Replication Checkpoint Prevents Two Types of Fork Collapse without Regulating Replisome Stability. *Mol. Cell* **59**, 998–1010 (2015).
176. Quinet, A., Lemaçon, D. & Vindigni, A. Replication Fork Reversal: Players and Guardians. *Mol. Cell* **68**, 830–833 (2017).
177. Mourón, S. *et al.* Repriming of DNA synthesis at stalled replication forks by human PrimPol. *Nat. Struct. Mol. Biol.* **20**, 1383–1389 (2013).
178. Tirman, S. *et al.* Temporally distinct post-replicative repair mechanisms fill PRIMPOL-dependent ssDNA gaps in human cells. *Mol. Cell* **81**, 4026–4040.e8 (2021).
179. Boos, D. & Ferreira, P. Origin firing regulations to control genome replication timing. *Genes (Basel)*. **10**, 1–21 (2019).
180. McIntosh, D. & Blow, J. J. Dormant origins, the licensing checkpoint, and the response to replicative stresses. *Cold Spring Harb. Perspect. Biol.* **4**, 1–11 (2012).
181. Truong, L. N. & Wu, X. Prevention of DNA re-replication in eukaryotic cells. *J. Mol. Cell Biol.* **3**, 13–22 (2011).
182. Berti, M., Cortez, D. & Lopes, M. The plasticity of DNA replication forks in response to clinically relevant genotoxic stress. *Nat. Rev. Mol. Cell Biol.* **21**, 633–651 (2020).
183. Chanoux, R. A. *et al.* ATR and H2AX cooperate in maintaining genome stability under replication stress. *J. Biol. Chem.* **284**, 5994–6003 (2009).
184. Ashour, M. E. & Mosammamarast, N. Mechanisms of damage tolerance and repair during DNA replication. *Nucleic Acids Res.* **49**, 3033–3047 (2021).
185. Voineagu, I., Narayanan, V., Lobachev, K. S. & Mirkin, S. M. Replication stalling at unstable inverted repeats: Interplay between DNA hairpins and fork stabilizing proteins. *Proc. Natl. Acad. Sci. U. S. A.* **105**, 9936–9941 (2008).
186. Kumar, C., Batra, S., Griffith, J. D. & Remus, D. The interplay of rna:Dna hybrid structure and g-quadruplexes determines the outcome of r-loop-replisome collisions. *Elife* **10**, 1–34 (2021).
187. Wootton, J. & Soutoglou, E. Chromatin and Nuclear Dynamics in the Maintenance of Replication Fork Integrity. *Front. Genet.* **12**, 1–18 (2021).
188. Topal, S., Van, C., Xue, Y., Carey, M. F. & Peterson, C. L. INO80C Remodeler Maintains Genomic Stability by Preventing Promiscuous Transcription at

- Replication Origins. *Cell Rep.* **32**, 108106 (2020).
189. Sfeir, A. *et al.* Mammalian Telomeres Resemble Fragile Sites and Require TRF1 for Efficient Replication. *Cell* **138**, 90–103 (2009).
  190. Xu, C., Xu, Y., Gursoy-Yuzugullu, O. & Price, B. D. The histone variant macro H2A1.1 is recruited to DSBs through a mechanism involving PARP1. *FEBS Lett.* **586**, 3920–3925 (2012).
  191. Rondinelli, B. *et al.* EZH2 promotes degradation of stalled replication forks by recruiting MUS81 through histone H3 trimethylation. *Nat. Cell Biol.* **19**, 1371–1378 (2017).
  192. Agudelo Garcia, P. A. *et al.* Histone acetyltransferase 1 is required for DNA replication fork function and stability. *J. Biol. Chem.* **295**, 8363–8372 (2020).
  193. Bester, A. C. *et al.* Nucleotide deficiency promotes genomic instability in early stages of cancer development. *Cell* **145**, 435–446 (2011).
  194. Papadopoulou, C., Guilbaud, G., Schiavone, D. & Sale, J. E. Nucleotide Pool Depletion Induces G-Quadruplex-Dependent Perturbation of Gene Expression. *Cell Rep.* **13**, 2491–2503 (2015).
  195. Tumini, E., Barroso, S., Pérez-Calero, C. & Aguilera, A. Roles of human POLD1 and POLD3 in genome stability. *Sci. Rep.* **6**, 1–13 (2016).
  196. Griffin, W. C. & Trakselis, M. A. The MCM8/9 complex: A recent recruit to the roster of helicases involved in genome maintenance. *DNA Repair (Amst)*. **76**, 1–10 (2019).
  197. García-Muse, T. & Aguilera, A. Transcription-replication conflicts: How they occur and how they are resolved. *Nat. Rev. Mol. Cell Biol.* **17**, 553–563 (2016).
  198. Lin, Y. L. & Pasero, P. Transcription-Replication Conflicts: Orientation Matters. *Cell* **170**, 603–604 (2017).
  199. Prado, F. & Aguilera, A. Impairment of replication fork progression mediates RNA polII transcription-associated recombination. *EMBO J.* **24**, 1267–1276 (2005).
  200. Huvet, M. *et al.* Human gene organization driven by the coordination of replication and transcription. *Genome Res.* **17**, 1278–1285 (2007).
  201. Aguilera, A. & García-Muse, T. R Loops: From Transcription Byproducts to Threats to Genome Stability. *Mol. Cell* **46**, 115–124 (2012).
  202. Sollier, J. & Cimprich, K. A. Breaking bad: R-loops and genome integrity. *Trends Cell Biol.* **25**, 514–522 (2015).
  203. Sollier, J. *et al.* Transcription-Coupled Nucleotide Excision Repair Factors Promote R-Loop-Induced Genome Instability. *Mol. Cell* **56**, 777–785 (2014).
  204. Huertas, P. & Aguilera, A. Cotranscriptionally formed DNA:RNA hybrids mediate transcription elongation impairment and transcription-associated recombination. *Mol. Cell* **12**, 711–721 (2003).
  205. Santos-Pereira, J. M. & Aguilera, A. R loops: New modulators of genome dynamics and function. *Nat. Rev. Genet.* **16**, 583–597 (2015).
  206. Ginno, P. A., Lim, Y. W., Lott, P. L., Korf, I. & Chédin, F. GC skew at the 59 and 39

- ends of human genes links R-loop formation to epigenetic regulation and transcription termination. *Genome Res.* **23**, 1590–1600 (2013).
207. Skourti-Stathaki, K., Proudfoot, N. J. & Gromak, N. Human Senataxin Resolves RNA/DNA Hybrids Formed at Transcriptional Pause Sites to Promote Xrn2-Dependent Termination. *Mol. Cell* **42**, 794–805 (2011).
  208. Gan, W. *et al.* R-loop-mediated genomic instability is caused by impairment of replication fork progression. *Genes Dev.* **25**, 2041–2056 (2011).
  209. Hatchi, E. *et al.* BRCA1 recruitment to transcriptional pause sites is required for R-loop-driven DNA damage repair. *Mol. Cell* **57**, 636–647 (2015).
  210. Niehrs, C. & Luke, B. Regulatory R-loops as effectors of gene expression and genome stability. **21**, 167–178 (2021).
  211. Bayona-Feliu, A., Barroso, S., Muñoz, S. & Aguilera, A. The SWI/SNF chromatin remodeling complex helps resolve R-loop-mediated transcription–replication conflicts. *Nat. Genet.* **53**, 1050–1063 (2021).
  212. Drolet, M. *et al.* Overexpression of RNase H partially complements the growth defect of an Escherichia coli  $\Delta$ topA mutant: R-loop formation is a major problem in the absence of DNA topoisomerase I. *Proc. Natl. Acad. Sci. U. S. A.* **92**, 3526–3530 (1995).
  213. Wahba, L., Amon, J. D., Koshland, D. & Vuica-Ross, M. RNase H and Multiple RNA Biogenesis Factors Cooperate to Prevent RNA:DNA Hybrids from Generating Genome Instability. *Mol. Cell* **44**, 978–988 (2011).
  214. García-Rubio, M. L. *et al.* The Fanconi Anemia Pathway Protects Genome Integrity from R-loops. *PLoS Genet.* **11**, 1–17 (2015).
  215. MacAlpine, D. M. & Almouzni, G. Chromatin and DNA replication. *Cold Spring Harb. Perspect. Biol.* **5**, 1–22 (2013).
  216. Salas-Armenteros, I. *et al.* Human THO –Sin3A interaction reveals new mechanisms to prevent R-loops that cause genome instability. *EMBO J.* **36**, 3532–3547 (2017).
  217. Ginno, P. A., Lott, P. L., Christensen, H. C., Korf, I. & Chédin, F. R-Loop Formation Is a Distinctive Characteristic of Unmethylated Human CpG Island Promoters. *Mol. Cell* **45**, 814–825 (2012).
  218. Castellano-Pozo, M. *et al.* R loops are linked to histone H3 S10 phosphorylation and chromatin condensation. *Mol. Cell* **52**, 583–590 (2013).
  219. Chen, P. B., Chen, H. V., Acharya, D., Rando, O. J. & Fazio, T. G. R-loops regulate promoter-proximal chromatin architecture and cellular differentiation. *Nat Struct Mol Biol* **22**, 999–1007 (2015).
  220. Boque-Sastre, R. *et al.* Head-to-head antisense transcription and R-loop formation promotes transcriptional activation. *Proc. Natl. Acad. Sci. U. S. A.* **112**, 5785–5790 (2015).
  221. Skourti-Stathaki, K., Kamieniarz-Gdula, K. & Proudfoot, N. J. R-loops induce repressive chromatin marks over mammalian gene terminators. *Nature* **516**, 436–439 (2014).

222. Hanahan, D. Hallmarks of Cancer: New Dimensions. *Cancer Discov.* **12**, 31–46 (2022).
223. Negrini, S., Gorgoulis, V. G. & Halazonetis, T. D. Genomic instability an evolving hallmark of cancer. *Nat. Rev. Mol. Cell Biol.* **11**, 220–228 (2010).
224. Choi, W. & Lee, E. S. Therapeutic targeting of the DNA damage response in prostate cancer. *Int. J. Mol. Sci.* **23**, (2022).
225. Lam, M. H., Liu, Q., Elledge, S. J. & Rosen, J. M. Chk1 is haploinsufficient for multiple functions critical to tumor suppression. *Cancer Cell* **6**, 45–59 (2004).
226. Halazonetis, T. D., Gorgoulis, V. G. & Bartek, J. An oncogene-induced DNA damage model for cancer development. *Science (80- )*. **319**, 1352–1355 (2008).
227. Kotsantis, P. *et al.* Increased global transcription activity as a mechanism of replication stress in cancer. *Nat. Commun.* **7**, 1–13 (2016).
228. Srinivasan, S. V., Dominguez-Sola, D., Wang, L. C., Hyrien, O. & Gautier, J. Cdc45 Is a Critical Effector of Myc-Dependent DNA Replication Stress. *Cell Rep.* **3**, 1629–1639 (2013).
229. Jones, R. M. *et al.* Increased replication initiation and conflicts with transcription underlie Cyclin E-induced replication stress. *Oncogene* **32**, 3744–3753 (2013).
230. Macheret, M. & Halazonetis, T. D. DNA replication stress as a hallmark of cancer. *Annu. Rev. Pathol. Mech. Dis.* **10**, 425–448 (2015).
231. Kuchenbaecker, K. B. *et al.* Risks of breast, ovarian, and contralateral breast cancer for BRCA1 and BRCA2 mutation carriers. *Jama* **317**, 2402–2416 (2017).
232. Oh, M. *et al.* The association of BRCA1 and BRCA2 mutations with prostate cancer risk, frequency, and mortality: A meta-analysis. *Prostate* **79**, 880–895 (2019).
233. Cavanagh, H. & Rogers, K. M. A. The role of BRCA1 and BRCA2 mutations in prostate, pancreatic and stomach cancers. *Hered. Cancer Clin. Pract.* **13**, 1–7 (2015).
234. Hill, S. J. *et al.* Systematic screening reveals a role for BRCA1 in the response to transcription-associated DNA damage. *Genes Dev.* **28**, 1957–1975 (2014).
235. Bhatia, V. *et al.* BRCA2 prevents R-loop accumulation and associates with TREX-2 mRNA export factor PCID2. *Nature* **511**, 362–365 (2014).
236. Curtin, N. J. Targeting the DNA Damage Response for Cancer Therapy. *Biochem. Soc. Trans.* **51**, 207–221 (2023).
237. Li, Q. *et al.* A new wave of innovations within the DNA damage response. *Signal Transduct. Target. Ther.* **8**, 1–26 (2023).
238. Lord, C. J. & Ashworth, A. PARP inhibitors synthetic lethality in the clinic. *Science (80- )*. **355**, 1152–1158 (2017).
239. Zhang, B. *et al.* The tumor therapy landscape of synthetic lethality. *Nat. Commun.* **12**, 1–11 (2021).
240. Jurkovicova, D., Neophytou, C. M., Gašparović, A. Č. & Gonçalves, A. C. DNA Damage Response in Cancer Therapy and Resistance: Challenges and

- Opportunities. *Int. J. Mol. Sci.* **23**, (2022).
241. Huang, D. *et al.* A highly annotated database of genes associated with platinum resistance in cancer. *Oncogene* **40**, 6395–6405 (2021).
  242. Erice, O. *et al.* MGMT expression predicts parp-mediated resistance to temozolomide. *Mol. Cancer Ther.* **14**, 1236–1246 (2015).
  243. Reinhardt, H. C., Jiang, H., Hemann, M. & Yaffe, M. B. Exploiting synthetic lethal interactions for targeted cancer therapy. *Cell cycle* **8**, 3112–3119 (2009).
  244. Ashworth, A. A synthetic lethal therapeutic approach: Poly(ADP) ribose polymerase inhibitors for the treatment of cancers deficient in DNA double-strand break repair. *J. Clin. Oncol.* **26**, 3785–3790 (2008).
  245. Farmer, H. *et al.* Targeting the DNA repair defect in BRCA mutant cells as a therapeutic strategy. *Nature* **434**, 917–921 (2005).
  246. D’Andrea, A. D. Mechanisms of PARP inhibitor sensitivity and resistance. *DNA Repair (Amst)*. **71**, 172–176 (2018).
  247. Wilson, Z. *et al.* ATR Inhibitor AZD6738 (Ceralasertib) Exerts Antitumor Activity as a Monotherapy and in Combination with Chemotherapy and the PARP Inhibitor Olaparib. *Cancer Res.* **82**, 1140–1152 (2022).
  248. Garralda, E. *et al.* MYC targeting by OMO-103 in solid tumors: a phase 1 trial. *Nat. Med.* (2024) doi:10.1038/s41591-024-02805-1.
  249. Thompson-Wicking, K. *et al.* Novel BRD4-NUT fusion isoforms increase the pathogenic complexity in NUT midline carcinoma. *Oncogene* **32**, 4664–4674 (2013).
  250. Shaw, G., Morse, S., Ararat, M. & Graham, F. L. Preferential transformation of human neuronal cells by human adenoviruses and the origin of HEK 293 cells. *FASEB J.* **16**, 869–871 (2002).
  251. T. Das, A., Tenenbaum, L. & Berkhout, B. Tet-On Systems For Doxycycline-inducible Gene Expression. *Curr. Gene Ther.* **16**, 156–167 (2016).
  252. Zengerle, M., Chan, K. H. & Ciulli, A. Selective Small Molecule Induced Degradation of the BET Bromodomain Protein BRD4. *ACS Chem. Biol.* **10**, 1770–1777 (2015).
  253. Vannam, R. *et al.* Targeted degradation of the enhancer lysine acetyltransferases CBP and p300. *Cell Chem. Biol.* **28**, 503–514.e12 (2021).
  254. Lai, W. S., Arvola, R. M., Goldstrohm, A. C. & Blackshear, P. J. Inhibition of transcription in cultured metazoan cells with actinomycin D to monitor mRNA turnover. *Methods* **155**, 77–87 (2019).
  255. Soucek, L. *et al.* Design and properties of a Myc derivative that efficiently homodimerizes. *Oncogene* **17**, 2463–2472 (1998).
  256. Manzo, A. *et al.* Lurbinectedin in small cell lung cancer. *Front. Oncol.* **12**, 1–8 (2022).
  257. Bailly, C. Irinotecan: 25 years of cancer treatment. *Pharmacol. Res.* **148**, (2019).
  258. Bou-Nader, C., Bothra, A., Garboczi, D. N., Leppla, S. H. & Zhang, J. Structural

- basis of R-loop recognition by the S9.6 monoclonal antibody. *Nat. Commun.* **13**, 1–14 (2022).
259. Dhar, S., Datta, A., Banerjee, T. & Brosh, R. M. Single-molecule DNA fiber analyses to characterize replication fork dynamics in living cells. in *Methods in Molecular Biology* vol. 1999 307–318 (Humana Press Inc., 2019).
  260. Pierce, A. J., Hu, P., Han, M., Ellis, N. & Jasin, M. Ku DNA end-binding protein modulates homologous repair of double-strand breaks in mammalian cells. *Genes Dev.* **15**, 3237–3242 (2001).
  261. Castroviejo-Bermejo, M. *et al.* A RAD 51 assay feasible in routine tumor samples calls PARP inhibitor response beyond BRCA mutation. *EMBO Mol. Med.* **10**, 1–16 (2018).
  262. Cruz, C. *et al.* RAD51 foci as a functional biomarker of homologous recombination repair and PARP inhibitor resistance in germline BRCA-mutated breast cancer. *Ann. Oncol.* **29**, 1203–1210 (2018).
  263. Ewels, P. A. *et al.* The nf-core framework for community-curated bioinformatics pipelines. *Nat. Biotechnol.* **38**, 276–278 (2020).
  264. Ritchie, M. E. *et al.* Limma powers differential expression analyses for RNA-sequencing and microarray studies. *Nucleic Acids Res.* **43**, e47 (2015).
  265. Robinson, M. D. & Oshlack, A. A scaling normalization method for differential expression analysis of RNA-seq data. 1–12 (2010).
  266. Robinson, M. D., McCarthy, D. J. & Smyth, G. K. edgeR: A Bioconductor package for differential expression analysis of digital gene expression data. *Bioinformatics* **26**, 139–140 (2009).
  267. Subramanian, A. *et al.* Gene set enrichment analysis: A knowledge-based approach for interpreting genome-wide expression profiles. *PNAS* **102**, 15545–15550 (2005).
  268. Yu, G., Wang, L. G., Han, Y. & He, Q. Y. ClusterProfiler: An R package for comparing biological themes among gene clusters. *Omi. A J. Integr. Biol.* **16**, 284–287 (2012).
  269. Liu, S. *et al.* Distinct roles for DNA-PK, ATM and ATR in RPA phosphorylation and checkpoint activation in response to replication stress. *Nucleic Acids Res.* **40**, 10780–10794 (2012).
  270. Jao, C. Y. & Salic, A. Exploring RNA transcription and turnover in vivo by using click chemistry. *Proc. Natl. Acad. Sci. U. S. A.* **105**, 15779–15784 (2008).
  271. Stirling, P. C. *et al.* R-loop-mediated genome instability in mRNA cleavage and polyadenylation mutants. *Genes Dev.* **26**, 163–175 (2012).
  272. Brown, T. A., Tkachuk, A. N. & Clayton, D. A. Native R-loops persist throughout the mouse mitochondrial DNA genome. *J. Biol. Chem.* **283**, 36743–36751 (2008).
  273. Murga, M. *et al.* Exploiting oncogene-induced replicative stress for the selective killing of Myc-driven tumors. *Nat. Struct. Mol. Biol.* **18**, 1331–1335 (2011).
  274. Pierce, A. J., Hu, P., Han, M., Ellis, N. & Jasin, M. Ku DNA end-binding protein

- modulates homologous repair of double-strand breaks in mammalian cells. *Genes Dev.* **15**, 3237–3242 (2001).
275. Lee, H. *et al.* Oncogenic Impact of TONSL, a Homologous Recombination Repair Protein at the Replication Fork, in Cancer Stem Cells. *Int. J. Mol. Sci.* **24**, (2023).
  276. Bagrodia, A. & AMatruda, J. F. *Testicular Germ Cell Tumors. Human press* (2021).
  277. Bonilla, B., Hengel, S. R., Grundy, M. K. & Bernstein, K. A. RAD51 gene family structure and function. *Annu Rev Genet* **53**, 25–46 (2020).
  278. Mekonnen, N., Yang, H. & Shin, Y. K. Homologous Recombination Deficiency in Ovarian, Breast, Colorectal, Pancreatic, Non-Small Cell Lung and Prostate Cancers, and the Mechanisms of Resistance to PARP Inhibitors. *Front. Oncol.* **12**, 1–28 (2022).
  279. Qiu, Z., Oleinick, N. L. & Zhang, J. ATR/CHK1 inhibitors and cancer therapy. *Radiother. Oncol.* **126**, 450–464 (2018).
  280. Kim, H. *et al.* Combining PARP with ATR inhibition overcomes PARP inhibitor and platinum resistance in ovarian cancer models. *Nat. Commun.* **11**, (2020).
  281. Beaulieu, M. E. *et al.* Intrinsic cell-penetrating activity propels omomyc from proof of concept to viable anti-myc therapy. *Sci. Transl. Med.* **11**, (2019).
  282. Trigo, J. *et al.* Lurbinectedin as second-line treatment for patients with small-cell lung cancer: a single-arm, open-label, phase 2 basket trial. *Lancet Oncol.* **21**, 645–654 (2020).
  283. Jr, P. N. L. *et al.* Phase III Trial of Irinotecan / Cisplatin Compared With Etoposide / Cisplatin in Extensive-Stage Small-Cell Lung Cancer : Clinical and Pharmacogenomic Results From SWOG S0124. *J. Clin. Oncol.* **27**, (2009).
  284. Gatta, G. *et al.* Burden and centralised treatment in Europe of rare tumours: results of RARECAREnet—a population-based study. *Lancet Oncol.* **18**, 1022–1039 (2017).
  285. Serrano, C. *et al.* Rethinking placebos: embracing synthetic control arms in clinical trials for rare tumors. *Nat. Med.* **29**, 2689–2692 (2023).
  286. Natsume, T., Kiyomitsu, T., Saga, Y. & Kanemaki, M. T. Rapid Protein Depletion in Human Cells by Auxin-Inducible Degron Tagging with Short Homology Donors. *Cell Rep.* **15**, 210–218 (2016).
  287. Xu, X. *et al.* Clinical characteristics and prognostic significance of DNA methylation regulatory gene mutations in acute myeloid leukemia. *Clin. Epigenetics* **15**, 1–13 (2023).
  288. Tang, M., Xu, W., Wang, Q., Xiao, W. & Xu, R. Potential of DNMT and its Epigenetic Regulation for Lung Cancer Therapy. *Curr. Genomics* **10**, 336–352 (2009).
  289. Edwards, C. & Johnson, R. W. Targeting histone modifications in bone and lung metastatic cancers. **19**, 230–246 (2021).
  290. Liu, Y. & Yang, Q. The roles of EZH2 in cancer and its inhibitors. *Med. Oncol.* **40**,

- 1–29 (2023).
291. Lovén, J. *et al.* Selective inhibition of tumor oncogenes by disruption of super-enhancers. *Cell* **153**, 320–334 (2013).
  292. Li, X. *et al.* BRD4 Promotes DNA Repair and Mediates the Formation of TMPRSS2-ERG Gene Rearrangements in Prostate Cancer. *Cell Rep.* **22**, 796–808 (2018).
  293. Stanlie, A., Yousif, A. S., Akiyama, H., Honjo, T. & Begum, N. A. Chromatin reader Brd4 functions in Ig class switching as a repair complex adaptor of nonhomologous end-joining. *Mol. Cell* **55**, 97–110 (2014).
  294. Floyd, S. R. *et al.* The bromodomain protein Brd4 insulates chromatin from DNA damage signalling. *Nature* **498**, 246–250 (2013).
  295. Zhang, J. *et al.* BRD4 facilitates replication stress-induced DNA damage response. *Oncogene* **37**, 3763–3777 (2018).
  296. Bisgrove, D. A., Mahmoudi, T., Henklein, P. & Verdin, E. Conserved P-TEFb-interacting domain of BRD4 inhibits HIV transcription. *Proc. Natl. Acad. Sci. U. S. A.* **104**, 13690–13695 (2007).
  297. Kong, X. *et al.* Cancer drug addiction is relayed by an ERK2-dependent phenotype switch. *Nature* **550**, 270–274 (2017).
  298. Vivanco, I. Targeting molecular addictions in cancer. *Br. J. Cancer* **111**, 2033–2038 (2014).
  299. Lam, F. C. *et al.* BRD4 prevents the accumulation of R-loops and protects against transcription–replication collision events and DNA damage. *Nat. Commun.* **11**, (2020).
  300. Pilié, P. G., Gay, C. M., Byers, L. A., O’Connor, M. J. & Yap, T. A. PARP inhibitors: Extending benefit beyond BRCA-mutant cancers. *Clin. Cancer Res.* **25**, 3759–3771 (2019).
  301. Brenner, J. C. *et al.* PARP-1 inhibition as a targeted strategy to treat Ewing’s sarcoma. *Cancer Res.* **72**, 1608–1613 (2012).
  302. Rieckhoff, J. *et al.* Exploiting chromosomal instability of pten-deficient triple-negative breast cancer cell lines for the sensitization against parp1 inhibition in a replication-dependent manner. *Cancers (Basel)*. **12**, 1–14 (2020).
  303. Laspata, N. *et al.* PARP1 associates with R-loops to promote their resolution and genome stability. *Nucleic Acids Res.* **51**, 2215–2237 (2023).
  304. Massó-Vallés, D. *et al.* MYC Inhibition Halts Metastatic Breast Cancer Progression by Blocking Growth, Invasion, and Seeding. *Cancer Res. Commun.* **2**, 110–130 (2022).
  305. Zacarías-Fluck, M. F. *et al.* Reducing MYC’s transcriptional footprint unveils a good prognostic gene signature in melanoma. *Genes Dev.* **37**, 303–320 (2023).
  306. Kotekar, A., Singh, A. K. & Devaiah, B. N. BRD4 and MYC: power couple in transcription and disease. *FEBS J.* **290**, 4820–4842 (2023).
  307. Sengupta, D. *et al.* Disruption of BRD4 at H3K27Ac-enriched enhancer region correlates with decreased c-Myc expression in Merkel cell carcinoma.

- Epigenetics* **10**, 460–466 (2015).
308. Shimamura, T. *et al.* Efficacy of BET bromodomain inhibition in KRAS-mutant non-small cell lung cancer. *Clin. Cancer Res.* **19**, 6183–6192 (2013).
  309. Devaiah, B. N. *et al.* MYC protein stability is negatively regulated by BRD4. *Proc. Natl. Acad. Sci. U. S. A.* **117**, 13457–13467 (2020).
  310. Nie, Z. *et al.* Dissecting transcriptional amplification by MYC. *Elife* **9**, 1–32 (2020).
  311. Papadopoulos, D., Uhl, L., Ha, S. A. & Eilers, M. Beyond gene expression: how MYC relieves transcription stress. *Trends in Cancer* **9**, 805–816 (2023).

# APPENDIX



Papers resulting from collaboration in other projects during this thesis::

- **Human Metastatic Cholangiocarcinoma Patient-Derived Xenografts and Tumoroids for Preclinical Drug Evaluation.** Serra-Camprubí Q, Verdaguer H, Oliveros W, Lupi3n-Garcia N, Llop-Guevara A, Molina C, Vila-Casadesús M, Turpin A, Neuzillet C, Frigola J, Querol J, Yáñez-Bartolomé M, Castet F, Fabregat-Franco C, **Escudero-Iriarte C**, Escorihuela M, Arenas EJ, Bernadó-Morales C, Haro N, Giles FJ, Pozo ÓJ, Miquel JM, Nuciforo PG, Vivancos A, Melé M, Serra V, Arribas J, Tabernero J, Peiró S, Macarulla T, Tian TV. *Clinical Cancer Research*. 2023 Jan 17; **29**(2):432-445. doi: 10.1158/1078-0432.CCR-22-2551.
- **LOXL2-mediated chromatin compaction is required to maintain the oncogenic properties of triple-negative breast cancer.** Serra-Bardenys, Gemma; Blanco, Enrique; **Escudero-Iriarte, Carmen**; Serra-Camprubí, Queral; Querol, Jessica Pascual-Renguant, Laura; Morancho, Beatriz; Escorihuela, Marta; Tissera, Natalia S.; Sabé, Anna; Martín, Luna; Segura-Bayona, Sandra; Verde, Gaetano; Aiese-Cigliano, Riccardo; Millanes-Romero, Alba; Kerónimo, Celia; Cebrià-Costa, Joan Pau; Nuciforo, Paolo; Simonetti, Sara; Viaplana, Cristina; Dienstmann, Rodrigo; Oliviera, Mafalda; Peg, Vicente; Stracker, Travis H.; Arribas, Joaquin; Canals, Francesc; Villanueva, Josep; Di Croce, Luciano; García de Herreros, Antonio; Tian, Tian V.; Peiró, Sandra. *The FEBS Journal*. 2024 March; **7** doi.org/10.1111/febs.17112
- **Fascin-1 expression is associated with neuroendocrine prostate cancer and directly suppressed by androgen receptor.** Anthony Turpin, Carine Delliaux, Pauline Parent, Hortense Chevalier, **Carmen Escudero-Iriarte**, Franck Bonardi, Nathalie Vanpouille, Anne Flourens, Jessica Querol, Aurélien Carnot, Xavier Leroy, Nicolás Herranz, Tristan Lane, Arnauld Villers, Jonathan Olivier, Hélène Touzet, Yvan de Launoit, Tian V. Tian, Martine Duterque-Coquillaud. *British Journal of Cancer*. 2023 Dec. **129**(12):1903-1914. doi: 10.1038/s41416-023-02449-x